2014

Advanced Distillation Curve For Alternate Aviation Fuel And Biofuels

Thomas Anison
North Carolina Agricultural and Technical State University

Advanced Distillation Curve for Alternate Aviation Fuel and Biofuels

Thomas Anison

North Carolina A&T State University

A thesis submitted to the graduate faculty

in partial fulfillment of the requirements for the degree of

MASTER OF SCIENCE

Department: Chemical, Biological and Bio Engineering

Major: Chemical Engineering

Major Professor: Dr. Vinayak Kabadi

Greensboro, North Carolina

2014

The Graduate School
North Carolina Agricultural and Technical State University
This is to certify that the Master's Thesis of

Thomas Anison

has met the thesis requirements of
North Carolina Agricultural and Technical State University

Greensboro, North Carolina
2014

Approved by:

Dr. Vinayak Kabadi Major Professor	Dr. Shamsuddin Ilias Committee Member
Dr. Mannur Sundaresan Committee Member	Dr. Stephen B Knisley Department Chair

Dr. Sanjiv Sarin
Dean, The Graduate School

Biographical Sketch

Thomas Anison was born in June 15, 1978 in Ghana and obtained his undergraduate degree in Chemical Engineering from Kwame Nkrumah University of Science and Technology, in the year 2001. He started his professional career with PZ Cussons Ghana as a management trainee and built it career from there. He worked in various capacities in the industries with Ghana Oil Palm Development Company, Ghana Specialty Fats Industries Limited and International Oils and Fats.

Thomas got admission to North Carolina A&T State University in Fall Semester, 2012 in the department of Chemical, Biological and BioEngineering to pursue his master's degree in Chemical Engineering.

Dedication

This thesis is dedicated to my lovely wife Doris Anison and my two daughters Michelle and Doreen Anison. Thank you all for the understanding and support during this time of my career.

Acknowledgements

I first of all want to give thanks to God for the grace and strength to go through this research. To my advisor Dr. Vinayak Kabadi, I say a big thank you for the instruction, directions and his valuable time throughout the research. I want to acknowledge the Chemical, Biological and Bio Engineering department for the admission and training to this end of my career. It has been wonderful experience here with you all. For the support of NASA grant No NNX09AV08A which has been at the backbone in the financing of the research, I say it is highly appreciated. To my committee members, Dr. Shamsuddin Ilias and Dr. Mannur Sundaresan, I say thank you for your time. Further I express my appreciation to Glas-col Company for their help in the operating of the Ramptrol heater used and also my appreciation to Knauf Insulation for the free piece of insulation given for the experiment. To my colleagues Derrick Amoabeng and Zaron Johnson, thank you for your help.

Table of Contents

List of Figures

List of Tables

List of Symbols

Symbols	Description
r_c	radius of cylindrical head of distillation flask
R	radius of spherical portion of distillation flask
r	radius of liquid level in the distillation flask
h_c	height of cylindrical head of the distillation flask
h_s	height of spherical portion of the distillation flask
h_l	height of liquid in flask
u	linear velocity of the vapor in the distillation flask
Q_v	Vapor volumetric flow rate in the flask
Q_l	Distillate volumetric flow rate
A	Cross-sectional area of the liquid in the distillation flask
t	Experimental recorded time
t_{rc}	Vapor travel time in the cylindrical head
trs	Vapor travel time in the spherical portion of the flask
tr	Overall travel time ($t_{rc} + t_{rs}$)
T0	Temperature of the liquid in the flask
T1	Temperature in the flask half-way from liquid surface to condenser intake
T2	Temperature at the condenser intake
T	Temperature
P	Atmospheric Pressure
M	Molecular weight
R	Gas constant
ρ_l	Density of distillate
ρ_v	Density of vapor

%V	Uncorrected percent volume distilled
%V1	1st volume correction from receiver to condenser intake
%V2	2nd volume correction from condenser intake to vapor take off (boiling)
V_{lo}	initial vapor volume in the flask
V_l	Liquid volume in the distillation flask
F_{vo}	Inlet stream molar flow rate (Material is Hydrocarbon)
F	Outlet stream molar flow rate (both Air and Hydrocarbon)
N	Total moles of Air and Hydrocarbon vapor in the control volume
y_v	mole fraction of hydrocarbon vapor in the Control volume
y_A	Mole fraction of Air in the control volume
N_A	Moles of Air in the control volume
N_v	Moles of Hydrocarbon vapor in the control volume
$\dot{U}$	Total molar internal energy of the system
H_{Vo}	Total enthalpy of the input stream
H	Total enthalpy of the exit stream
$\dot{U}_v$	Molar internal energy of Hydrocarbon vapor in the control volume
$\dot{U}_A$	Molar internal energy of Air in the control volume
C_v	Molar concentration of hydrocarbon vapor
C_A	Molar concentration of Air
Pc	Critical Pressure
Tc	Critical Temperature
Tr	Reduced Temperature
Pr	Reduced Pressure
Psat	Saturation Pressure
ω	Acentric factor

Abstract

Distillation curve is an important indicator in industry and academia for characterizing fuels. The advanced distillation curve apparatus developed by Smith and Bruno[1] was used to carry out this research. The boiling temperature vs volume curve of a distillation curve can further be improved or corrected if the time delay of the distillate in the condenser and the vapor travel time from vaporization to condensation is known.

Experiment for a four component mixture of decane, dodecane, tetradecane and hexadecane was conducted and the experimental data used to develop an empirical model for the process as a pure pseudo-hydrocarbon compound. The recorded observed delay time and the calculated travel time were used to correct the temperature-volume profile.

Furthermore, the experiment was repeated to test the model. The model was then applied to a seven component mixture of octane, decane, dodecane, tetradecane, hexadecane, heptadecane and octadecane.

The empirical model developed predicts very closely the behavior of the batch distillation process.

CHAPTER 1

Introduction

The rapid growth of worldwide air travel has prompted concern about the fuel quality and consumption of aviation activities globally. The world energy consumption has doubled from 1970 to 2005, growing at 2% per year until 2002 and 4.5% per year from 2003 to 2005 when consumption reached 463 quadrillion British thermal units (463 quads). [2] With transportation sector consuming 68% of oil [2] it has become globally imperative to look into alternative fuel as far as sustainability is concern in the future. One area which plays an integral role in the search of fuels and its characterization is the distillation curve of the fuel.

The distillation (or boiling) curve of a complex fluid is a critically important indicator of the bulk behavior or response of the fluid. For this reason, the distillation curve, usually presented graphically as the boiling temperature against the volume fraction distilled, is often cited as a primary design and testing criterion for liquid fuels, lubricants, and other important industrial fluids. While the distillation curve gives a direct measure of fluid volatility fraction by fraction, the information the curve contains can be taken much further; there are numerous engineering and application-specific parameters that can be correlated to the distillation curve. [3]

Over the past few years the American society for Testing Materials (ASTM D-86) [4] method for distillation has been widely used by most institutions. A wide search by engineers and researchers since the introduction of the ASTM has been carried out to further improve the ASTM distillation procedure and the reliability of the measurements. The ASTM test method covers the atmospheric distillation of fuel products using a laboratory batch distillation unit to determine quantitatively the boiling range characteristics of various fuels.

There are significant disadvantages associated with the ASTM D-86 test. Large uncertainties can be expected when using this method where specifications for complex fluids are presented in tabular form for the 10, 20, 50, and 90 vol. % fractions. It is common to give such specifications in terms of temperature ranges spanning up to 25 °C. This very large variability encompasses more the uncertainty inherent in the measurement than the variability of the fluid. Further the results from the ASTM D-86 test have little theoretical significance and cannot be modeled thermodynamically due to shortcomings with the approach..[3]

As an improvement on the ASTM D-86, Bruno [3] developed the Advanced distillation curve apparatus. The ADC method presents several modifications to the measurement of distillation curves that provide. It gives (1) temperature and volume measurement(s) of low uncertainty and, most important, (2) a composition-explicit data channel in addition to the usual temperature-volume relationship. This latter modification is achieved with a new sampling approach that allows precise qualitative as well as quantitative analyses of each fraction.[3]

Though the ADC proposed by Smith and Bruno[1] gives better reliability of distillation curve measurements, the boiling temperature measurements and volume distilled are concurrently at the same experimental time. This approach fails to take into consideration the time delay that the vapor takes from the boiling temperature to the condensation temperature. This time delay if properly estimated helps to shift the boiling temperatures of the fluid as propose by Bruno. This research initially started by Laya [5] looks further into this time delay and how the boiling temperature curves of fuels can be improved.

CHAPTER 2

Literature Review

2.1 Batch Distillation

Batch distillation is where a liquid mixture is charged to a still-pot and heated to boiling. The vapor formed is continuously removed and condensed to produce a distillate. The compositions of the initial charge and distillate change with time and the still temperature increases and the amount of lower-boiling components in the still pot decreases as distillation proceeds.[6]

2.2 Advanced Distillation Curves (ADC)

The distillation (or boiling) curve of a complex fluid is a critically important indicator of the bulk behavior or response of the fluid. For this reason, the distillation curve, usually presented graphically as the boiling temperature against the volume fraction distilled, is often cited as a primary design and testing criterion for liquid fuels, lubricants, and other important industrial fluids.

While the distillation curve gives a direct measure of fluid volatility fraction by fraction, the information the curve contains can be taken much further; there are numerous engineering and application-specific parameters that can be correlated to the distillation curve.[3] One of the most important and informative properties that is measured for complex fluid mixtures is the distillation (or boiling) curve.[3, 7] Simply stated, the distillation curve is a graphical depiction of the boiling temperature of a fluid mixture plotted against the volume fraction distilled.

2.2.1 Applications of Distillation Curve Distillation curve can be used in environmental applications as a guide for blending virgin stock with reclaimed oil, guiding the formulation of

product that will be suitable in various applications. Moreover, the distillation curve can be related to mutagenicity and the composition of the pollutant suite. It is therefore desirable to enhance or extend the usual approach to distillation curve measurement to allow optimal information content.[3]

The information that can be inferred from the distillation curve extends well beyond the rough description in terms of fluid mixture volatility. It has been possible in recent years to relate the distillation curve to operational parameters of complex liquid fuels.[3, 8-11] These parameters include engine starting ability, vehicle drivability, fuel system icing and vapor lock, the fuel injection schedule, and fuel auto-ignition, etc. For example, it is possible to directly correlate the fuel system icing rate (a consequence of intake manifold rarefaction) with the distillation temperature of various fractions of gasoline [3, 12, 13]. The front end (low temperature region) of the distillation curve of gasoline (up to approximately 70 °C) is used to assess and optimize ease of starting and the potential for hot weather vapor lock in engines. The mid-range of the gasoline curve (up to a temperature of approximately 100 °C) is used to assess and optimize cold weather performance, the operational readiness of a hot engine, and the acceleration behavior of a hot engine under load. The top range of the distillation curve is used to assess and optimize fuel economy in a hot engine. In addition to these applications to performance optimization and design, the distillation curve provides an avenue to long-term trend analysis of fuel performance, since changes in the distillation curve are related to changes in fuel performance

2.3 ASTM measurements of Distillation Curve

The most common procedure for measurement of distillation curves is that of American Society for Testing Materials (ASTM) D-86[4] The distillation curve is simply a plot of boiling temperature (at ambient pressure) against volume fraction.

In the ASTM D-86 test, the data obtained are the initial boiling point *(IBT)*, the temperature at volume fractions of 10, 20, 30, 40, 50, 60, 70, 80, and 90%, and then the final boiling temperature (FBT). The *IBP*, is the corrected thermometer reading that is observed at the instant the first drop of condensate falls from the lower end of the condenser tube and the end point *(EP)* or final boiling point *(FBP)*, is the maximum corrected thermometer reading obtained during the test.[4]

The simplest apparatus for the measurement of distillation curves as set forth in ASTM D-86 embodies a Bunsen burner chamber for heating, a liquid bath with a condensate tube, and a graduated cylinder covered with blotting paper for a calibrated volume receiver.[4]

The temperature sensor is fitted through a snug-fitting device, to mechanically center the sensor in the neck of the flask. In the case of a thermometer, the bulb is centered in the neck and the lower end of the capillary is level with the highest point on the bottom of the inner wall of the vapor tube and the temperature of the saturated vapor is measured in the neck of the flask below the vapor tube as shown in figure 2.1 below.[4]

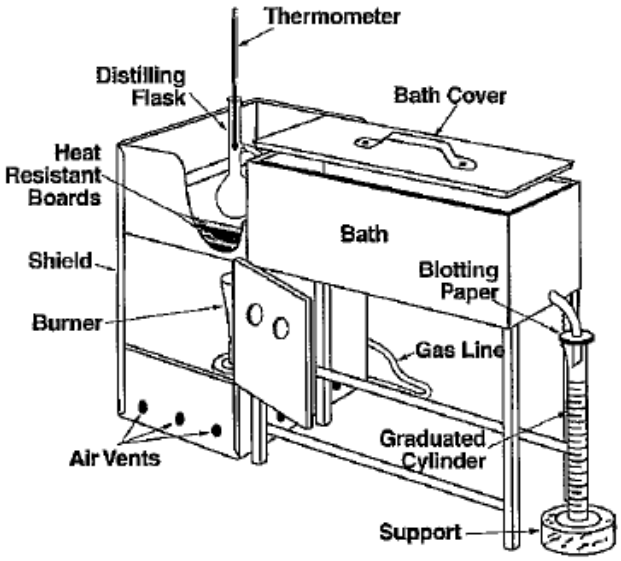

Figure 2.1 ASTM Batch distillation setup for obtaining distillation curves [4]

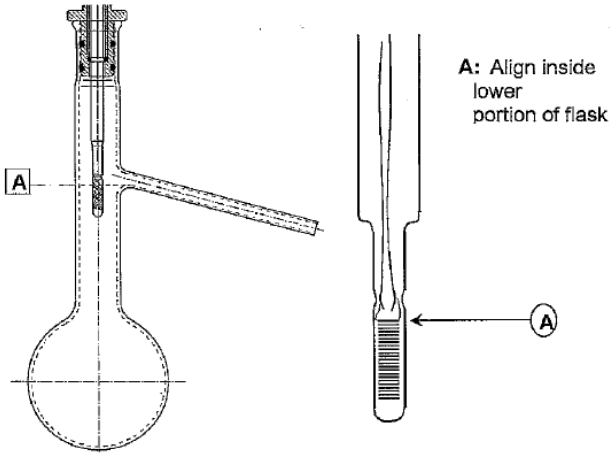

Figure 2.2 Placement of thermometer probe relative to Distillation Flask [4]

2.3.1 Disadvantages of ASTM distillation curve measurement. The fact that the ASTM D-86 test remains important to industry, and is the only test that appears to be standardized [4] makes it important to improve the method and get as much information as possible from it. There are significant disadvantages associated with the ASTM D-86 test, and

these have been well-documented. Large uncertainties can be expected when using the method. Often, specifications for complex fluids are presented in tabular form for the 10, 20, 50, and 90 vol. % fractions. It is common to give such specifications in terms of temperature ranges spanning up to 25 °C.[3] Note that this very large variability encompasses more the uncertainty inherent in the measurement than the variability of the fluid. The results from the ASTM D-86 test have little theoretical significance and cannot be modeled thermodynamically due to shortcomings with the approach. [3] This has led to calculation methods applied to the method to produce the true boiling point curve and the equilibrium flash vaporization curve.[3]

The ASTM test has clear hazards associated with an open flame, even if it is shrouded in a heating chamber, when applied to hydrocarbon fluids. The use of a graduated cylinder as a receiver is problematic because distillate tends to splash into the cylinder, making a precise volume measurement difficult if not impossible. Deflectors are sometimes used to ameliorate (but not eliminate) this difficulty. This basic approach is embodied in several commercial instruments that function under essentially manual control.[3]

2.4 Bruno's Advanced Distillation Curve Measurement

To improve on the reliability of the results from the distillation curve, Bruno [3] developed an apparatus for the measurement of distillation curves with a composition-explicit information channel as depicted schematically in figures 2.3, 2.4 and 2.5. The distillation flask is a 500 mL round-bottom flask that is placed in a two-part aluminum heating jacket (alloy 6061), the lower part of which is contoured to fit the flask. The upper part is placed around the flask after the flask has been inserted into the contoured (lower) part of the jacket. This two-part enclosure effectively surrounds approximately four-fifths of the spherical section of the flask. [3] Above the distillation flask, a centering adapter provides access for two thermally tempered J-

type thermocouples that enter the distillation head. One thermocouple (T2) is centered at the low point of distillate takeoff (the typical distillation head placement, as recommended graphically in ASTM-86), and the other (T1) enters the distillation flask and is submerged in the fluid, to monitor the temperature of the bulk fluid.

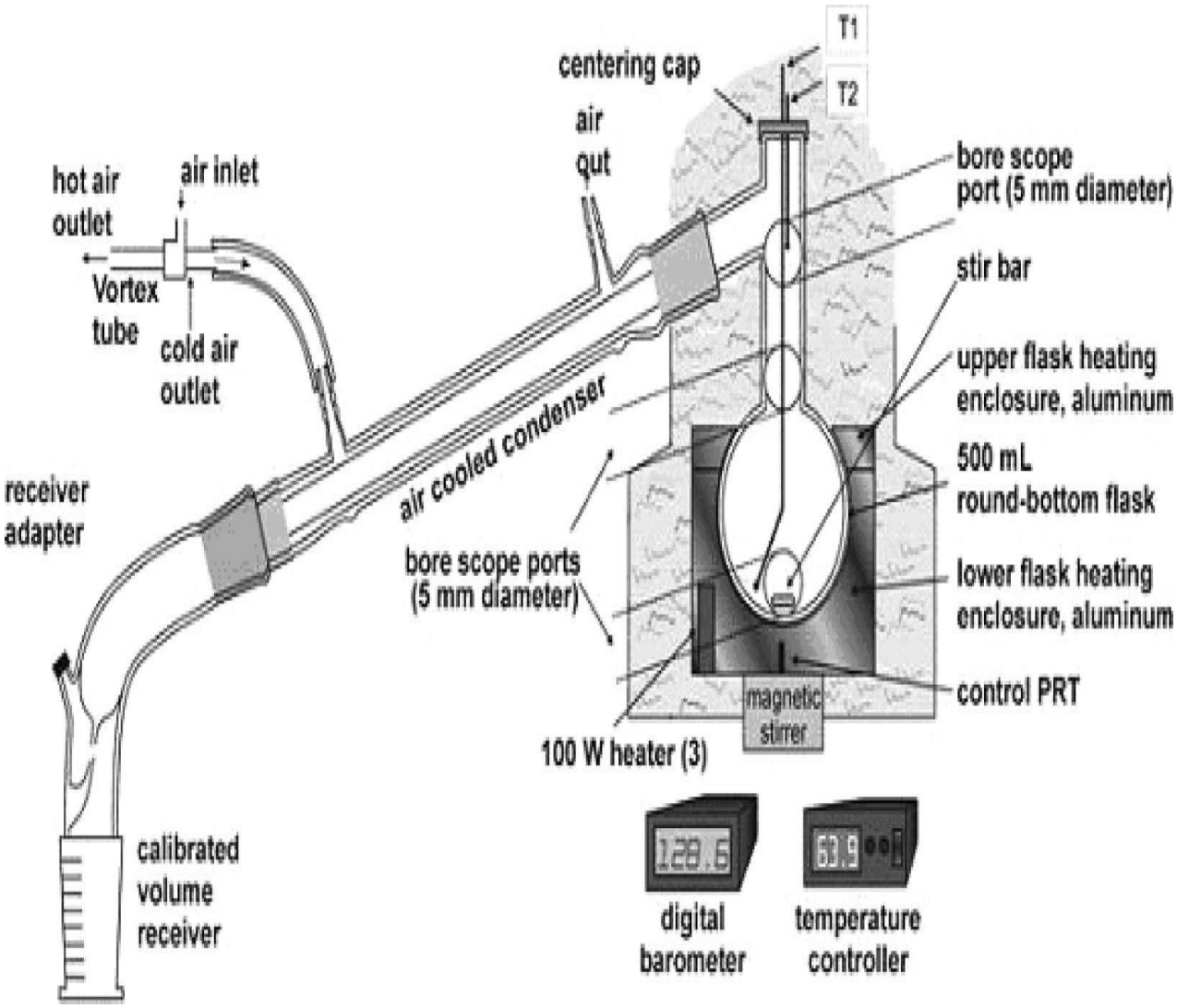

Figure 2.3 Overall apparatus used for the measurement of distillation curves[14]

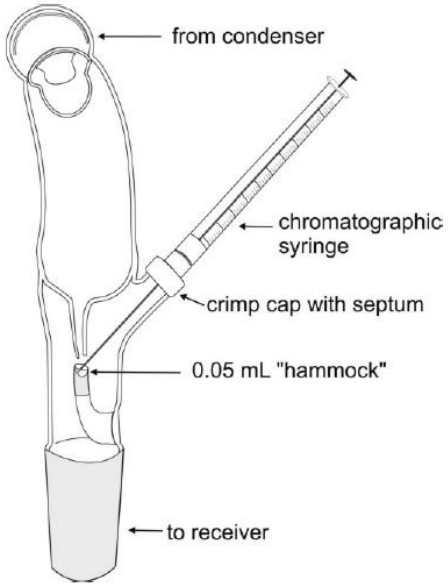

Figure 2.4 Schematic diagram of the receiver adapter. [3]

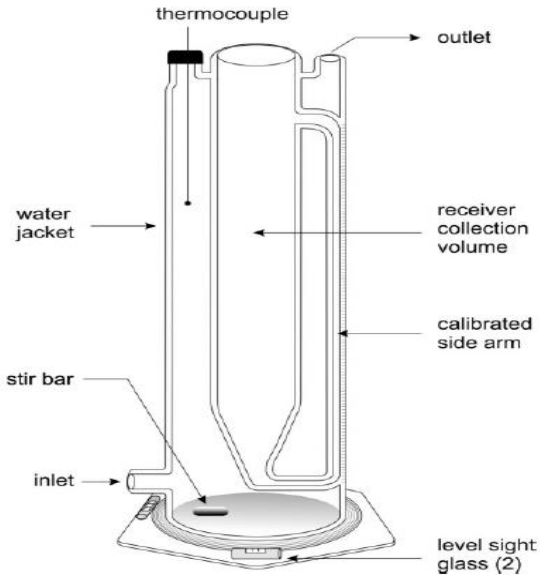

Figure 2.5 Schematic diagram of the level-stabilized receiver developed for this work. [3]

To improve the precision of the volume measurement, the calibrated receiver that is shown in figure 2.5 was developed. Constructed of glass, this receiver consists of a central volume that gradually decreases in diameter at the base and connects to a small-diameter sidearm sight glass that is calibrated. The sidearm stabilizes the fluid level for a precise volume

measurement as the distillation proceeds. The large inner volume and the sight glass are enclosed in a water jacket that contains a thermometer and a magnetic stir bar for circulation. The tube of the sight glass is actually glass-welded to the inside wall of the water jacket, to eliminate parallax in reading the volume. The water jacket allows the receiver to be maintained at a suitable temperature, and the stirrer ensures acceptable temperature.[3]

The more common approach is to measure the temperature in the distillation head, represented as TC2 but the common difficulty with this temperature measurement location is that even slight variations in mass-flow rate through the head will cause aberrations in T2. Such aberrations are sometimes called hesitation. This measurement is very dependent on the heating rate throughout the measurement, thus a change in mass-flow rate through the head results changing fluid composition. However the behavior of the T1 curve is unaffected by heating rate but it is controlled only by the fluid behavior. Clearly, the TC1 curve does not represent the actual fluid behavior, and it is unreliable and not repeatable.[1, 3]

As earlier said the specific location of the thermocouple in the liquid in the boiling flask or kettle, T1, allows the process to be modeled, because it represents a thermodynamic state point, and is easily reproducible and preferable to the head temperature, which is very sensitive to placement in the apparatus as well as the heating rate.[14]

Thomas Bruno's correction was to use TC2 in place of TC1 as in ASTM method for the temperature vs. percent volume distilled or recovery curve.

2.5 Volume Correction of Distillation Curves

Until recently not much effort had been made in correction of the distillate volume. M. L. Huber et *al* [14] used computational approach to model the distillation curve of a surrogate mixture with the help of an equation of state. They assumed the pressure was constant, and a

bubble-point calculation was made to determine the bubble-point temperature and the compositions of the resulting equilibrium vapor phase. The entire distillation procedure for a volume of 200 mL was divided into a fixed number of volume increments, with a constant volume of fluid removed from the still at each volume step. [14]

However the volume recovery from the model was far more done the experimental results and the volume was shifted by adjusting the value of the shift until agreement between the calculated and the observed distillation curves was achieved. The calculated results capture much of the experimental behavior but do not agree with the experimental data exactly. [14]

To further improve on the volume correction, Laya [5] considered the hold-up volume by assuming that the time taken for distillate drop that appears at the condenser intake travels through the condenser until it falls into the receiver is constant. The times the first vapor appears in the condenser (t_0) as well as the receiver (t_1) was recorded and the difference was calculated as the delay time or hold-up time (t_{hup}). From a numerical fitting of the distillate percent volume recovery ($\%V_r$) as a function of time, the $\%V_r$ was shifted by adding the delay time (t_{hup}) to the experimentally observed times (t_1) and the calculated shifted time ($t_1 + t_{hup}$) were used to calculate the $\%V_r$. The assumption here was that the distillate started appearing at a time t_0 but not time (t_1).[5] The apparatus used by Laya[5] was one built by Bruno[3].

In this present research, the goal was to further correct the distillation curve with the work done by Laya as a starting reference. While Laya[5] corrected the curve by shifting volume distilled from the receiver to the condenser intake, this research further looked at shifting the volume to the time the vapor starts rising. As a result of the limited tools and sophisticated equipment, it was difficult to observe when the first vapor started to rise and as such the basic

assumption used was that the first vapor appears when the liquid was observed to have started boiling. Further details on the procedure can be seen at chapter 3, subsection 3.4 and 3.7.

2.6 Sydney Young's Temperature Correction

The boiling temperatures of distillation curve are measured during the course of a distillation curve determination are dependent upon the local atmospheric pressure. Since the atmospheric pressure not only varies diurnally, but also with elevation, this is an important consideration [15] . The usual technique that is applied to correct the observed temperature for variations in the atmospheric pressure is the application of the Sydney Young (SY) equation as cited in [15]. This equation was developed during the course of Young's work on distillation separations and (vapor + liquid) equilibrium measurements.[16, 17]

Young advocated the measurement of atmospheric pressure multiple times during long distillations, or when performing distillations in unsettled weather, since the effect of the pressure variations on the observed temperatures is so significant.

A simplified SY equation is specified in the ASTM standard[4] as in equation (2.1).

$$C_c = C\,(101.30 - P_a)\,(273.15 + T_c) \qquad (2.1)$$

Where $C_{c\ is}$ the correction added to the observed temperature in degree centigrade, C = 0.0009 is a constant, and P_a is the atmospheric pressure in kPa, and T_c is the measured temperature in °C.

2.7 Distillation Curves of Aviation Fuel JP-8 and a Coal-Based Jet Fuel

The major gas turbine fuel that is currently the most commonly used by the United States military is JP-8 (MILDTL-83133), a kerosene fraction that has a higher flash point than the main military predecessor, JP-4 and for this reason, the physical and chemical properties of JP-8 are receiving renewed interest. [18]

Beverly and Bruno [18] applied distillation curve measurements to develop a comparison between JP-8 and CDF fluid is a mixture of coal-derived liquid (a derivative of bituminous coal tar) and light cycle oil, a byproduct of catalytic cracking units in petroleum refining. The composition of the sample of CDF is significantly different from that of JP-8, as one would expect from the very different feedstock.

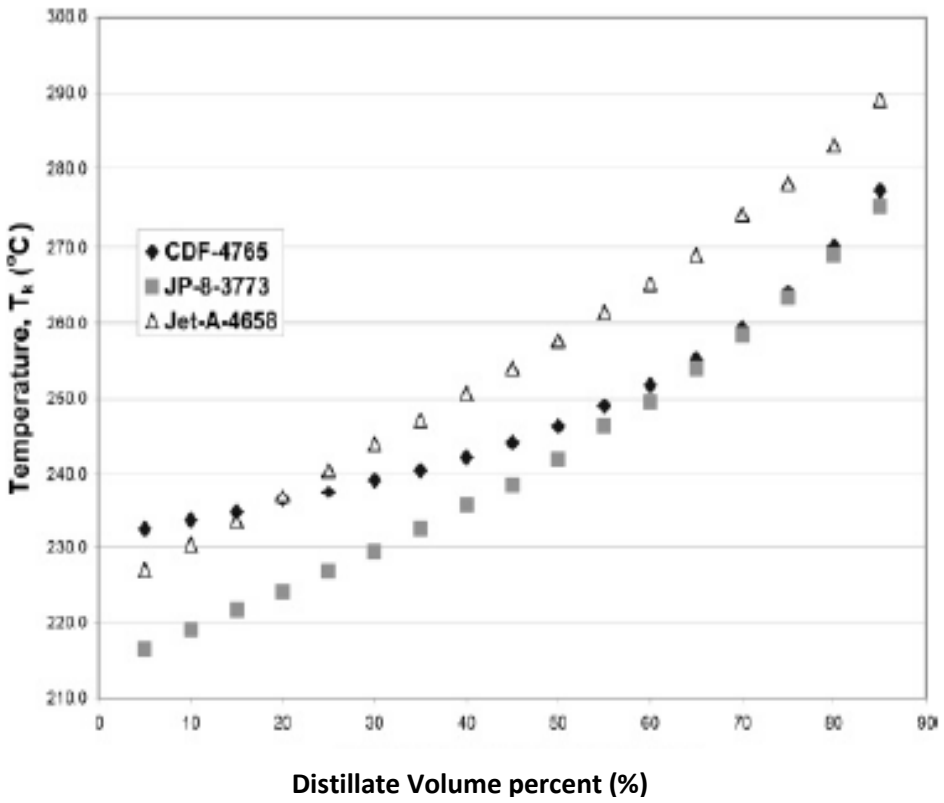

Figure 2.6 Distillation curves for JP-8, Jet A and Coal Derived Fuel [18]

The figure 2.6 above shows that JP-8 is the most volatile of the three fluids examined. The composite Jet-A sample is a relatively low-volatility fluid. The CDF shows an initial behavior that is less volatile than either the JP-8 or the composite Jet-A. As the distillation curves show, however, by the 60% volume fraction, the curve of CDF closely approaches the curve of JP-8. It might be tempting to conclude from this observation that the heavier fractions of CDF

are indeed similar in chemical composition to JP-8. Beverly and Bruno [18] later showed that the composition-explicit data channel of the advanced distillation curve shows a very different character, consistent with the different feedstock. Another interesting observation concerns the shape of the curve for CDF, the slope of which is far less pronounced than those of the JP-8 or Jet-A samples. A curve that flattens in this way is similar in behavior to that of either a pure fluid or an azeotrope. If the fluid were showing azeotropic characteristics, one would observe the azeotropic convergence of T0 and T2, and this is not seen. Another explanation of this behavior is that the distillation curve is being dominated to some extent by the presence of a constituent that is present in a large concentration, whereas the distribution of components of JP-8 and Jet-A is more disperse in terms of individual boiling temperatures. [18]

CHAPTER 3

Calibrations and Experimental Section

3.1 Calibration of Level-Equalizing Receiver (LER)

The level-equalizing receiver, LER, is the part of the experimental equipment which serves as a holding ‘vessel’ for collecting the condensed vapor from the condenser. The LER is constructed of glass, with two same diameter side tube (one calibrated) volumes that decreases in volume at the base, and connects to each other. The calibrated side stabilizes the fluid level for a precise volume measurement during the distillation process. Both tubes are enclosed in a water jacket with running water that ensures almost stable distillate temperature.

The tube of the sight glass is glass welded to the inside wall of the water jacket, to eliminate parallax in reading the volume.[1] The LER was calibrated from 0 to 17 with each division subdivided into 10 subdivisions on one side of the jacked tube. The distance between two points in the subdivisions is 1mm. To calibrate the LER volume for measurements, a burette was used to discharge distilled water at 5ml interval until it 200ml was discharged and the corresponding reading on the LER recorded for every 5ml that was discharged. The choice of 200ml was as a result of a batch size of 200ml to be used for the distillation process.

The recorded distilled water volume (ml) discharged and the corresponding reading on the LER was plotted and a correlation was generated from the plot which gave the volume (ml) of LER as a function of the LER reading on the side glass tube.

3.1.1 Fitted equation for calibrated receiver. From the experimental data of discharged distilled water volume and the LER readings the following expression was generated from the fitted data.

$$V_R = 18.83 - 7.3189x \qquad 1 \leq x \leq 17 \qquad (3.1)$$

Where V_R = Volume of receiver (ml)

x = Reading on the receiver

3.1.2 Experimental data for receiver calibration. Table 3.1 and figure 3.1 provide information regarding data used to generate equation (3.1).

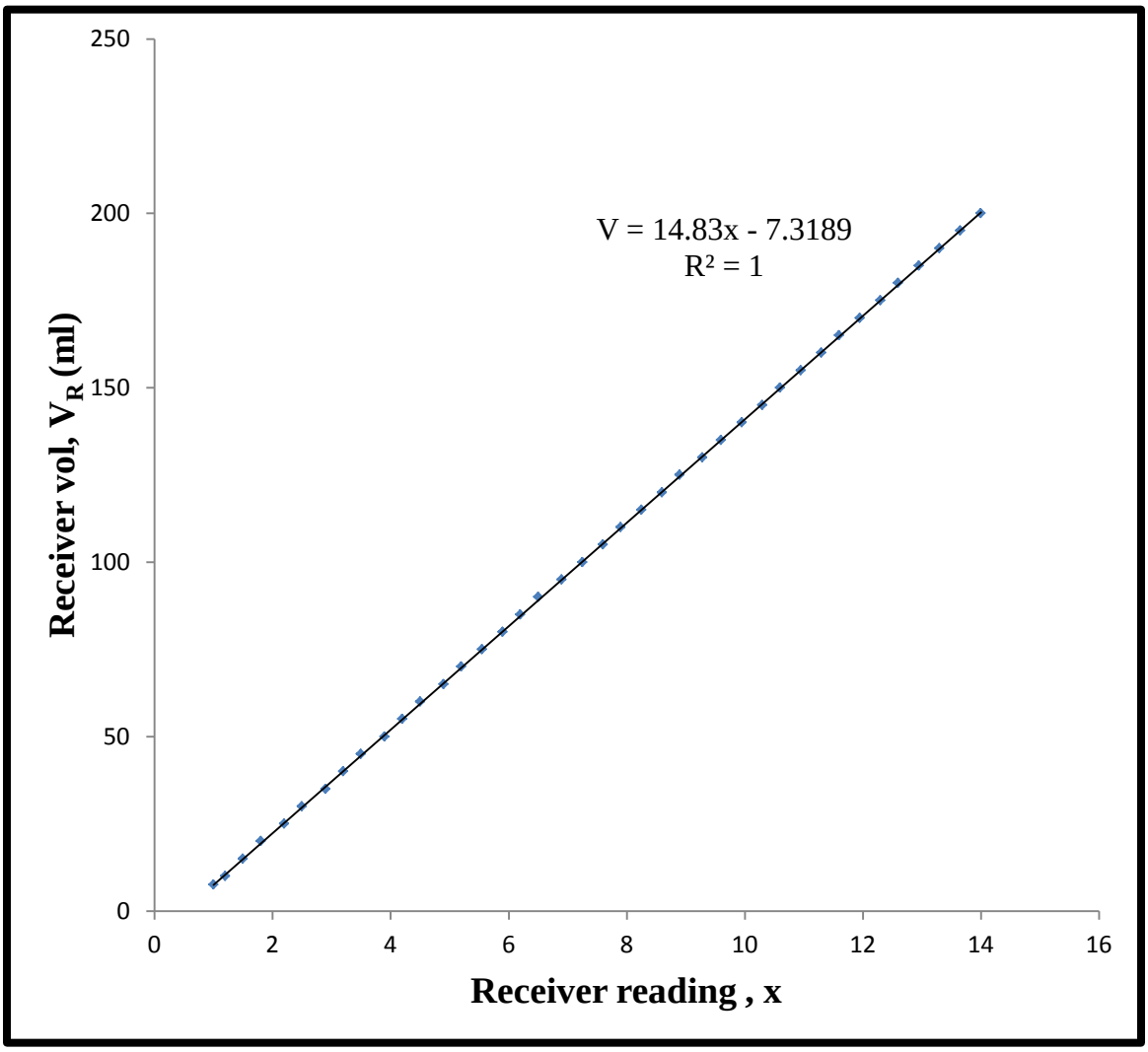

Figure 3.1 Plot of distilled water discharged vs. receiver reading

Table 3.1

Data used for calibration

Measurement	Receiver Reading (x)	Distilled Water (ml)	Cumulative Vol. (ml)
1	1	7.6	7.6
2	1.2	2.4	10
3	1.5	5	15
4	1.8	5	20
5	2.2	5	25
6	2.5	5	30
7	2.9	5	35
8	3.2	5	40
9	3.5	5	45
10	3.9	5	50
11	4.2	5	55
12	4.5	5	60
13	4.9	5	65
14	5.2	5	70
15	5.55	5	75
16	5.9	5	80
17	6.2	5	85
18	6.5	5	90
19	6.9	5	95
20	7.25	5	100
21	7.6	5	105
22	7.9	5	110
23	8.25	5	115
24	8.6	5	120
25	8.9	5	125
26	9.28	5	130
27	9.6	5	135
28	9.95	5	140
29	10.3	5	145
30	10.6	5	150
31	10.95	5	155
32	11.3	5	160
33	11.6	5	165
34	11.95	5	170
35	12.3	5	175
36	12.6	5	180
37	12.95	5	185
38	13.3	5	190
39	13.65	5	195
40	14	5	200

3.2 Calibration of Thermocouple

The K-type thermocouples were used in all experiments. Thermocouples were used in their original factory calibrated state and hence no further calibration was done. However all the readings of the three thermocouples used were compared to each other to double check their reliability and consistency.

Thermocouple 1 (T0), thermocouple 2 (T1) and thermocouple 3 (T2) were placed in distilled water at room temperature and also in boiling distilled water and table 3.2 and table 3.3 shows the comparison data of the average readings observed for three different cases.

Table 3.2

Thermocouple Calibration at room temperature (Room Temperature = 20.1^{o}C)

	T0	**T1**	**T2**
Case1	20.1	19.9	20.0
Case 2	19.9	19.7	19.9
Case 3	20.5	20.4	20.6
Average	**20.1**	**20.0**	**20.1**

Table 3.3

Thermocouple Calibration in boiling distilled water. (Room Pressure = 98.9 kPa)

	T0	**T1**	**T2**
Case1	99.7	99.7	99.8
Case 2	99.8	99.8	99.8
Case 3	99.9	99.8	99.8
Average	**99.8**	**99.76**	**99.8**

Since T0, T1 and T2 readings are fairly close it was assumed that the factory calibration is enough for direct reading from the experiment.

3.3 Experimental Section

The apparatus that has been developed for the measurement of distillation curves with a composition-explicit information channel is depicted pictorially in Figure 3.2, with additional detail labeling provided in Figures 3.3. The receiver used works on the same principle as that used by Thomas Bruno, but differ slightly in design as shown in figure 3.4. The distillation flask is a 500 mL round-bottom flask that is placed in a two-part aluminum heating jacket, the lower part of which is contoured to fit the flask. The upper part is placed around the flask after the flask has been inserted into the contoured (lower) part of the jacket. This two-part enclosure effectively surrounds approximately four-fifths of the spherical section of the flask. [3]

Figure 3.2 Pictorial view of un-insulated apparatus for measurement of distillation curves

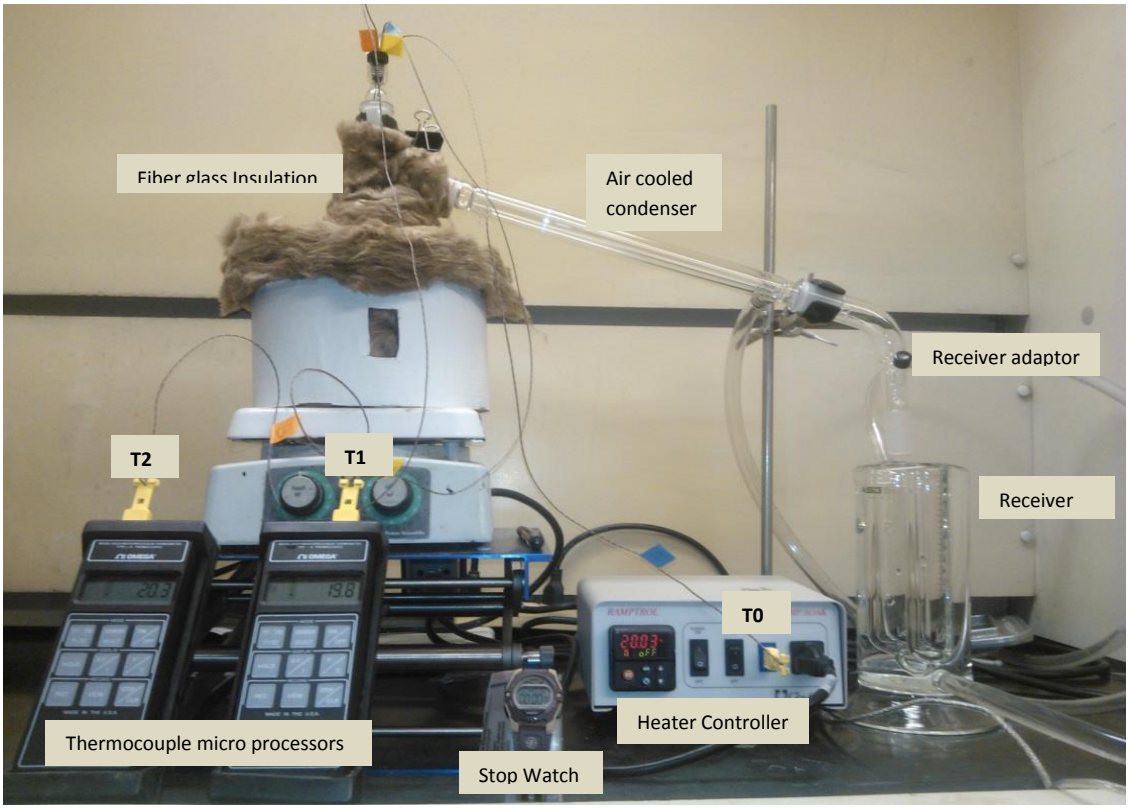

Figure 3.3 Pictorial view of insulated apparatus for measurement of distillation curves

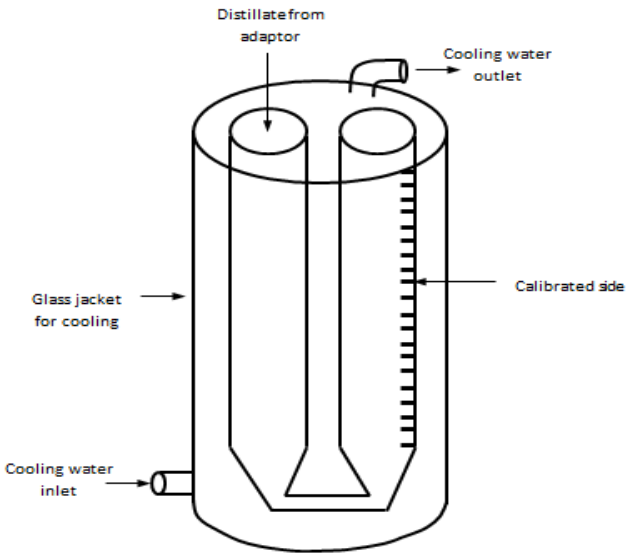

Figure 3.4 Schematic diagram of the level-stabilized receiver developed for this work.

A Ramptrol heater is placed in the lower, contoured part of the jacket, to provide uniform heating axially about the radius of the enclosure. The heater which can be controlled with a proportional integral derivative was run the manual control mode since the flask liquid temperature is independent on the heat rate and the upper thermocouple (T2) placed in the flask as recommended graphically in ASTM-86), and the other (T0) enters the distillation flask and is submerged in the fluid, to monitor the temperature of the bulk fluid. A third Thermocouple (T1) was introduced in the middle (half-way from the initial liquid height to thermocouple T2) to monitor any back-mixing in the distillation flask vapor region.

At the bottom of the distillation flask is a glass magnetic stirrer bar (7/8 x ¼ inches) which stirs the contents of the distillation flask to maintaining horizontal temperature uniformity in the fluid with the aid of a magnetic stirrer plate placed beneath the jacketed distillation flask. The stirring is controlled to avoid vortex forming on the surface of the liquid and also to avoid lift-out of thermocouple T1 from the fluid.

3.4 Comparison of Experimental Data with Previous Work and Literature

In order to ascertain the accuracy of the experimental readings, an experiment was run with a equimolar mixture of decane and tetradecane and the distillation curve was compared to that of literature [1] and that generated by Laya[5] in his thesis. The thesis of Laya was used as a reference in this research to further improve the distillation boiling curves measurement. The same apparatus used by Laya and designed by Bruno was used in this research. Table 3.4 shows the results of the recorded experimental data. The percent volume distilled comparison for the experimental data has been plotted for the thermocouple (T0) embedded in the liquid as in figure 3.5. Data for (1)Smith and Bruno and (2) Laya were from references [1] and [5] respectively.

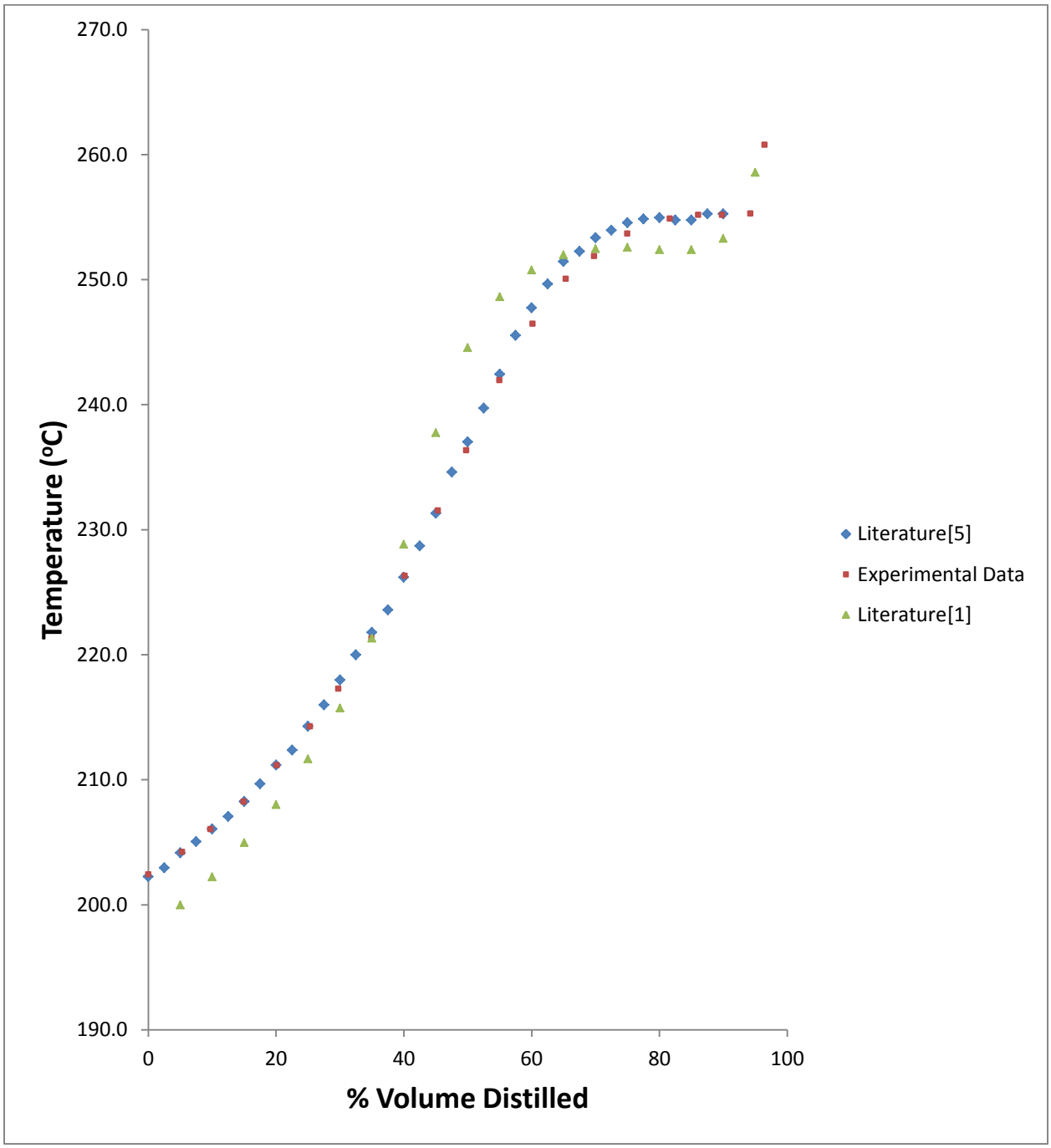

Figure 3.5 Comparison of measured distillation curved for equimolar mixture of decane and tetradecane with literature data

Table 3.4

Experimental data for Equimolar mixture of decane and dodecane

					Head Temp	mid-way Temp	Liquid Temp	T0 Temp correction	Corrected T0	Receiver Reading	Receiver vol, ml	% Vol Distilled
Time	Duration, min	Step time (min)	Distillate Cum. Time	Receiver Cum. Time	T0	T1	T0	c	T0 + c	x	V_f	$V_{\%}$
0:00:00	0	0			20.0	19.9	20.5	0.83	21.33			
0:15:00	15.0	15.0			19.9	22.2	48.01	0.91	48.92			
0:30:00	30.0	15.0			21.5	35.2	96.1	1.05	97.15			
0:45:00	45.0	15.0			23.6	55.3	143.3	1.18	144.48			
0:55:00	55.0	10.0			26.5	73.4	172.6	1.26	173.86			
0:55:30	55.5	0.5			26.7	74.2	173.8	1.27	175.07			
0:58:33	58.6	3.1			30.5	80.7	182.8	1.29	184.09			
1:00:49	60.8	2.3			32.0	85.6	188.8	1.31	190.11			
1:03:04	63.1	2.3			35.1	91.8	194.5	1.33	195.83			
1:07:12	67.2	4.1	0.0		143.9	163.7	200.2	1.34	201.54			
1:07:30	67.5	0.3	0.3		167.8	178.9	200.7	1.34	202.04			
1:07:47	67.8	0.3	0.6	0.0	186.6	181.8	201.1	1.34	202.44	0	0.000	0.00
1:10:17	70.2	2.4	3.0	2.4	192.2	187.2	202.9	1.35	204.25	1.2	10.477	5.24
1:11:42	71.7	1.5	4.5	3.9	194.0	190.4	204.7	1.35	206.05	1.8	19.375	9.69
1:13:30	73.5	1.8	6.3	5.7	191.0	193.2	206.9	1.36	208.26	2.5	29.756	14.88
1:15:17	75.3	1.8	8.1	7.5	194.0	196.0	209.8	1.37	211.17	3.2	40.137	20.07
1:17:06	77.1	1.8	9.9	9.3	196.6	199.3	212.9	1.38	214.28	3.9	50.518	25.26
1:18:40	78.7	1.6	11.5	10.9	199.3	203.2	215.9	1.39	217.29	4.5	59.416	29.71
1:20:36	80.6	1.9	13.4	12.8	201.0	207.2	219.9	1.41	221.31	5.2	69.797	34.90
1:22:58	83.0	2.4	15.8	15.2	206.7	212.3	224.9	1.43	226.33	5.9	80.178	40.09
1:25:08	85.1	2.2	17.9	17.4	212.2	219.3	230.1	1.44	231.54	6.6	90.559	45.28
1:27:18	87.3	2.2	20.1	19.5	217.6	224.7	234.9	1.46	236.36	7.2	99.457	49.73
1:29:47	89.8	2.5	22.6	22.0	228.1	232.1	240.5	1.47	241.97	7.9	109.838	54.92
1:32:17	92.3	2.5	25.1	24.5	237.6	239.8	245	1.48	246.48	8.6	120.219	60.11
1:34:22	94.4	2.1	27.2	26.6	243.3	244.9	248.6	1.48	250.08	9.3	130.600	65.30
1:36:00	96.0	1.6	28.8	28.2	248.2	247.9	250.4	1.49	251.89	9.9	139.498	69.75
1:37:40	97.7	1.7	30.5	29.9	251.6	249.7	252.2	1.49	253.69	10.6	149.879	74.94
1:39:39	99.7	2.0	32.5	31.9	252.4	251.0	253.4	1.49	254.89	11.5	163.226	81.61
1:40:57	101.0	1.3	33.8	33.2	252.9	251.4	253.7	1.49	255.19	12.1	172.124	86.06
1:42:28	102.5	1.5	35.3	34.7	253.0	251.7	253.7	1.49	255.19	12.6	179.539	89.77
1:43:25	103.4	1.0	36.2	35.6	251.5	252.0	253.8	1.49	255.29	13.2	188.437	94.22
1:44:27	104.45	1.0	37.3	36.7	202.5	252.3	259.3	1.51	260.81	13.5	192.886	96.44

3.5 Homogeneity of Liquid Temperature in the Flask

To determine the effect of the mixing by the magnetic bar stirrer, an experiment was conducted with equimolar mixture of decane and tetradecane. The batch volume for this experiment was 180ml was used due to some loss as a result of natural evaporation of the recovered distillate which had been in the fume hood for about 5 days. Here the batch volume (20 ml less than the norm) was not an issue because the interest was just to study the temperature homogeneity in the liquid mixture. Table 3.5 below and figures 3.6 and 3.76 gives the results obtained. The suden increase in the liquid bottom and middle temperature as well as the decrease in the head temperature signifies the end of the distillation as the flask is then exposed directly to the heater.

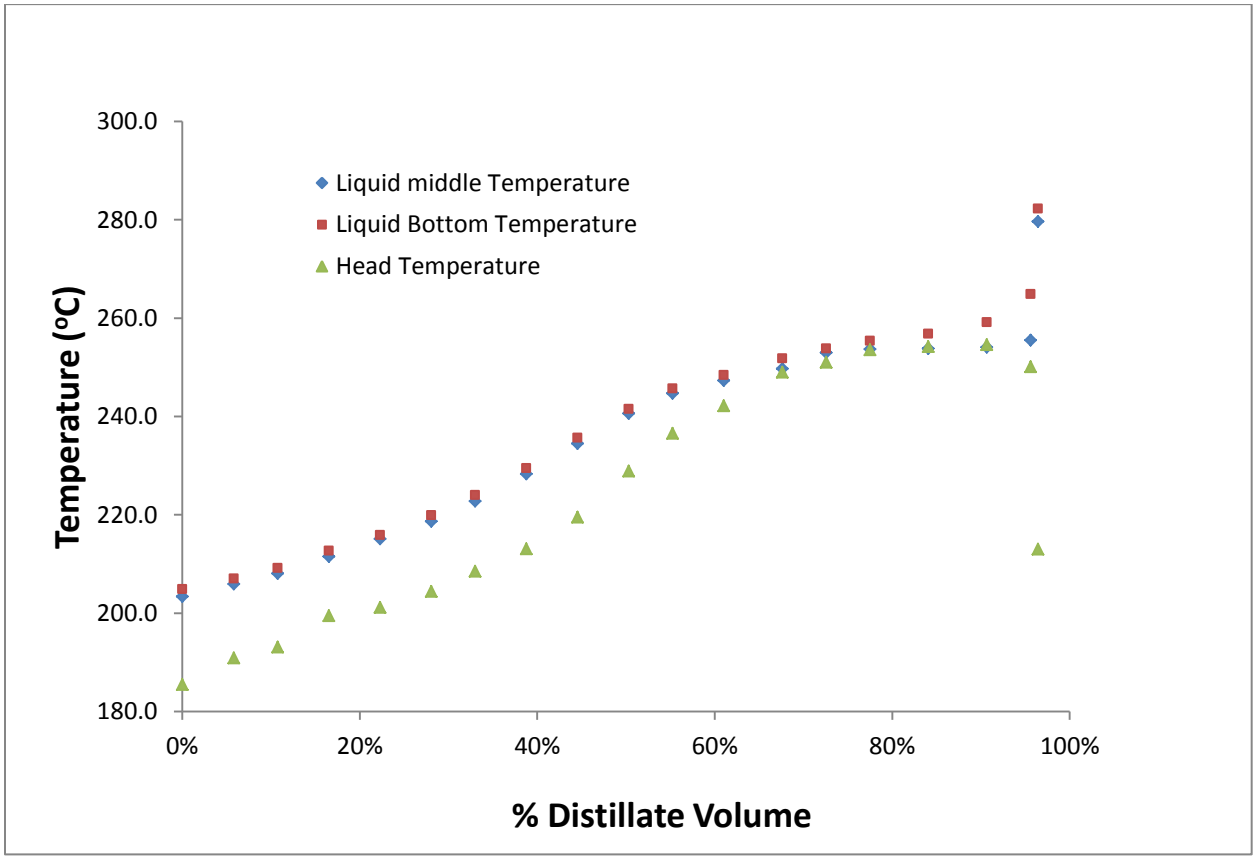

Figure 3.6 Liquid Temperature Homogeneity profile

Table 3.5

Results for liquid homogeneity with 50/50 mole % Decane and Dodecane spent solvent

					Head Temp	Liq mid Temp	Bottom Temp	T0 Temp correction	Corrected T0	Receiver Reading	Receiver vol, ml	% Vol Distilled
Time	**Duration, min**	**Step time (min)**	**Distillate Cum. Time**	**Receiver Cum. Time**	**T2**	**T1**	**T0**		**T0**	**x**	**V_f**	**$V_{\%}$**
0:00:00	0	0			21.4	20.8	21.7	0.70	22.40			
0:15:00	15.0	15.0			21.2	51.0	52.47	0.78	53.25			
0:30:00	30.0	15.0			22.4	100.1	102	0.89	102.89			
0:45:00	45.0	15.0			25.0	148.4	150.4	1.01	151.41			
0:55:00	55.0	10.0			27.4	175.9	177.9	1.08	178.98			
0:57:17	57.3	2.3			28.2	182.2	183.7	1.09	184.79			
1:00:05	60.1	2.8			29.0	188.8	190.5	1.11	191.61			
1:03:17	63.3	3.2			102.9	196.5	197.3	1.14	205.74			
1:07:15	67.3	4.0	0.0		145.8	203.2	204.6	1.14	205.84			
1:07:32	67.5	0.3	0.3		168.3	203.2	204.7	1.14	206.04			
1:07:55	67.9	0.4	0.7	0.0	185.5	203.4	204.9	1.14	208.14	0	0.000	0.00%
1:10:18	70.3	2.4	3.1	2.4	190.9	205.9	207	1.15	210.35	1.2	10.477	5.82%
1:11:15	71.3	1.0	4.0	3.3	193.1	208.1	209.2	1.15	210.35	1.8	19.375	10.76%
1:14:00	74.0	2.8	6.8	6.1	199.5	211.5	212.7	1.16	213.86	2.5	29.756	16.53%
1:15:47	75.8	1.8	8.5	7.9	201.2	215.1	215.9	1.17	217.07	3.2	40.137	22.30%
1:17:50	77.8	2.1	10.6	9.9	204.4	218.7	219.9	1.18	221.08	3.9	50.518	28.07%
1:19:48	79.8	2.0	12.6	11.9	208.5	222.8	224	1.19	225.19	4.5	59.416	33.01%
1:22:24	82.4	2.6	15.2	14.5	213.1	228.3	229.5	1.21	230.71	5.2	69.797	38.78%
1:25:08	85.1	2.7	17.9	17.2	219.5	234.5	235.7	1.23	236.93	5.9	80.178	44.54%
1:28:03	88.1	2.9	20.8	20.1	228.9	240.6	241.5	1.24	242.74	6.6	90.559	50.31%
1:30:23	90.4	2.3	23.1	22.5	236.6	244.7	245.7	1.24	246.94	7.2	99.457	55.25%
1:32:10	92.2	1.8	24.9	24.3	242.2	247.3	248.4	1.25	249.65	7.9	109.838	61.02%
1:35:17	95.3	3.1	28.0	27.4	249.0	249.7	251.8	1.26	253.06	8.7	121.702	67.61%
1:37:06	97.6	2.3	30.4	29.7	251.0	253.0	253.8	1.26	255.06	9.3	130.600	72.56%
1:38:19	98.3	0.7	31.1	30.4	253.6	253.7	255.4	1.27	256.67	9.9	139.498	77.50%
1:38:55	98.9	0.6	31.7	31.0	254.2	253.8	256.8	1.28	260.48	10.7	151.362	84.09%
1:41:20	101.3	2.4	34.1	33.4	254.6	254.1	259.2	1.32	266.22	11.5	163.226	90.68%
1:42:30	102.5	1.2	35.3	34.6	250.1	255.5	264.9	0.65	282.95	12.1	172.124	95.62%
1:43:38	103.6	1.1	36.4	35.7	213.0	279.7	282.3	0.65	282.95	12.2	173.607	96.45%

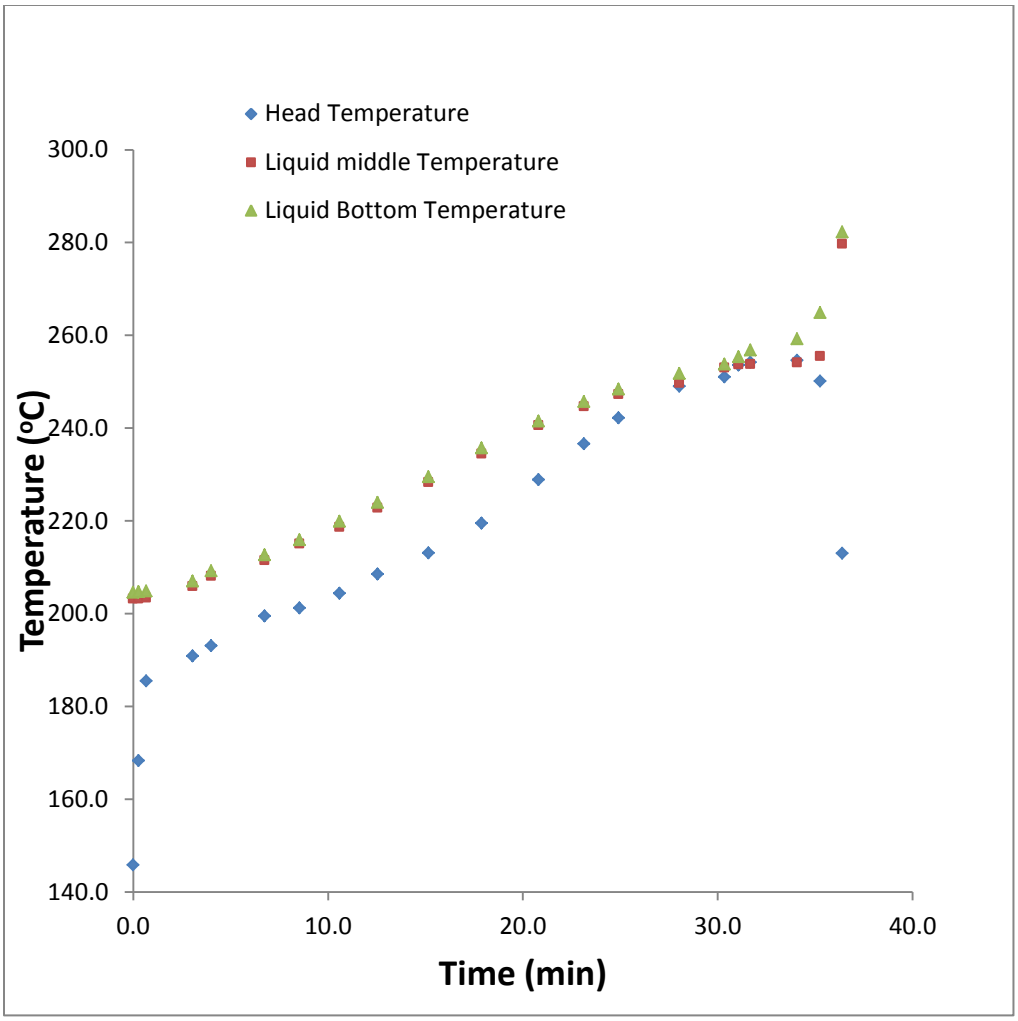

Figure 3.7 Liquid Temperature Homogeneity profile of equimolar mixture of decane and tetradecane

3.6 Correction to the Distillation Curve

Distillation curves are nothing new in today's 21st century. However the distillation curve has always been a representation of the boiling temperature measured directly inside the fluid and the percent distillate recovered measure from a calibrated receiver or tank.

The short-fall here is that the temperature (boiling point) is taking simultaneously with the % volume distilled. For example, if for a mixture of solvents, the first drop of the distillate is taken at a reference time zero and the corresponding boiling temperature, T0 = 150°C is also

measured at the same time zero reference, you will agree with me that the actual boiling temperature occurred at a time earlier than $150^{o}C$. This is because the vapors of the boiling mixture will take some time to rise up through the flask and then condense through the condenser before dropping into the collecting receiver.

This helps us to generate the distillation curve of the boiling temperature as a function of time and then deducing from that how long ('travel time') it took the vapors to rise through the flask and through the condenser.

Knowing the 'travel time' will help us estimate the actual boiling temperatures for every % volume distilled and as a result correct the distillation curve. This will be further discussed in the experiment used for the correction.

3.7 Experiment Used for Correction of the Distillation Curve

A mixture of equal volume of 50*ml* each of four components straight chain alkanes (decane, dodecane, tetradecane and hexadecane) were measured with a burette into the round bottom distillation flask. The chemicals were all purchased from Sigma Aldrich with purity $\geq 99\%$.

The magnetic stirring bar was then placed in the flask and the flask placed in the ramptrol heating pot. The condenser, receiver adaptor, thermocouples and the receiver were all connected as required. Care was taken to ensure that all connectors were firmly in place to avoid vapor leak during heating when the vapors starts rising. The fiber glass insulation was then put in place as in figure 3.3b to avoid heat loss. The ramptrol heater was then turned on to start heating and the magnetic stirring bar also started. The magnetic bar was regulated to prevent vigorous mixing of the fluid in order to avoid the vortex effect at the surface. The heater was run in the

manual mode at 100% heat power. Whiles the heating was ongoing, the distillation flask was intermittently viewed through the inspection hole and the initial boiling temperature and time were recorded for T0, T1 and T2. Similarly the temperature and time at which the first distillate appeared at the condenser intake were recorded for T0, T1 and T2. The same recordings were done when the first drop of distillate fell in the receiver. The rest of the recordings were done at some intervals for the receiver. At every receiver reading the corresponding time, T0, T1 and T2 were recorded. The experimental process was then modeled with both plug flow and completely mixed approach and then compared the vapor travel time in the flask to the experimental data. The physical properties of the hydrocarbon used can be found in Table 3.6 and table 3.7 gives details of all experimental data recorded and used in the modeling process and

Table 3.6

Physical properties of straight chain alkanes (C_{10} to C_{16}) [19]

	Density @ 20^{o}C	Molecular Wt	Boiling Pt (^{o}C) @1atm	Moles used
n-decane	0.730	142.29	174.10	0.2565
n-dodecane	0.749	170.41	216.28	0.2198
n-tetradecane	0.763	198.40	253.50	0.1923
n-hexadecane	0.773	226.45	286.80	0.1707

Table 3.7

Experimental data for distillation curve measurement for a mixture of equal volume of decane, dodecane, tetradecane and hexadecane at Room Pressure of 98.1kPa

Time (min)			Recorded Temperature			Corrected Temperature			Rec. reading	Receiver Vol (ml)	% V
t	t_b	t_{con}	T2	T1	T0	T2c	T1c	T0c	X	V	
0.00			20.3	20.00	20.06	21.14	20.84	20.90			
5.00			20.6	21.00	24.78	21.45	21.85	25.64			
10.00			20.6	25.20	36.51	21.45	26.06	37.40			
15.00			20.6	32.10	51.54	21.45	32.98	52.47			
20.00			20.9	41.00	68.08	21.75	41.90	69.06			
25.00			21.2	53.40	85.00	22.05	54.34	86.03			
30.00			21.6	62.90	101.9	22.45	63.87	102.98			
35.00			22.2	66.5	118.7	23.05	67.48	119.83			
40.00			23.0	76.5	134.9	23.85	77.51	136.07			
45.00			24.0	88.0	150.5	24.86	89.04	151.72			
50.00			25.2	99.9	165.6	26.06	100.97	166.86			
55.00			26.3	114.2	180.2	27.16	115.32	181.51			
58.75			26.9	126.7	190.1	27.76	127.85	191.43			
63.55	0.00		28.7	150.5	201.6	29.57	151.72	202.97			
68.42	4.87	0.00	184.5	188.9	210.1	185.82	190.23	211.49			

Table 3.7

Cont.

69.15	5.60	0.73	193.5	194.6	210.7	194.84	195.95	212.09	0.0	0.00	0.0%
70.70	7.15	2.28	198.9	201.3	212.3	200.26	202.67	213.70	1.0	7.51	3.8%
71.97	8.42	3.55	202.7	203.8	213.9	204.07	205.17	215.30	1.5	14.93	7.5%
73.32	9.77	4.90	206.0	206.3	216.0	207.38	207.68	217.41	2.0	22.34	11.2%
74.62	11.07	6.20	207.9	208.2	218.1	209.28	209.59	219.51	2.5	29.76	14.9%
75.95	12.40	7.53	211.0	211.2	220.3	212.39	212.59	221.72	3.0	37.17	18.6%
77.32	13.77	8.90	214.2	214.7	222.8	215.60	216.10	224.23	3.5	44.59	22.3%
78.63	15.08	10.22	216.7	217.6	225.3	218.11	219.01	226.74	4.0	52.00	26.0%
79.95	16.40	11.53	219.7	220.3	227.9	221.12	221.72	229.34	4.5	59.42	29.7%
81.42	17.87	13.00	223.2	223.8	230.9	224.63	225.23	232.35	5.0	66.83	33.4%
82.93	19.38	14.52	226.6	227.3	234.1	228.04	228.74	235.56	5.5	74.25	37.1%
84.50	20.95	16.08	230.9	231.2	237.5	232.35	232.65	238.97	6.0	81.66	40.8%
86.08	22.53	17.67	234.6	235.0	240.9	236.06	236.46	242.38	6.5	89.08	44.5%
87.63	24.08	19.22	238.0	238.6	244.3	239.47	240.07	245.79	7.0	96.49	48.2%
89.27	25.72	20.85	242.0	242.9	247.8	243.48	244.39	249.30	7.5	103.91	52.0%
90.82	27.27	22.40	246.0	246.6	251.1	247.49	248.10	252.61	8.0	111.32	55.7%
92.45	28.90	24.03	249.6	250.6	254.5	251.11	252.11	256.02	8.5	118.74	59.4%

Table 3.7

Cont.

93.98	30.43	25.57	253.2	254.4	257.7	254.72	255.92	259.23	9.0	126.15	63.1%
95.48	31.93	27.07	256.6	257.8	260.8	258.13	259.33	262.34	9.5	133.57	66.8%
97.12	33.57	28.70	260	261.3	264.0	261.54	262.84	265.55	10.0	140.98	70.5%
98.70	35.15	30.28	263.5	264.8	267.1	265.05	266.35	268.66	10.5	148.40	74.2%
100.35	36.80	31.93	266.9	267.8	270	268.45	269.36	271.56	11.0	155.81	77.9%
102.00	38.45	33.58	270.4	271.3	273	271.96	272.87	274.57	11.5	163.23	81.6%
103.67	40.12	35.25	273.5	274.5	275.9	275.07	276.08	277.48	12.0	170.64	85.3%
105.53	41.98	37.12	277.2	278.0	278.8	278.78	279.59	280.39	12.5	178.06	89.0%
107.23	43.68	38.82	280.3	281.3	281.9	281.89	282.90	283.50	13.0	185.47	92.7%
108.67	45.12	40.25	282.9	283.9	284	284.50	285.50	285.60	13.3	189.92	95.0%
109.93	46.38	41.52	253.1	286.0	302.5	254.62	287.61	304.16	13.5	192.89	96.4%

3.7.1 Plots of experimental data recorded. The temperatures for the thermocouple (T0) inserted in the liquid and just above the bottom of the flask, the thermocouple (T1) placed in the half-way the distance from the initial liquid surface to the thermocouple (T2) placed at the condenser intake were plotted against time and the figure 3.8 gives the details.

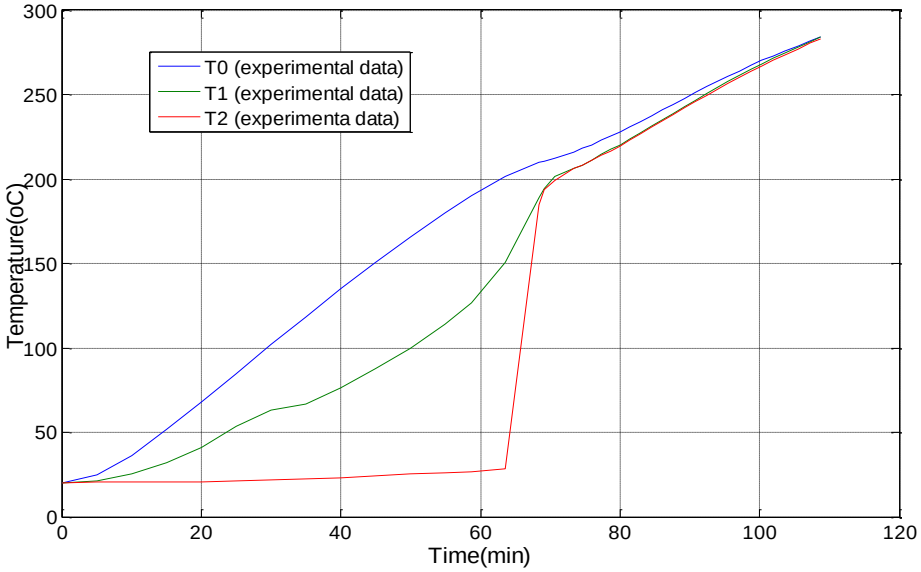

Figure 3.8 Plot of measured temperature vs. experimental time

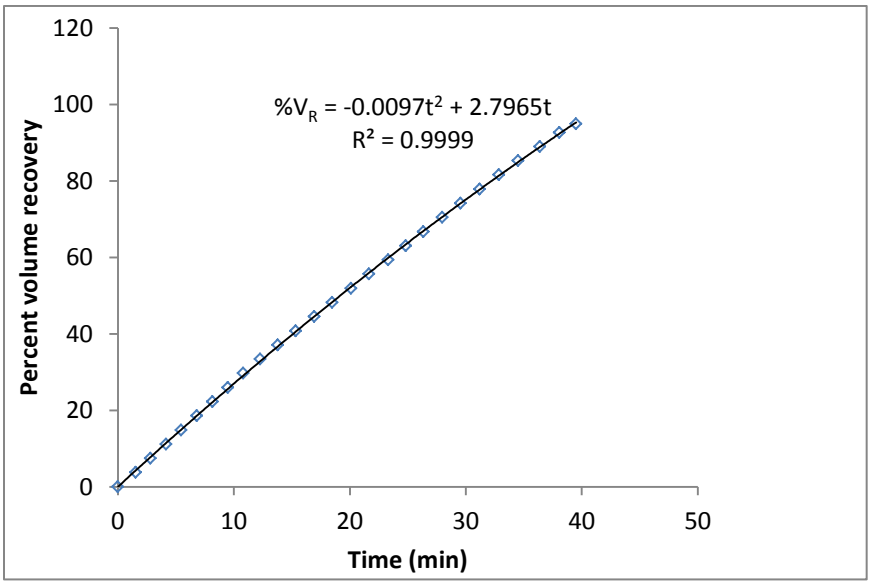

Figure 3.9 Plot of measured % volume recovered vs. experimental time

3.7.2 Fitted correlation for plug flow and complete mixing modeling. The experimental data for the bottom temperature T0 (beginning from when boiling was observed to start) and time were fitted to 2nd order polynomial using MS excel and used in both plug flow and complete mixing modeling of the experiment. Equation 3.2 and equation 3.3 give the correlations for the fitted curves. The fit for the percent recovered volume can be seen as shown earlier in figure 3.9 and that of T0 is in figure 3.10

$$T0 = 0.0039\,t^2 + 1.7495\,t + 200.99 \qquad (3.2)$$

$$\%\,V = -0.0097\,t^2 + 2.7965\,t \qquad (3.3)$$

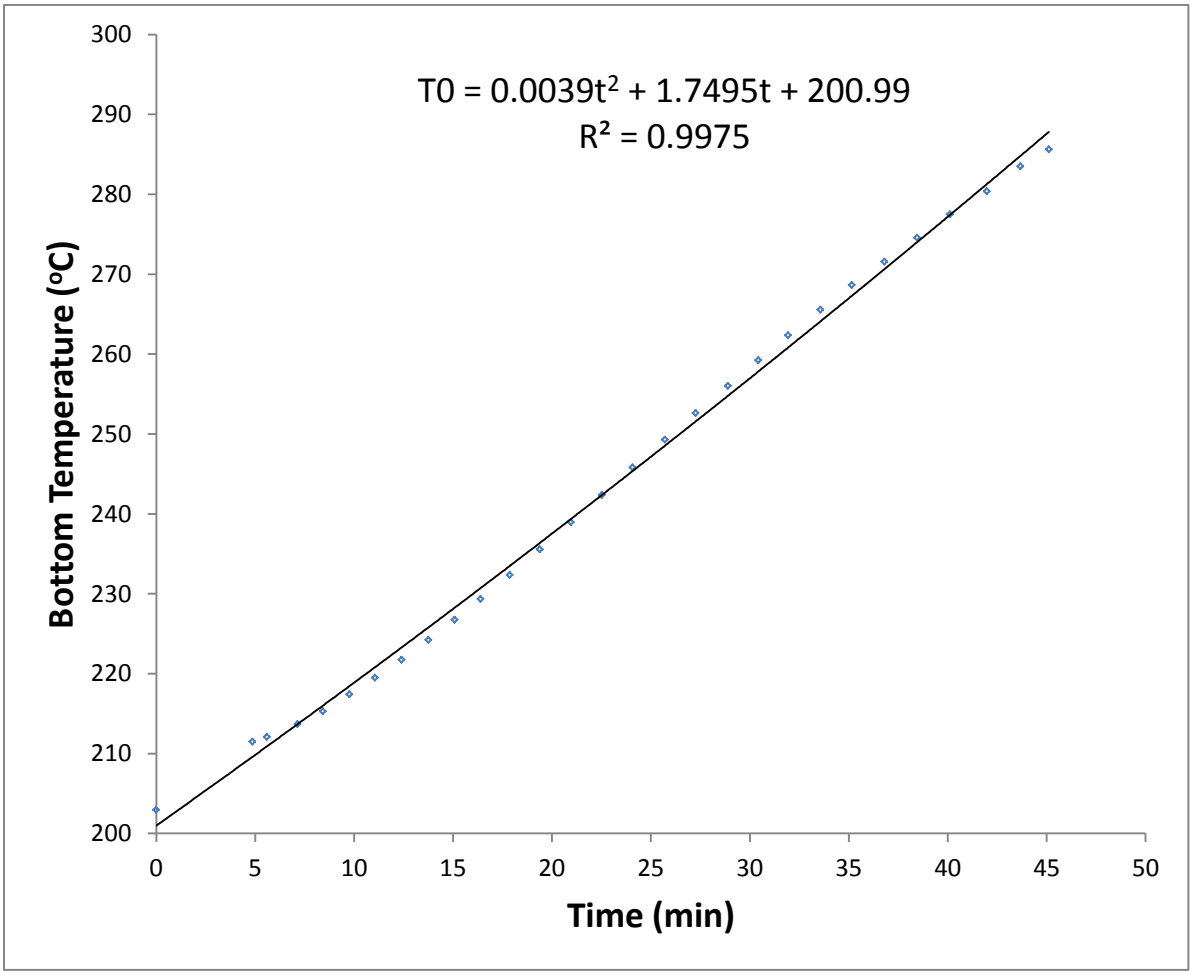

Figure 3.10 Plot of measured T0 vs. experimental time with fitted curve

CHAPTER 4

Modeling the Results

4.1 Plug Flow Modeling for Vapor Travel Time

The figure 4.1 below shows the schematic diagram of the flask used for the distillation experiment. This is used in the plug flow modeling to determine the travel time of the vapor as it rises (vaporizes) from the surface of the liquid to the exit of the flask (at the end of point h_c).

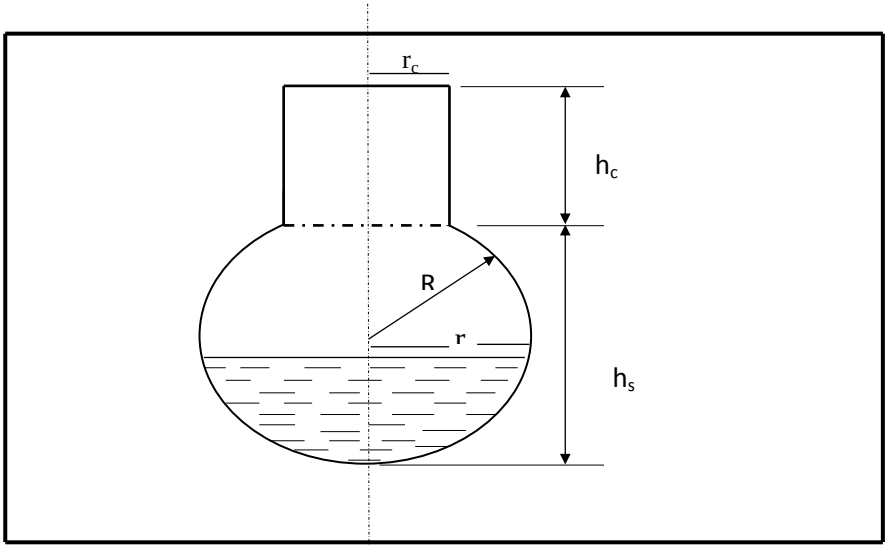

Figure 4.1 Batch distillation setup flask (control volume used in modeling)

4.1.1 Plug Flow Assumptions. To model the process as a plug flow, some assumptions as were made as bulleted below**.**

1. Constant mass flow rate of the hydrocarbon vapor
2. The liquid density of distillate is assumed constant
3. The distillate volumetric flow rate is assumed constant based on the almost linearity profile of the volume distilled and time from the experimental data

For a given hydrocarbon vapor that escapes from the liquid being heated (boiled) in a round bottom flask, the linear velocity of the hydrocarbon vapor is given as

$$u = \frac{dh}{dt_r} = \frac{Q_v}{A} \qquad (4.1)$$

Where t_r = Travel time of the vapor from the liquid surface to the condenser entrance

Qv is the volumetric flow rate of the vapor

h = the height of distance travelled by the vapor

4.1.2 Vapor travel time for the spherical portion of the flask. The cross-sectional area for the spherical portion of the flask or kettle can be given as

$$A = \pi r^2 = \pi\,[R^2 - (R-h)^2] = \pi\,(2Rh - h^2) \qquad (4.2)$$

Also since Q_v is changing with time, we will express Q_v in terms of time using the ideal gas law.

Base on a constant mass flow rate we can write

$$Q_v = \frac{Q_l \rho_l}{\rho_V} \qquad (4.3)$$

Where Q_l and ρ_l are the average distillate volumetric flow rate and density respectively

Now from ideal gas law

$$\rho_v = \frac{PM}{RT} \qquad (4.4)$$

But from the experimental data the temperature of the thermocouple (T0) embedded in the fluid can be written as a function of time as in equation 4.5.

$$T = at^2 + bt + c \qquad (4.5)$$

Where T is in Celsius and a, b and c are constants generated from a plot of temperature (T) vs. time (t) using experimental data. The plot for the fitted temperature time profile is shown in figure 4.2

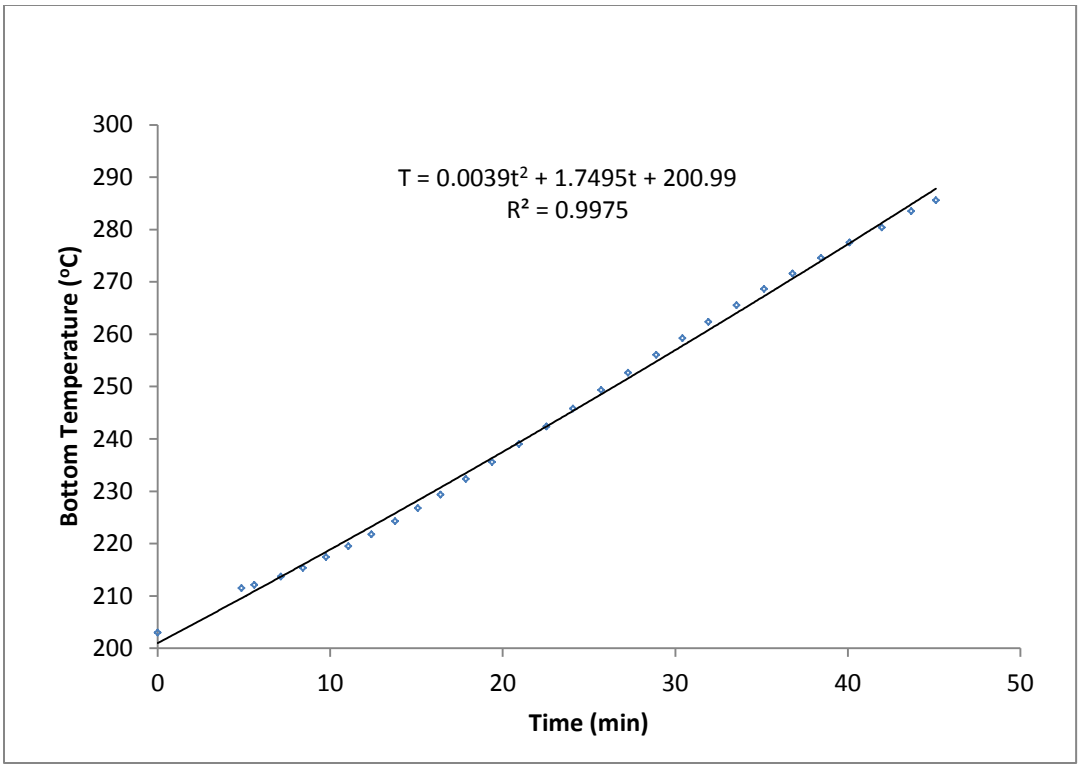

Figure 4.2 Flask Bottom Temperature vs. time graph

Substituting (4.5) into (4.4) gives

$$\rho_v\,(t) = \left(\frac{PM}{R}\right)\left(\frac{1}{at^2 + bt + c'}\right) \qquad (4.6)$$

Where

$$T(t) = at^2 + bt + c' \qquad \text{(in Kelvin)}$$

$$c' = \text{c} + 273.15$$

$$let \qquad K_1 = \frac{PM}{R}$$

$$\rho_v(t) = \frac{K_1}{at^2 + bt + c'} \qquad (4.7)$$

Substituting (4.7) into (4.3) gives

$$Q_v\,(t) = \frac{\rho_l Q_l}{K_1}\,(at^2 + bt + c')$$

$$Q_v\,(t) = K_2\,(at^2 + bt + c') \qquad (4.8)$$

Where

$$K_2 = \frac{\rho_l Q_l}{K_1} = \frac{\dot{m}}{K_1}$$

$$\dot{m} = \rho_l Q_l$$

From (4.1.0) the travel time for the spherical portion of the flask can be written as

$$\frac{dh}{dt_{rs}} = \frac{K_2 (at^2 + bc + c')}{\pi (2Rh - h^2)}$$

Separating variables gives

$$dt_{rs} = \frac{\pi (2Rh - h^2)}{K_2 (at^2 + bt + c')} dh$$

Integrating both sides

$$\int_0^{t_{rs}} dt_{rs} = \int_{h_l}^{h_s} \frac{\pi(2Rh - h^2)}{K_2(at^2 + bt + c')} dh \qquad where\ h_l = liqui\ height$$

The travel time is given as below

$$t_{rs} = \frac{\pi}{K_2(at^2 + bt + c')} \left[R(h_s^2 - h_l^2) - \frac{1}{3}(h_s^3 - h_l^3)\right] \qquad (4.9)$$

4.1.3 Travel time for the cylindrical (head) portion. For the cylindrical portion, the linear velocity in terms of the height and travel time is given as

$$\frac{dh}{dt_{rc}} = \frac{Q_v}{\pi r_c^2} \qquad (4.10)$$

$$\int_0^{t_{rc}} dt_{rc} = \frac{\pi r_c^2}{k_2(at^2 + bt + c')} \int_0^{h_c} dh$$

$$t_{rc} = \frac{\pi r_c^2 h_c}{k_2(at^2 + bt\, c')} \qquad (4.11)$$

4.1.4 Overall vapor travel time. The total travel time is given as

$$t_r = t_{rs} + t_{rc}$$

$$t_r = \frac{\pi}{k_2(at^2 + bt + c')}\left[R(h_s^2 - h_l^2) - \frac{1}{3}(h_s^3 - h_l^3) + r_c^2 h_c\right] \qquad (4.12)$$

4.1.5 Liquid changing height calculations. Now we need to determine the values of h_l changing with time. The volume of the liquid is given as

$$V_l = \frac{1}{3}\pi h_l^2 (3R - h_l) \qquad (4.13)$$

Where V_{v0} is the initial vapour volume at t = 0.

For changing liquid height or level (h_l) we write the liquid volume as

$$V_{lo} - Q_l t = \frac{1}{3}\pi h_l^2 (3R - h_l)$$

Where V_{lo} is the initial liquid volume at time t = 0

$$V_{lo} - Q_l t = \pi R h_l^2 - \frac{1}{3}\pi h_l^3$$

$$\pi h_l^3 - 3R\pi h_l^2 + V_{lo} - 3Q_l t = 0 \qquad (4.14)$$

Where

$Q_l = 4.73\ ml/\min = 4730\ mm^3/min$

$V_{lo} = 200ml = 200 \times 10^3\ mm^3$

$R = 49.2\ mm$

Let

$$f(h_l, t) = \pi h_l^3 - 3\pi R h_l^2 + 3V_{lo} - 3Q_l t = 0 \qquad (4.15)$$

Since t values are known from experiment, we use numerical method to calculate h_l values at corresponding t values. See appendix A.1 for the M – file used to generate h_l values.

4.1.6 Calculating the travel time for plug flow. The steps written below were used to calculate the travel time for the plug flow.

1. With equation (4.15), h_l values are calculated using experimented data for time and the m.file in appendix A.1.
2. With h_l values calculated, we then have a matrix of time and liquid height data
3. The values of h_l and t from step (1) and (2) with the m.file in appendix A.2 are used to calculate the total travel time for both the spherical portion and cylindrical portion using equation (4.12).
4. The travel time $t_r = t_{rs} + t_{rc}$ where t_{rs} = travel time for spherical and t_{rc} = travel time for cylindrical.
5. Measured values for the height of the spherical portion, radius and height of the cylindrical portion are as noted below.

$h_s = 89.7mm$ $r_c = 13.0mm$ $h_c = 62.0m$m

Table 4.1 shows how the liquid level in the flask goes down with the assumptions made during the distillation process and table 4.2 gives details of the results of plug flow modeling and the volume correction for plug flow. The vapor travel time results in table 4.2 were used to correct the percent volume recovered $\%V_2$ as shown in table 4.1. The first volume corrections, $\%V_1$, were calculated as proposed by Laya [5] by adding the hold-up time of the first drop of the distillate in the condenser to the experimentally recorded time for the distillate in the receiver. The 2nd correction was done by adding the vapor travel time to Laya' time approach to take care of the volume recovered with respect to when the vapors took off the surface (bubble point temperature) of the liquid. In all the corrected volume corrections, the fitted correlation for % volume recovered vs. time in figure 3.9 or equation 3.7.4b was used. Values for $\%V_1$ and $\%V_2$

were calculated with times t_1 and t_2 respectively as in table 4.2. The vapor travel time plots with time and bottom temperature (T0) are shown in figures 4.3 and 4.4 and the corrected volume plot is shown in figure 4.5.

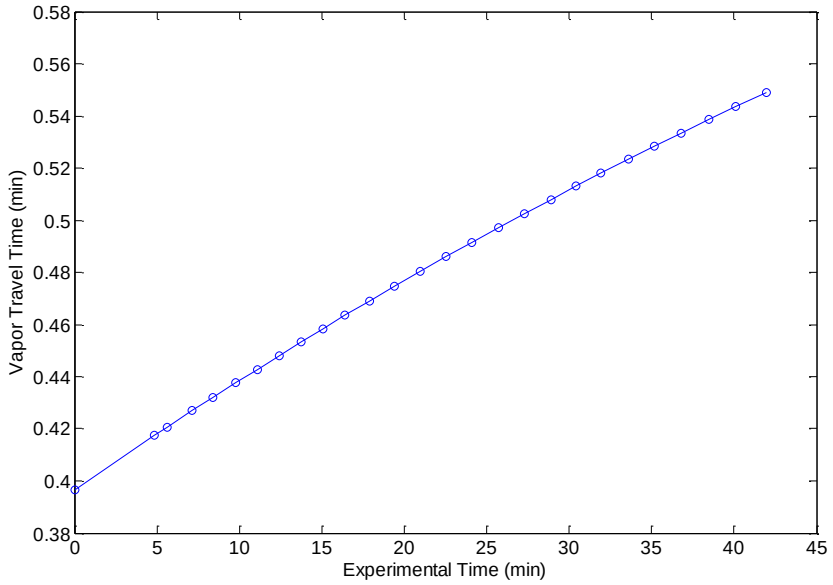

Figure 4.3 Travel time vs. experimental time graph

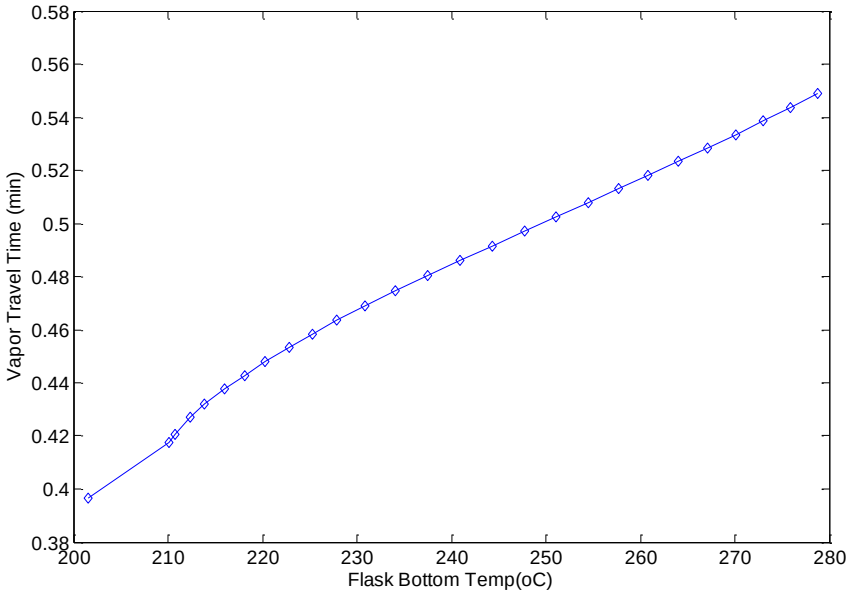

Figure 4.4 Travel time vs. experimental Flask bottom temperature graph

Table 4.1

Calculated values of liquid level and travel time for plug flow model

Experiment Time (t) (min)	Liquid height (h_l) (mm)	Travel time (t_r) (min)
0	42.66	0.3966
4.9	39.55	0.4175
5.6	39.07	0.4205
7.2	38.06	0.427
8.4	37.23	0.4322
9.8	36.33	0.4376
11.1	35.46	0.4428
12.4	34.55	0.448
13.8	33.61	0.4534
15.1	32.7	0.4584
16.4	31.77	0.4634
17.9	30.72	0.469
19.4	29.61	0.4745
20.9	28.44	0.4803
22.5	27.23	0.4859
24.1	26	0.4914
25.7	24.67	0.4971
27.3	23.36	0.5024
28.9	21.93	0.508
30.4	20.53	0.513
31.9	19.07	0.518
33.6	17.39	0.5233
35.1	15.62	0.5283
36.8	13.59	0.5334
38.5	11.27	0.5385
40.1	8.38	0.5436
42	3.08	0.5491

Table 4.2

Results of corrected volume for plug flowmodel

Time (min)	Liquid Temperature	% Volume Recovered	Time from Receiver (min)	1st Time shift from Receiver to condenser	2nd Time shift from Cond to vapor take off	Vapor travel time inside flask (min)	Liquid height in mm	1st corrected % Vol using fitted equation	2nd corrected % Vol using fitted equation
t	T0	% V	t	t_c	$t_b = t_r + tc$	t_r	h_l	$\%V_1$	$\%V_2$
0.0	203.0				0.0		42.66		0
4.9	211.5			0.0	0.397	0.3966	39.55	0	1.11
5.6	212.1	0.0	0.0	0.73	1.151	0.4175	39.07	2.05	3.22
7.2	213.7	3.8	1.6	2.28	2.704	0.4205	38.06	6.36	7.52
8.4	215.3	7.5	2.8	3.55	3.977	0.427	37.23	9.84	11.01
9.8	217.4	11.2	4.2	4.90	5.332	0.4322	36.33	13.52	14.69
11.1	219.5	14.9	5.5	6.20	6.638	0.4376	35.46	17.02	18.20
12.4	221.7	18.6	6.8	7.53	7.976	0.4428	34.55	20.58	21.76
13.8	224.2	22.3	8.2	8.90	9.348	0.448	33.61	24.19	25.37
15.1	226.7	26.0	9.5	10.22	10.670	0.4534	32.7	27.63	28.81
16.4	229.3	29.7	10.8	11.53	11.992	0.4584	31.77	31.04	32.21
17.9	232.4	33.4	12.3	13.00	13.463	0.4634	30.72	34.79	35.96
19.4	235.6	37.1	13.8	14.52	14.986	0.469	29.61	38.62	39.79

Table 4.2

Cont.

21.0	239.0	40.8	15.4	16.08	16.558	0.4745	28.44	42.53	43.70
22.5	242.4	44.5	16.9	17.67	18.147	0.4803	27.23	46.43	47.60
24.1	245.8	48.2	18.5	19.22	19.703	0.4859	26	50.19	51.36
25.7	249.3	52.0	20.1	20.85	21.341	0.4914	24.67	54.11	55.27
27.3	252.6	55.7	21.7	22.40	22.897	0.4971	23.36	57.77	58.94
28.9	256.0	59.4	23.3	24.03	24.536	0.5024	21.93	61.58	62.74
30.4	259.2	63.1	24.8	25.57	26.075	0.508	20.53	65.10	66.26
31.9	262.3	66.8	26.3	27.07	27.580	0.513	19.07	68.51	69.66
33.6	265.5	70.5	28.0	28.70	29.218	0.518	17.39	72.16	73.30
35.2	268.7	74.2	29.6	30.28	30.807	0.5233	15.62	75.64	76.79
36.8	271.6	77.9	31.2	31.93	32.462	0.5283	13.59	79.22	80.36
38.5	274.6	81.6	32.9	33.58	34.117	0.5334	11.27	82.75	83.87
40.1	277.5	85.3	34.5	35.25	35.789	0.5385	8.38	86.25	87.37
42.0	280.4	89.0	36.4	37.12	37.660	0.5436	3.08	90.10	91.21
43.7	283.5	92.7	38.1	38.82	39.366	0.5491		93.55	94.65
45.1	285.6	95.0	39.5	40.25					
46.4	304.2	96.4	40.8	41.52					

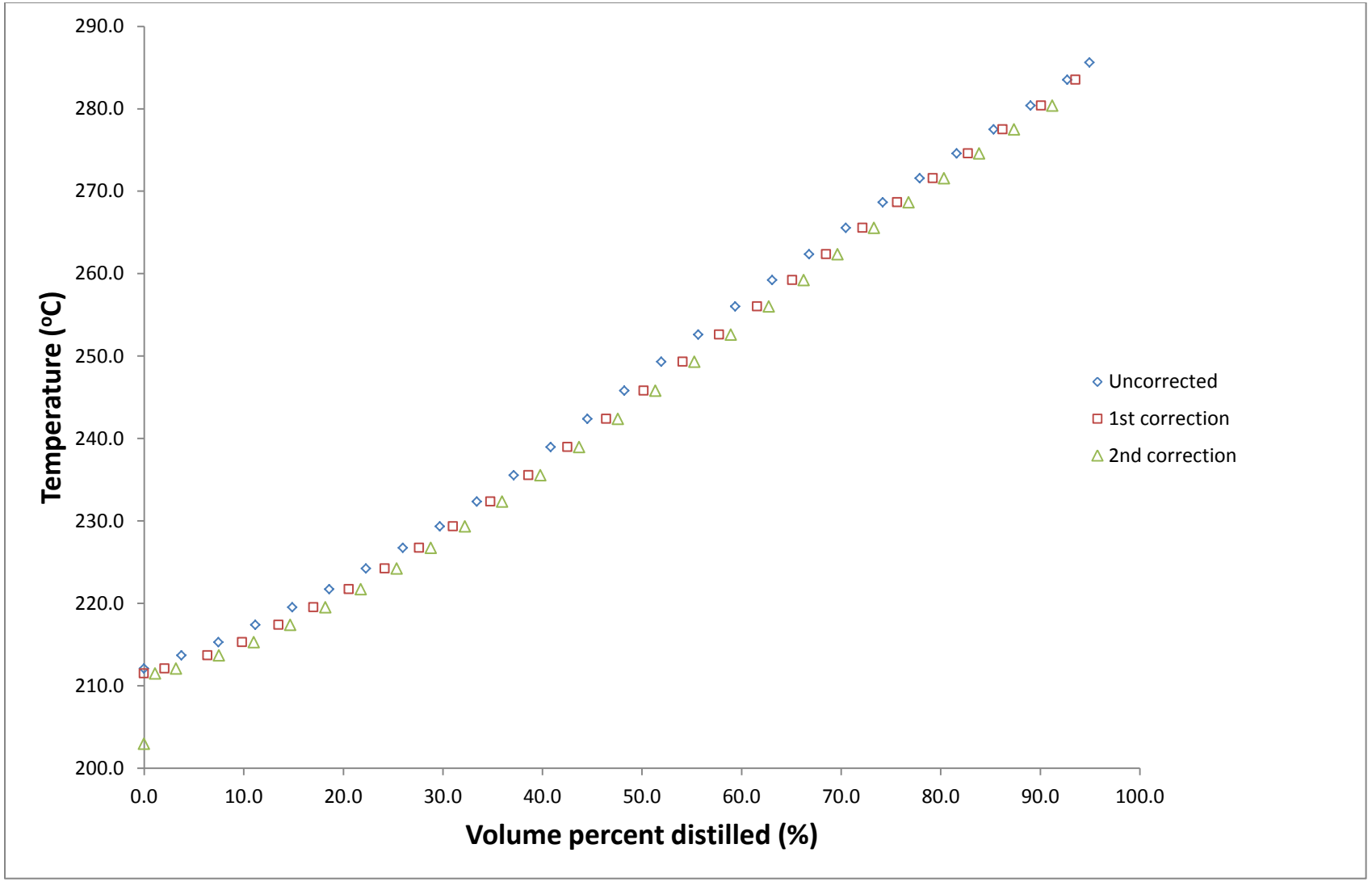

Figure 4.5 Uncorrected and corrected distillation curve for plug flow model

4.2 Complete Mixing Model

4.2.1 Mole and Energy balance derivations. A simple representation of the control volume used for modeling is shown below in figure 4.5. The initial control volume (vapor space) is the volume above the liquid surface before the first vapor rise. As the experiment starts and the vapors start rising the control volume increases with time. The increase in the control volume is as a result of the drop in liquid volume due to vaporization by boiling.

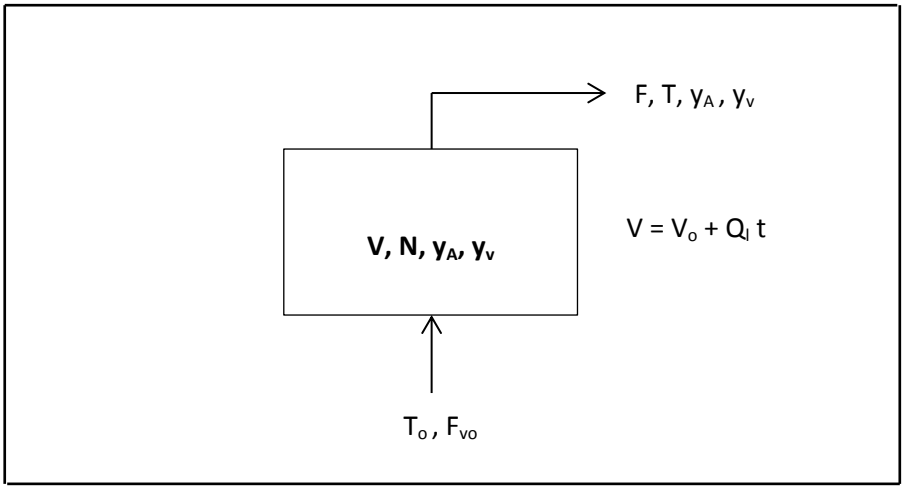

Figure 4.6 Representation of control volume for complete mixing model

Note: V_o, Q_l, F_{vo} are known constants from experimental data.

Total mole balance:

$$\frac{dN}{dt} = F_{vo} - F \qquad (4.16)$$

Molar balance for hydrocarbon vapor:

$$\frac{dNy_v}{dt} = F_{vo} - y_v F \qquad (4.17)$$

$$\frac{Ndy_v}{dt} = F_{vo} - y_v F - y_v F_{vo} + y_v F \qquad (4.18)$$

$$\frac{dy_v}{dt} = \frac{F_{vo}}{N}\,(1 - y_v) \tag{4.19}$$

Energy balance

$$\frac{dN\dot{U}}{dt} = F_{vo}\dot{H}_{vo} - F\left(y_A\dot{H}_A + y_v\dot{H}_v\right) \tag{4.20}$$

$$\frac{dN\left(y_A\dot{U}_A + y_v\dot{U}_v\right)}{dt} = F_{vo}\dot{H}_{vo} - F\left(y_A\dot{H}_A + y_v\dot{H}_v\right) \tag{4.21}$$

$$(y_AC_{vA} + y_vC_{vv})T\frac{dN}{dt} + N\frac{d}{dt}\,(y_AC_{vA}T + y_vC_{vv}T)$$

$$= F_{vo}Cp_{vo}T_o - F\left(y_AC_{P_A} + y_vC_{P_v}\right)T \tag{4.22}$$

The unknowns in equation (4.19) to be determined are N, F, y_v *and* T.

The total number of moles in the control volume is given as

$$N = \frac{PV}{RT} = \frac{P(V_o + Q_lt)}{RT} \tag{4.23}$$

$$\frac{dN}{dt} = \frac{PQ_l}{RT} - \frac{P(V_o + Q_lt)}{RT^2}\frac{dT}{dt} \tag{4.24}$$

From equation (4.16)

$$F = F_{vo} - \frac{dN}{dt} \tag{4.25}$$

Substituting for dN/dt gives

$$F = F_{vo} - \frac{PQ_l}{RT} + \frac{P(V_o + Q_lt)}{RT^2}\frac{dT}{dt} \tag{4.26}$$

Equation (4.18) can be further written as

$$\frac{dy_v}{dt} = \frac{FV_oRT}{P(V_o + Q_lt)}\quad(1 - y_v) \tag{4.27}$$

Now we will simplify equation (4.19) by substitution

$$\left[(1-\ y_v)\ C_{v_A}+\ y_v C_{v_v}\right] T\ \frac{dN}{dt}+NC_{v_A}\ \frac{d}{dt}\ (y_A T)+NC_{v_v}\ \frac{d(y_v T)}{dt}$$

$$=\ F_{vo} C p_{vo}\ T_o - F\ \left(y_A C_{p_A}+\ y_v C_{p_v}\right) T \qquad (4.28)$$

$$\left[C_{v_A}+\ y_v\ \left(C_{v_v}-\ C_{v_A}\right)\right] T\ \frac{dN}{dt}+NC_{v_A}\ \frac{d}{dt}\ [(1-\ y_v)\ T]+NC_{v_v}\ \frac{dy_v T}{dt}$$

$$=\ F_{vo}\ C_{p_{vo}}\ T_o - F\ \left(y_A C_{p_A}+\ y_v C_{p_v}\right) T \qquad (4.29)$$

Substitute for equation (5) for dN/dt gives

$$\left[C_{v_A}+\ y_v\ \left(C_{v_v}-\ C_{v_A}\right)\right] T\ \left[\frac{PQ_l}{RT}-\ \frac{P(v_o+\ Q_l t)}{RT^2}\ \frac{dT}{dt}\right]+NC_{v_A}\ \frac{dT}{dt}+\ \left(NC_{v_v}-NC_{v_A}\right)\frac{dy_v T}{dt}$$

$$=\ F_{vo}\ C_{p_{vo}}\ T_o - F\left[(1-\ y_v)\ C_{p_A}+\ y_v\ C_{p_v}\right] T \qquad (4.30)$$

$$\left[C_{v_A}+\ y_v\ \left(C_{v_v}-\ C_{v_A}\right)\right] T\ \left(\frac{PQ_l}{RT}-\ \frac{P(v_o+\ Q_l t)}{RT^2}\ \frac{dT}{dt}\right)+\ NC_{v_A}\ \frac{dT}{dt}$$

$$+\ N\left(C_{v_v}-\ C_{v_A}\right) T\ \left(\frac{F_{vo}}{N}\ (1-\ y_v)\right)+\ \left(C_{v_v}-\ C_{vA}\right) y_v\ \frac{dT}{dt}$$

$$=\ F_{vo}\ C p_{vo}\ T_o - \left[F_{vo}-\ \frac{PQ_l}{RT}+\ \frac{P(V_o+\ Q_l t)}{RT^2}\ \frac{dT}{dt}\right]\ \left[C_{p_A}+\ y_v\ \left(C_{p_v}-\ C_{p_A}\right)\right] T \qquad (4.31)$$

$$\frac{PQ_l}{R}\left[C_{v_A}+\ y_v\ \left(C_{v_v}-\ C_{v_A}\right)\right]-\ \frac{P(v_o+\ Q_l t)}{RT}\left(C_{v_A}+\ y_v\ \left(C_{v_v}-\ C_{v_A}\right)\right)\frac{dT}{dt}\ +\ NC_{v_A}\ \frac{dT}{dt}$$

$$+\ \left(C_{v_v}-\ C_{v_A}\right) TF_{vo}(1-\ y_v)+\ N\left(C_{v_v}-\ C_{vA}\right) y_v\ \frac{dT}{dt}$$

$$= F_{vo}\, Cp_{vo}\, T_o \; - \left(F_{vo} - \frac{PQ_l}{RT}\right)\left[C_{p_A} + y_v\left(C_{p_v} - C_{p_A}\right)\right]T$$

$$- \frac{P(V_o + Q_L t)}{RT}\left[C_{p_A} + y_v\left(C_{p_v} - C_{p_A}\right)\right]\frac{dT}{dt} \qquad (4.32)$$

$$\frac{P(V_o + Q_L t)}{RT}\left[C_{p_A} + y_v C_{p_v} - y_v C_{p_A} - C_{v_A} - y_v C_{v_v} + y_v C_{v_A}\right]\frac{dT}{dt} + NC_{v_A}\frac{dT}{dt}$$

$$+ N\left(C_{v_v} - C_{v_A}\right) y_v \frac{dT}{dt}$$

$$= F_{vo}\left[C_{p_{vo}}\, T_o - \left\{C_{p_A} + y_v\left(C_{p_v} - C_{p_A}\right)\right\}T\right]$$

$$+ \frac{PQ_l}{R}\left[C_{p_A} + y_v\left(C_{p_v} - C_{p_A}\right) - C_{vA} - y_v\left(C_{v_v} - C_{v_A}\right)\right]$$

$$- \left(C_{v_v} - C_{v_A}\right) T\, F_{vo}\,(1 - y_v) \qquad (4.33)$$

$$\frac{P(V_o + Q_l t)}{T}\frac{dT}{dt} + NC_{vA}\frac{dT}{dt}\, N\left(C_{v_v} - C_{vA}\right) y_v \frac{dT}{dt}$$

$$= PQ_l + F_{vo}\left[C_{p_{vo}}\, T_o - C_{p_A}\, T - y_v\, T\left(C_{p_v} - C_{p_A}\right) - \left(C_{v_v} - C_{vA}\right) T\,(1 - y_v)\right] \qquad (4.34)$$

$$\frac{P\,(V_o + Q_l t)}{T}\frac{dT}{dt} + \left[NC_{v_A} + NC_{v_v}\, y_v - NC_{v_A}\, y_v\right]\frac{dT}{dt}\, PQ_L$$

$$+ F_{vo}\left[C_{p_{vo}}\, T_o - C_{p_A} T - y_v T\left(C_{p_v} - C_{p_A} - C_{v_v} + C_{vA}\right) - T\left(C_{v_v} - C_{vA}\right)\right]$$

$$+ \left[\frac{P\,(V_o + Q_l t)}{T} + N\left\{C_{v_A} + y_v\left(C_{v_v} - C_{v_A}\right)\right\}\frac{dT}{dt}\right]$$

$$= PQ_L + F_{vo}\left[C_{p_{vo}}\, T_o - C_{p_A} T - T\left(C_{v_v} - C_{vA}\right)\right] \qquad (4.35)$$

4.2.2 Summary of equations. The equations used to solve for the flask exit or head temperature (T2) and the corresponding vapor composition (y_v) simultaneously have been summarized as below.

$$N = \frac{P\,(V_o + Q_l t)}{RT} \tag{4.36}$$

$$\frac{dN}{dt} = \frac{PQ_l}{RT} - \frac{P(V_o + Q_l t\,)}{RT^2}\,\frac{dT}{dt} \tag{4.37}$$

$$F = F_{vo} - \frac{PQ_l}{RT} + \frac{P(V_o + Q_l t)}{RT^2}\,\frac{dT}{dt} \tag{4.38}$$

$$\frac{dy_v}{dt} = \frac{F_{vo}}{N}\,(1 - y_v) \tag{4.39}$$

$$\frac{dT}{dt} = \frac{PQ_L + F_{vo}\left[C_{p_{vo}}T_o - C_{p_A}T - T\left(C_{v_v} - C_{vA}\right)\right]}{\frac{P\,(V_o + Q_l t)}{T} + N\left\{C_{v_A} + y_v\left(C_{v_v} - C_{v_A}\right)\right\}} \tag{4.40}$$

4.2.3 Heat Capacity data used in modeling. To model the experiment, the hydrocarbon fluid mixture was assumed to be pure n-dodecane and the nitrogen was used as air for approximate calculations. To represent the four component mixture (decane, dodecane, tetradecane and hexadecane), n-dodecane was chosen as a good representation of the average properties of the mixture though not exact. Selecting n-decane will be on the extreme low side as well as using n-hexadecane will also be on the extreme high side in terms of representing the hydrocarbon mixture as one pure compound for sake of the modeling. Heat capacity data were

referenced from the text book ‘’The Properties of gases and liquids’’[19] as in equation 4.41. The heat capacity constants used can be seen in table 4.3.

$$\frac{C_P}{R} = a_o + a_1 T + a_2 T^2 + a_3 T^3 + a_4 T^4 \qquad (4.41)$$

Table 4.3

Heat capacity constants for Dodecane and Nitrogen [19]

Constants	**n-dodecane**	**Nitrogen**
a_o	17.229	3.539
a_1	-7.242 x 10^{-3}	-0.261 x 10^{-3}
a_2	31.922 x 10^{-5}	0.007 x 10^{-5}
a_3	-42.322 x 10^{-8}	0.157 x 10^{-8}
a_4	17.022 x 10^{-11}	-0.099 x 10^{-11}

4.2.4 Calculating for head (exit) temperature (T2) and exit mole fraction (yv). To calculate for the exit temperature and exit vapor fraction, Matlab ODE solver “ode45” was used to solve equations 4.26 and 4.27 simultaneously. The m.file ‘’compmix’’ in appendix A.3 was written to generate the expressions for equations 4.39 and 4.40 and the Matlab inbuilt function ode45 was used to compute the m.file ‘’compmix’’ in the command window. The time step was automatically chosen by ode 45 and the results can be seen in appendix B1. Input to the ode 45 were the function, time span (0 to 45) and the initial conditions for the vapor composition (yv = 0) and that of the exit temperature (T2 = 293.15K).

4.2.5 Graphs for complete mixing modeling. The results from the complete mixing modeling for the flask exit or head temperature (T2) and the bottom temperature (T0) were plotted and shown in figure 4.6 with expanded views from figures 4.7 to 4.10.

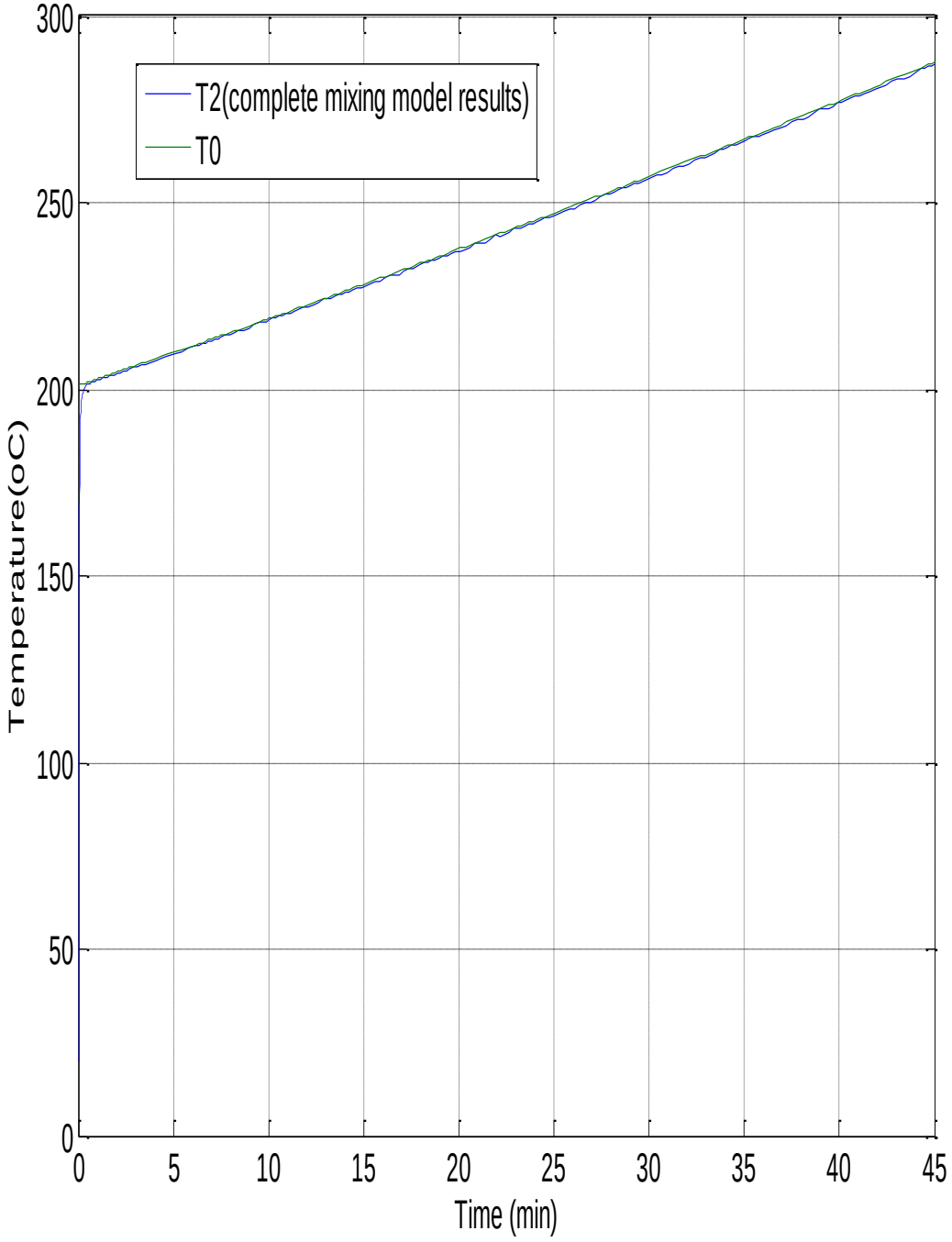

Figure 4.7 Temperature –Time profile of equal volume of decane, dodecane, tetradecane and hexadecane for complete mixing model

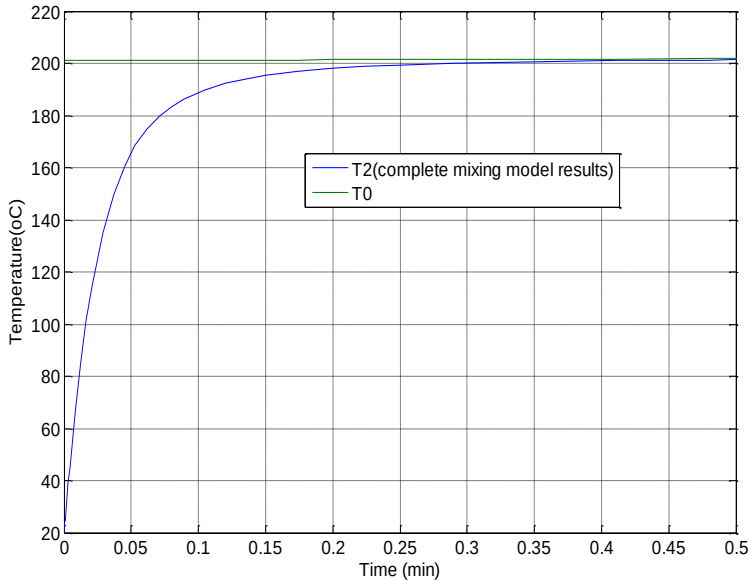

Figure 4.8 Expanded view of figure 4.7

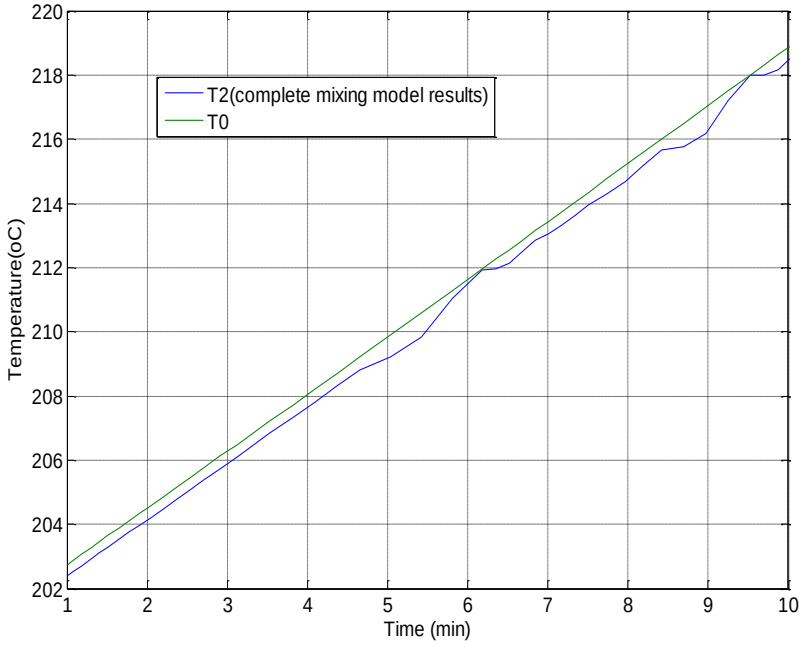

Figure 4.9 Expanded view of figure 4.7

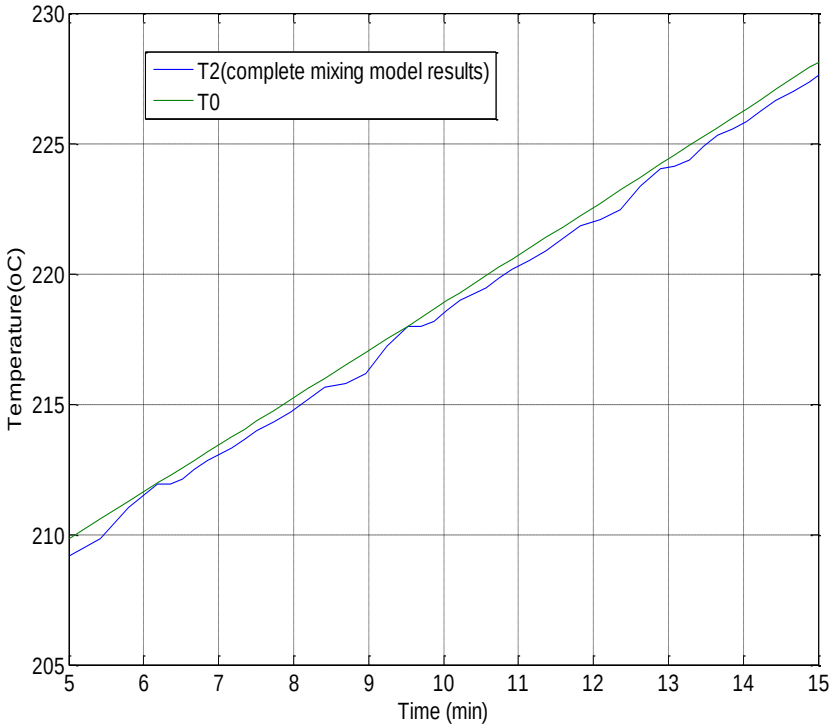

Figure 4.10 Expanded view of figure 4.7

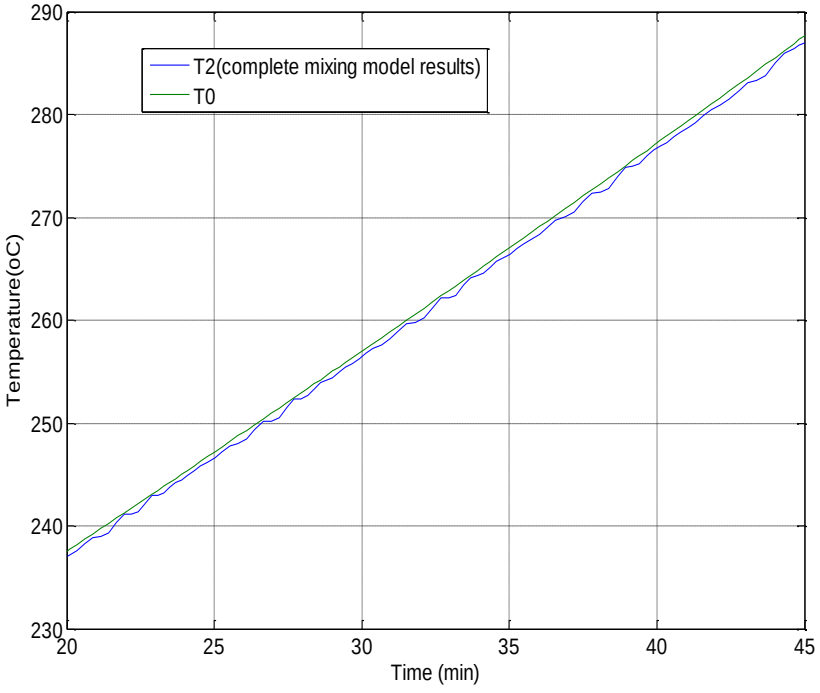

Figure 4.11 Expanded view of figure 4.7

To determine the vapor travel time, the 'wavy' portion of the exit temperature (T2) curve was fitted with least square quadratic fitting from time (1.4min to 45min) and the fitted curve was used to calculate the travel time for the said time interval.

The vapor travel time for times for $0 = t \leq 1.4$ were calculated directly from the ode45 time and exit temperature results, while that for $1.4 \leq t \leq 45.12$ were calculated from the least square fit for the exit temperature (T2) and time. The least square quadratic fit equation generated is given in equation 4.42.

$$a_{of} = 3.9333 \times 10^{-3}; \quad b_{of} = 1.7418; \quad c_{of} = 473.7858$$

$$T_2 = a_{of}t^2 + b_{of}t + c_{of} \qquad (4.42)$$

$$where\ T_2\ is\ in\ kelvin$$

The travel time was calculated as

$$t_r = t_{T_o=T} - t_T \qquad (4.43)$$

Where t_r is the travel time

$t_{To=T}$ is the time when the inlet temperature (T2) was equal to the exit temperature (T0)

t_T is the time at the exit temperature (T2)

The plot of travel time vs. the flask bottom temperature is shown below in figure 4.12 and matlab interpolation function 'interp1' was used to calculate the time at which the T0 equals T2. The interpolation was done in two phases. For time starting from 0 to 1.4minutes the ode results for T2 were used directly whiles from 1.4 minutes to 45 minutes the smoothed T2 curve fitted equation 4.29 was used. The interpolated times results ($t_{T0=T2}$) were to calculate the vapor travel time with equation (4.43) and the plotted results can be seen at figure 4.12. Results of the travel time from ode45 calculations can be seen in in appendix B1 and figure 4.12 and 4.13

shows the trend of the vapor composition. The exit temperature (T2) with the smoothed (T2) curve can be seen in figures 4.15 to 4.17. Note that the exit temperature (T2) results in appendix B1 are the direct ode 45 results and not T2 from fitted curve.

The volume correction based on the travel time calculated can be seen in table 4.4 and figure 4.18 shows the volume correction profile.

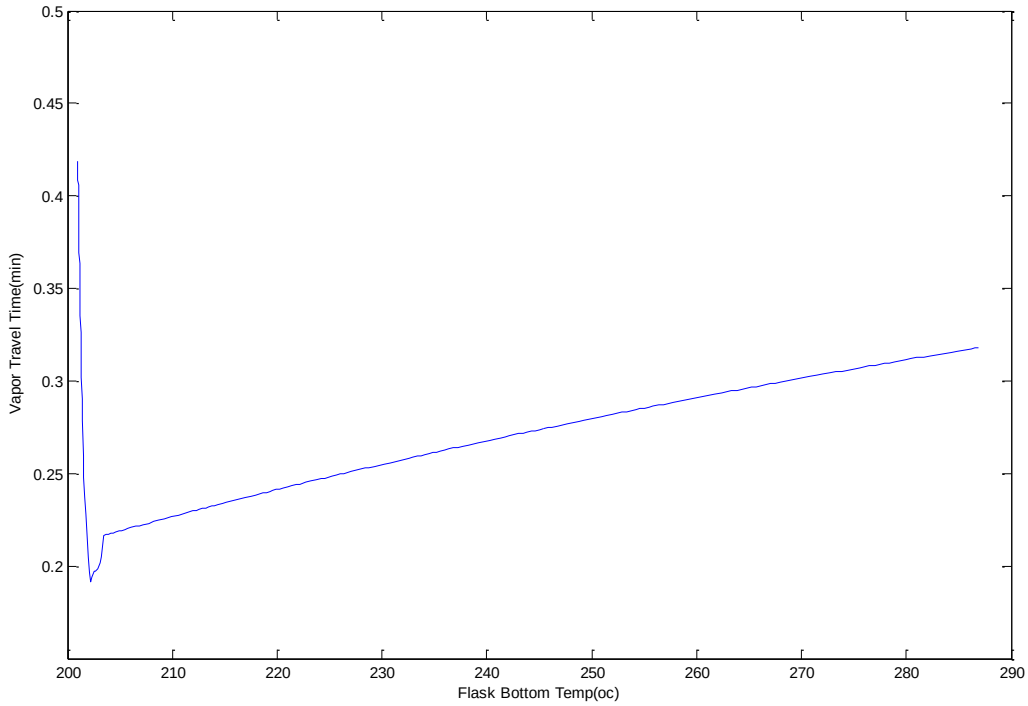

Figure 4.12 Complete mixing model vapor travel time profile

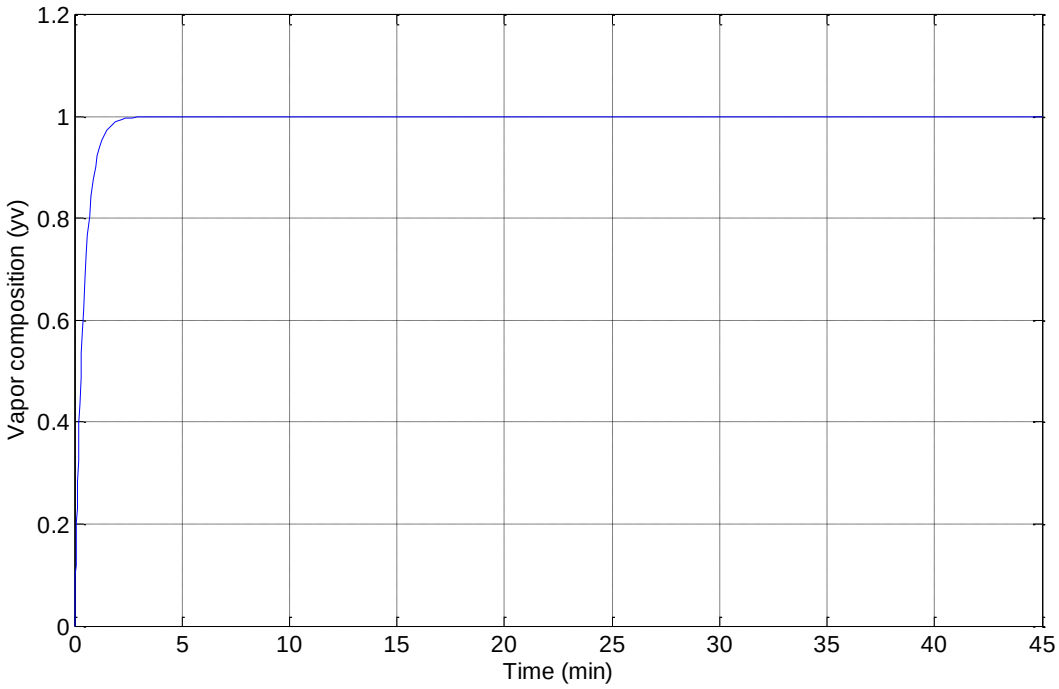

Figure 4.13 Vapor composition vs. time profile for complete mixing model

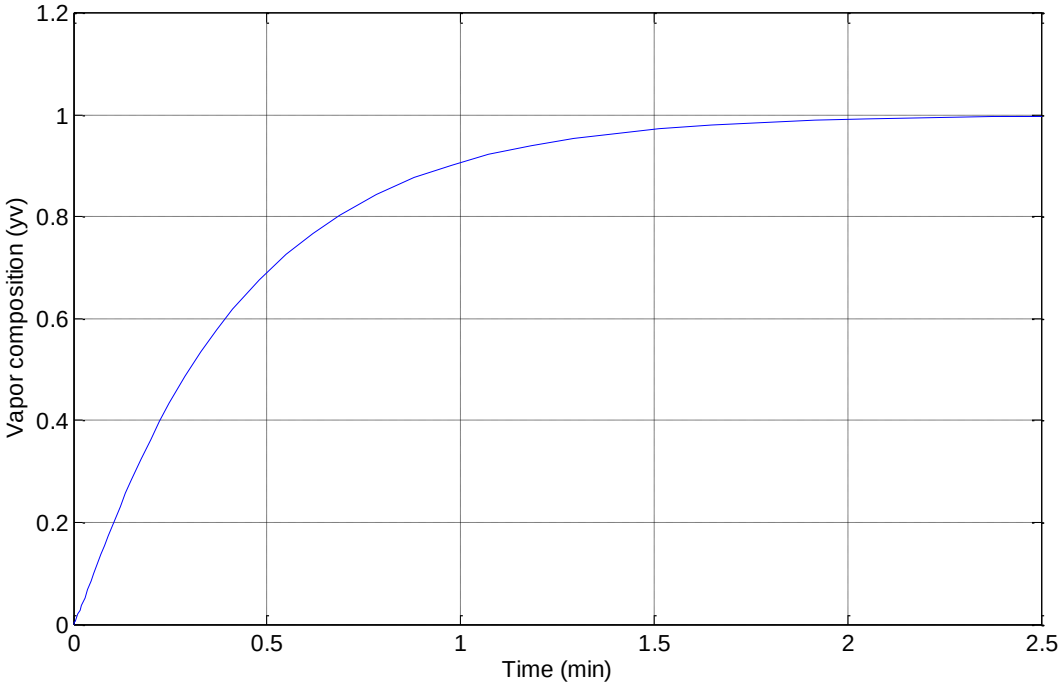

Figure 4.14 Expanded view of vapor composition vs. time profile for complete mixing

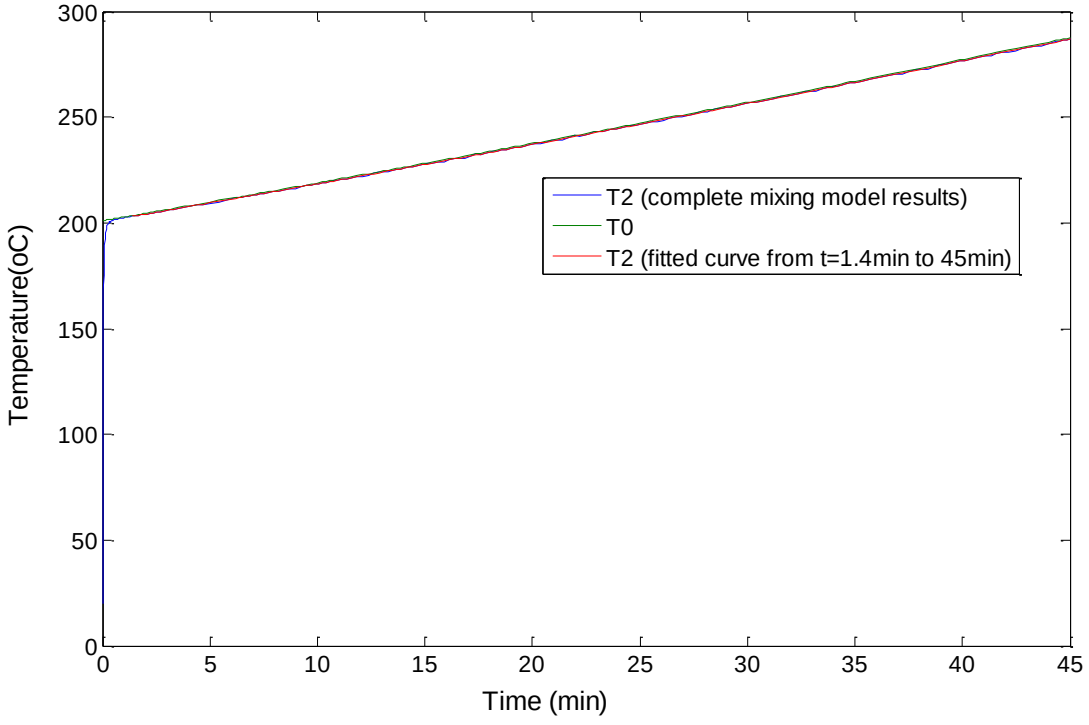

Figure 4.15 Temperature –Time profile with smoothened T2 curve for complete mixing model

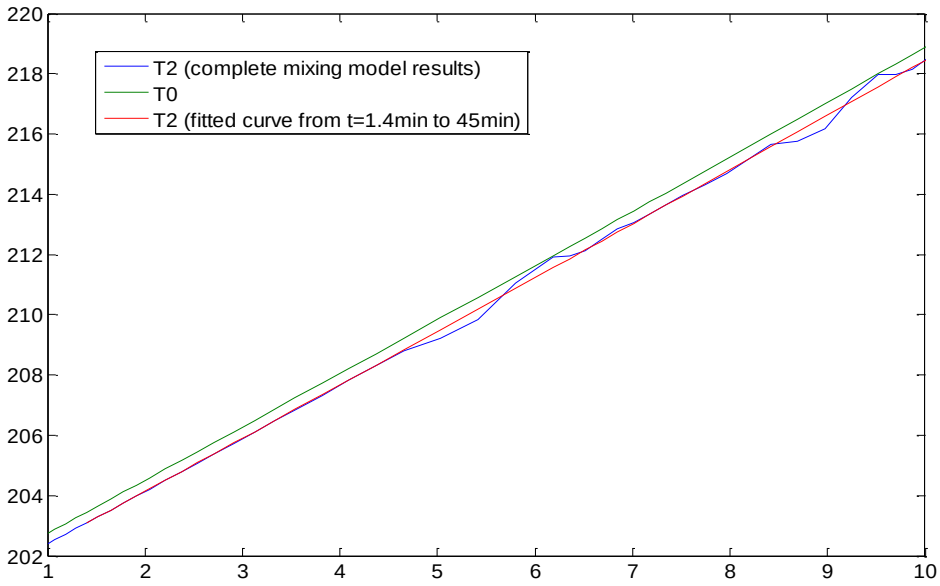

Figure 4.16 Expanded view of figure 4.15

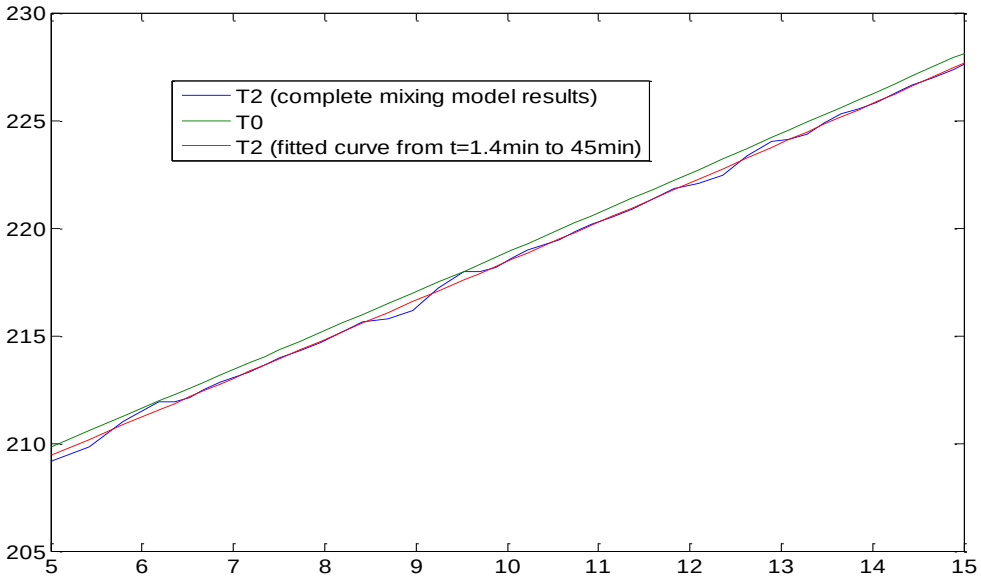

Figure 4.17 Expanded view of figure 4.15

Table 4.4

Results of volume correction for complete mixing model

Time (min)	Bottom Temp	% Volume Recovered	Time from Receiver (min)	1st Time shift from Receiver to condenser	2nd Time shift from Cond to liquid suf	Vapor travel time (min)	Exit Temp Time (min)	Bottom Temp Time (min)	1st corrected % Vol	2nd corrected % Vol
t	T0	% V	t	t_c	$t_b = t_r + t_c$	t_r	t_T	t_{To}	$\%V_1$	$\%V_2$
0.0	203.0				0.0					0
4.9	211.5			0.0	0.226	0.226	5.643	5.417	0	0.64
5.6	212.1	0.0	0.0	0.73	0.961	0.227	6.151	5.924	2.05	2.69
7.2	213.7	3.8	1.6	2.28	2.513	0.230	6.488	6.257	6.36	7.00
8.4	215.3	7.5	2.8	3.55	3.783	0.233	7.384	7.151	9.84	10.48
9.8	217.4	11.2	4.2	4.90	5.136	0.236	8.272	8.036	13.52	14.16
11.1	219.5	14.9	5.5	6.20	6.439	0.239	9.436	9.197	17.02	17.67
12.4	221.7	18.6	6.8	7.53	7.775	0.242	10.589	10.347	20.58	21.22
13.8	224.2	22.3	8.2	8.90	9.145	0.245	11.797	11.552	24.19	24.83
15.1	226.7	26.0	9.5	10.22	10.465	0.249	13.161	12.912	27.63	28.28
16.4	229.3	29.7	10.8	11.53	11.786	0.252	14.517	14.265	31.04	31.68
17.9	232.4	33.4	12.3	13.00	13.257	0.257	15.915	15.658	34.79	35.44

Table 4.4

Cont.

19.4	235.6	37.1	13.8	14.52	14.778	0.261	17.522	17.261	38.62	39.27
21.0	239.0	40.8	15.4	16.08	16.348	0.265	19.224	18.959	42.53	43.18
22.5	242.4	44.5	16.9	17.67	17.936	0.269	21.019	20.749	46.43	47.08
24.1	245.8	48.2	18.5	19.22	19.490	0.273	22.800	22.527	50.19	50.85
25.7	249.3	52.0	20.1	20.85	21.127	0.277	24.569	24.292	54.11	54.77
27.3	252.6	55.7	21.7	22.40	22.682	0.282	26.377	26.096	57.77	58.43
28.9	256.0	59.4	23.3	24.03	24.318	0.285	28.069	27.785	61.58	62.24
30.4	259.2	63.1	24.8	25.57	25.855	0.288	29.801	29.513	65.10	65.76
31.9	262.3	66.8	26.3	27.07	27.359	0.293	31.422	31.129	68.51	69.16
33.6	265.5	70.5	28.0	28.70	28.996	0.296	32.981	32.686	72.16	72.81
35.2	268.7	74.2	29.6	30.28	30.582	0.299	34.581	34.282	75.64	76.30
36.8	271.6	77.9	31.2	31.93	32.235	0.302	36.121	35.820	79.22	79.87
38.5	274.6	81.6	32.9	33.58	33.888	0.305	37.550	37.245	82.75	83.39
40.1	277.5	85.3	34.5	35.25	35.557	0.307	39.024	38.716	86.25	86.89
42.0	280.4	89.0	36.4	37.12	37.427	0.310	40.441	40.131	90.10	90.73
43.7	283.5	92.7	38.1	38.82	39.130	0.313	41.851	41.538	93.55	94.18
45.1	285.6	95.0	39.5	40.25	40.566	0.316	43.350	43.034		
46.4	304.2	96.4	40.8	41.52	41.517	0.000				

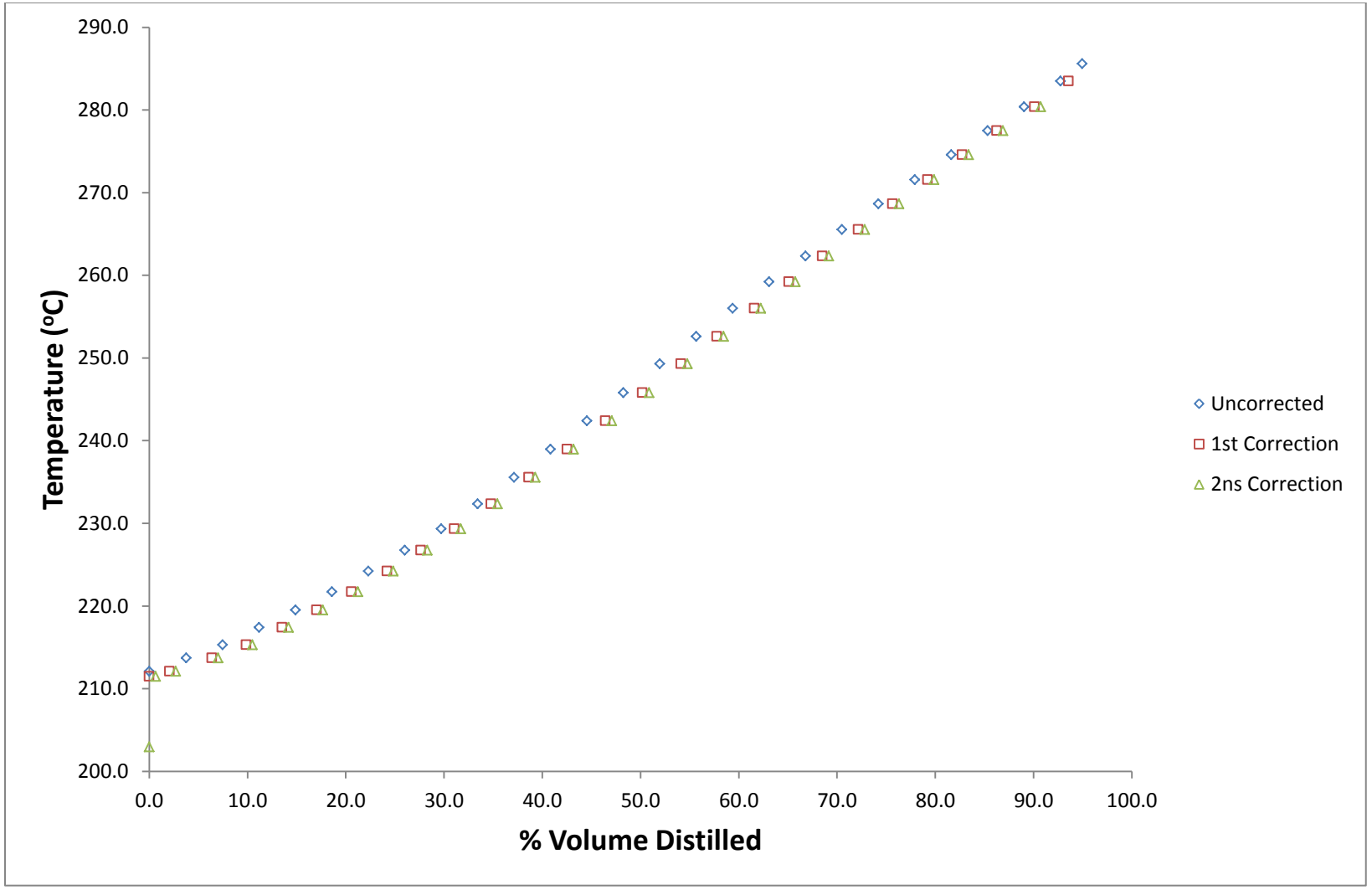

Figure 4.18 Uncorrected and corrected distillation curve for complete mixing model

4.3 Empirical Modeling of the Results

To better predict the behavior of the experimental data, an empirical modeling was done to represent the experimental data. To do this some assumptions were made.

4.3.1 Assumptions for empirical modeling. To model the process as completely mixing, some assumptions as were made as bulleted below**.**

1. It was assumed boiling hydrocarbon mixture was a pure pseudo carbon compound of different boiling points.
2. The pseudo carbon compounds condenses at its dew point
3. The Raoult's law [20] applies in this case because the activity coefficients of pure hydrocarbons are almost unity.
4. The first drop of distillate that appears at the condenser intake is the first hydrocarbon that vaporizes from the liquid.
5. The first hydrocarbon vaporizes at the observed initial boiling temperature during the experiment, thus when the fluid was observed to have started boiling at 201.6^{o}C.
6. The vapor that takes off is in equilibrium with its liquid just at the liquid surface.
7. The pseudo hydrocarbon vapor condenses at a temperature (T2) lower than its dew point due to the presence of air in the control volume.
8. The air in the control volume decay exponentially due to the profile of the experimental data of the flask head temperature T2

4.3.2 Procedure for empirical modeling. The steps written below were followed in modeling the experimental data to calculate the dew point temperatures as well as the pseudo hydrocarbon vapor compositions**.**

1. To better represent the experimental data for T0 and T2 to be used in the modeling process, fitted polynomial correlations were generated for both T0 and T2 after the Sydney Young correction [4] to atmospheric pressure. Equations 4.44 and 4.45 respectively represent T0 and T2 correlations. Figures 4.19 and 4.20 also respectively represent T0 and T2 fitted plots. The correlation coefficients for T0 and T2 curves are 0.9986 and 0.9976 respectively.

$$r_1 = -7.0074 \times 10^{-8};\ r_2 = 1.0966 \times 10^{-5};\ r_3 = -6.5719 \times 10^{-4}$$

$$r_4 = 0.01808;\ r_5 = -0.20469;\ r_6 = 2.2786;\ r_7 = 202.94$$

$$T_0 = r_1 t^6 + r_2 t^5 + r_3 t^4 + r_4 t^3 + r_5 t^2 + r_6 t + r_7 \qquad (4.44)$$

$$s_1 = -3.9746 \times 10^{-7};\ s_2 = 6.5263 \times 10^{-5};\ s_3 = -4.2467 \times 10^{-3};\ s_4 = 0.13838$$

$$s_5 = -2.3465;\ s_6 = 21.628;\ s_7 = 124.32;$$

$$T_2 = s_1 t^6 + s_2 t^5 + s_3 t^{43} + s_4 t^3 + s_5 t^2 + s_6 t + s7 \qquad (4.45)$$

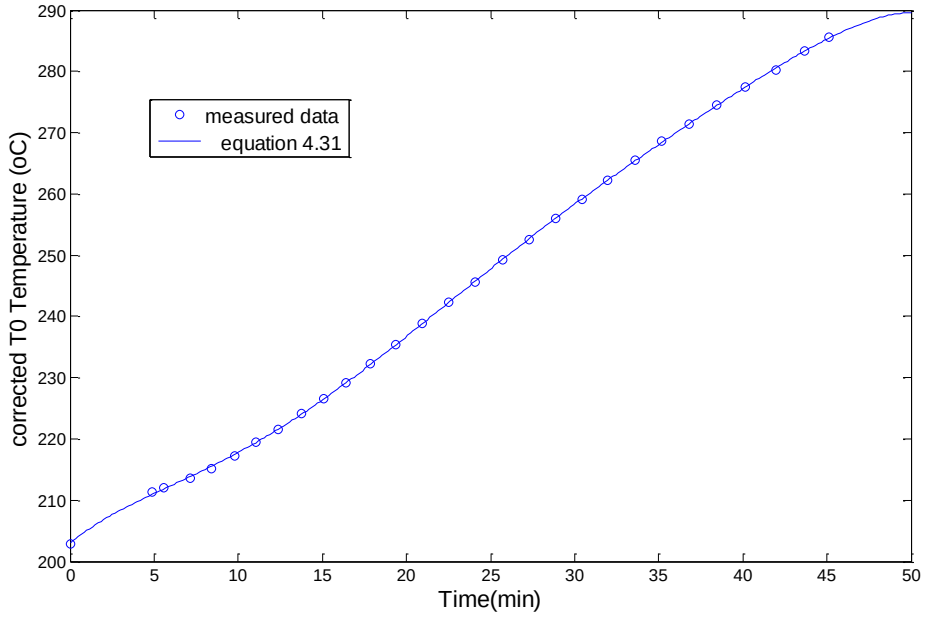

Figure 4.19 Measured T0 and T0 calculated from equation 4.44are plotted as a function of time

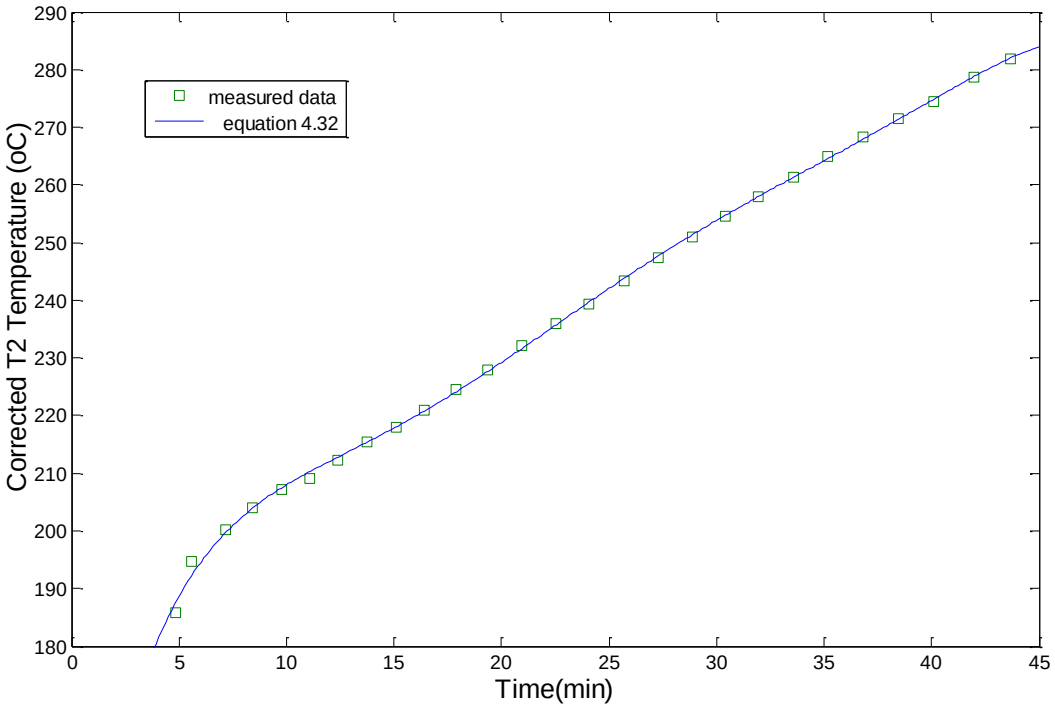

Figure 4.20 Measured T2 and T2 calculated from equation 4.45 are plotted as a function of time

2. To model the mixture as a pseudo pure carbon compound, the boiling point temperatures (T_0) correlation from equation 4.44 was used to calculate the carbon numbers (C_n) for each time step using the m.file in appendix A4 sub-function 'calCn' with the bisection [21] sub-function 'Bisect2'code in appendix A4
3. From the experimental data, the first drop of distillate appeared 4.87 minutes from time the fluid was observed to have started boiling, however 4.6 minutes was used as it gave a temperature (184.6^{o}C) using the T2 fit which was closer to the experimental time of 184.5^{o}C. This initial time (t_o) was used to calculate for the corresponding $T2_o$ using the fitted curve correlation in equation 4.33. The calculated value $T2_o$ at this time is 184.6^{o}C.

4. The critical temperature in Kelvin of the initial pseudo pure carbon number which vaporized first at T0 = 201.6°C was calculated with equation 4.46 [22]

$$ln(960 - T_c) = 6.8162 - 0.2115\ {C_n}^{2/3} \qquad (4.46)$$

5. The reduced temperature Tr for T2o was calculated with equation 4.47

$$T_r = \frac{T2_o}{T_c} \qquad (4.47)$$

6. The critical pressure Pc in bar was then calculated with equation 4.48 [19, 22]

$$P_c = \frac{M}{(0.339 + 0.226\ C_n)^{\,2}} \qquad (4.48)$$

Where M, is the molecular or molar mass of the hydrocarbon which was calculated from a fitted correlation generated from carbon number vs. molar mass data from reference [19]. The carbon numbers used for the fitting was C_7H_{16} (Heptane) to $C_{20}H_{42}$ (Icosane). Equation 4.49 gives the correlation for M as a function of carbon number. See appendix B, figure B2 for fitted curve.

$$M = -7.327e-007Cn^4 + 4.137e-005Cn^3 - 0.0008.337Cn^2 + 14.03Cn + 1.995 \qquad (4.49)$$

7. The equations 4.50 and 4.51 were used for the representation of the vapor-pressure P^{sat} is the four-constant form by Wagner. [22]

$$ln\left(\frac{P^{sat}}{P_c}\right) = lnP_r^{(0)} + \omega\ lnP_r^{(1)} + \omega^2\ lnP_r^{(2)} \qquad (4.50)$$

$$ln\left(P_r^{(i)}\right) = \frac{(a_i\ \tau + b_i\ \tau^{1.5} + c_i\ \tau^{2.5} + d_i\ \tau^5)}{T_r} \qquad (4.51)$$

$$where \quad \tau = 1 - T_r \quad and \quad i = 0, 1, 2$$

The constants for a b c and d are given in table 4.5.

The acentric factor was fitted as a function of carbon number and the correlation used all calculations. The data used for fitting were taken from reference [22]. The correlation is given below. See appendix B, figure B1 for fitted curve.

$$k_1 = 5.925 \times 10^{-7};\ k_2 = -4.518 \times 10^{-5};\ k_3 = 0.001404;\ k_4 = 0.02272;$$

$$k_5 = 0.2013;\ k_6 = -0.8766;\ k_7 = 1.735$$

$$\omega = k_1 Cn^6 + k_2 Cn^5 + k_3 Cn^4 + k_4 Cn^3 + k_5 Cn^2 + k_6 Cn + k_7 \qquad (4.52)$$

Table 4.5

Constants for calculating vapor pressure [22]

	$P_r^{(0)}$	$P_r^{(1)}$	$P_r^{(2)}$
a	-5.97616	-5.03365	-0.64771
b	1.29874	1.1150	2.41539
c	-0.60394	-5.41217	-4.26979
d	-1.06841	-7.46628	3.25259

8. With the vapor pressure calculated for the first pseudo hydrocarbon vapor that condenses, Raoult's Law was applied to calculate the initial vapor composition (y_{vo}) at the time the first drop of distillate was observed with equation 4.53. The Raoult's vapor liquid equilibrium equation [20] is given as

$$y_v P = x P^{sat} \qquad (4.53)$$

Since the liquid is assumed as pure pseudo compound, just at the surface he vapor is in equilibrium with the liquid and we assumed vapor is almost air, hence $x = 1$.

$$y_v = \frac{P^{sat}}{P} \qquad (4.54)$$

$$y_{vo} = \frac{P^{sat}|_{T2_0=188\,o_C}}{P} \qquad (4.55)$$

9. Equation 4.56 was then used to calculate for the air composition at when the first drop of distillate appeared.

$$y_{Ao} = 1 - y_{vo} \qquad (4.56)$$

10. With the assumption that the air decay exponentially we can write

$$y_A = y_{Ao}\, exp\left(-\frac{t - t_{initial}}{\tau}\right) \qquad (4.57)$$

$$y_v = 1 - y_{Ao}\, exp\left(-\frac{t - t_{initial}}{\tau}\right) \qquad (4.58)$$

where τ is the mean residence time of the vapor in the control volume which has to be determined to represent the behavior of the experimental data.

11. After calculating the initial air composition from using the initial observed condensation temperature, with the help of equation 4.55 and equation 4.56, the next step is to calculate the saturation pressure for the next carbon number.
12. Since the vapor composition for the next carbon number is not known, we assume that the vapor composition is the same as the previously calculated one ($y_{vinitial}$).
13. The saturation pressure is then calculated using equation 4.50.
14. Equation 4.47 is then used to calculate for the condensation temperature
15. The saturation temperature is then used to calculate for the time (t2) from the fitted condensation temperature data correlation in equation 4.45.

16. The condensation time (t2) is then substituted in equation 4.58 to calculate for the actual vapor composition with an iteration error of 0.000001. The error is given as

$$error = \frac{y_{vnew} - yv_{guess}}{y_{vnew}} \times 100 \qquad (4.59)$$

17. The iterated vapor composition (y_v), is then used to calculate for the actual saturation pressure of that carbon number in consideration.
18. The calculation is repeated for the next carbon number which is calculated from the boiling temperature correlation in equation 4.44 in conjunction with the bisection iteration sub-function as in appendix A4.
19. The next now is to calculate the vapor travel time using calculated t2 values and the T0 time scale used in calculating the carbon numbers. The vapor travel time is finally calculated as the difference in the bubble point temperature time (t) and the calculated dew point temperature time (t2) from step 15. This is represented in equation 4.60.

$$t_r = t_2 - t \qquad (4.60)$$

20. The vapor travel time are then added to the time delay or the hold-up time as described by Laya [5] and the total time is then used to correct the %V using equation 3.3.

4.3.3 Results of empirical modeling. See appendix B2 for calculated values of the empirical modeling. Figure 4.21 shows the travel time of the vapor for varying mean residence time and figure 4.22 shows the corresponding hydrocarbon vapor composition profile. Further figures 4.23, 4.24 and 4.25 illustrates the profile of T0 and T2 with boiling and condensation tie-points for varying mean residence time of 5, 7 and 10.

Since the mean residence time (τ) was not exactly known, the experimental results were used to model for varying τ to see the effect of the results compared to the experimental data. It was found out that τ between 5 and 10 were within the experimental region. When the time constant was increased to 15, the travel time went into the negative time zone. This is actually not practical and does not make sense as a negative travel time suggest condensation occurred before the liquid started boiling. The boiling-condensation tie points for τ=15 have not been shown due to the explanation just mentioned above.

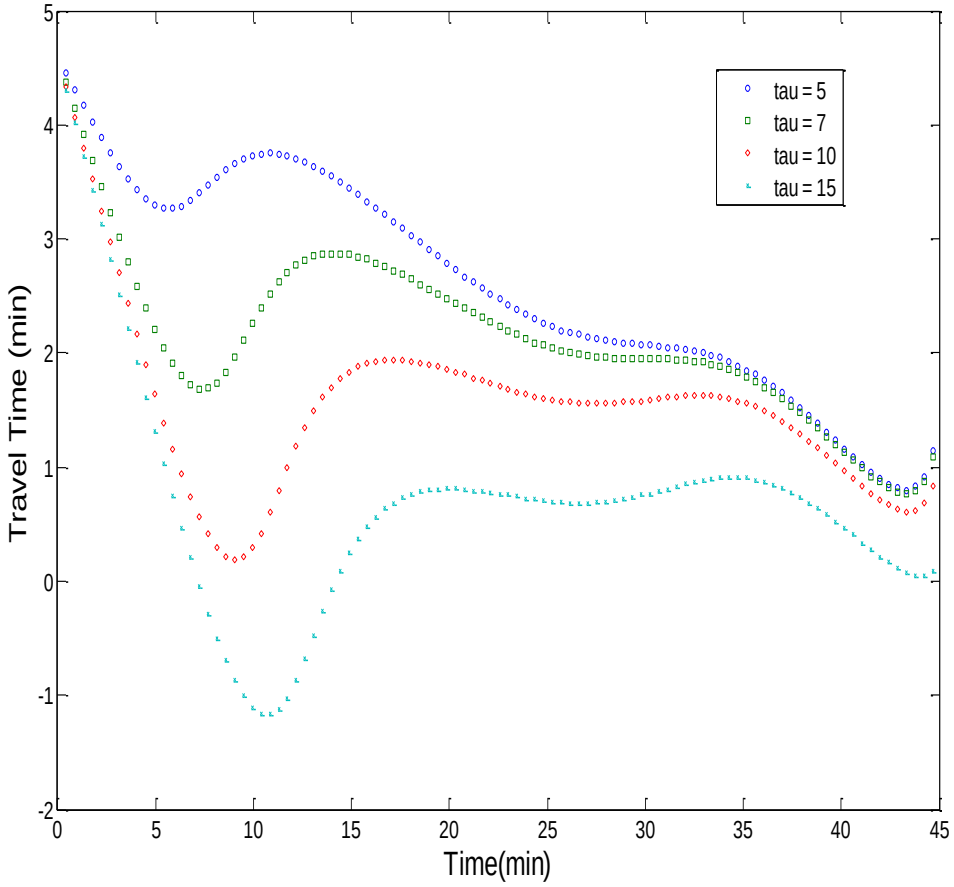

Figure 4.21 Hydrocarbon Vapor Travel Time for varying time constants

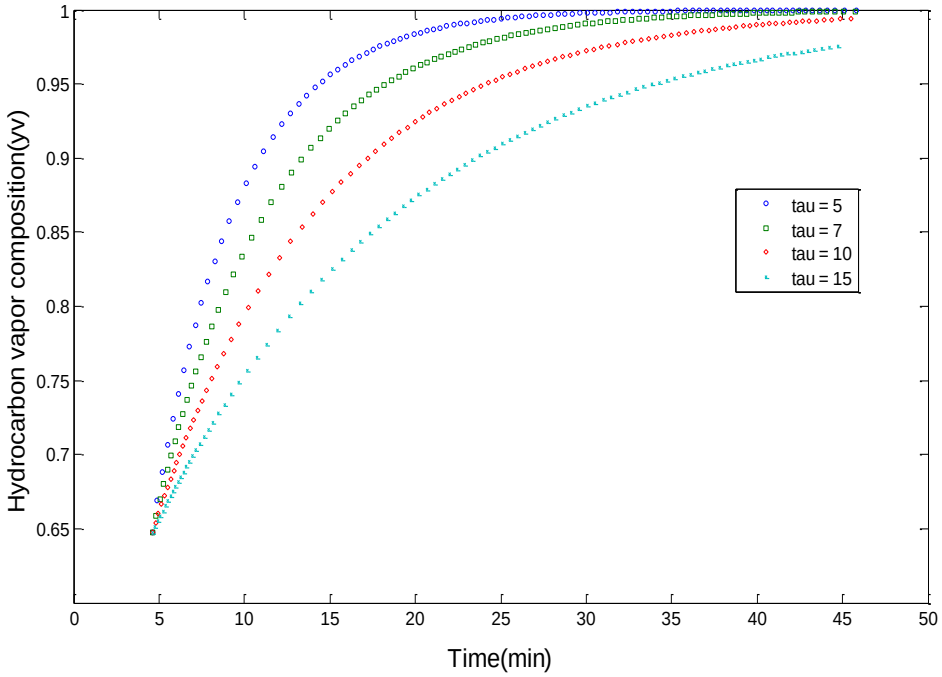

Figure 4.22 Hydrocarbon Vapor Composition for varying time constants

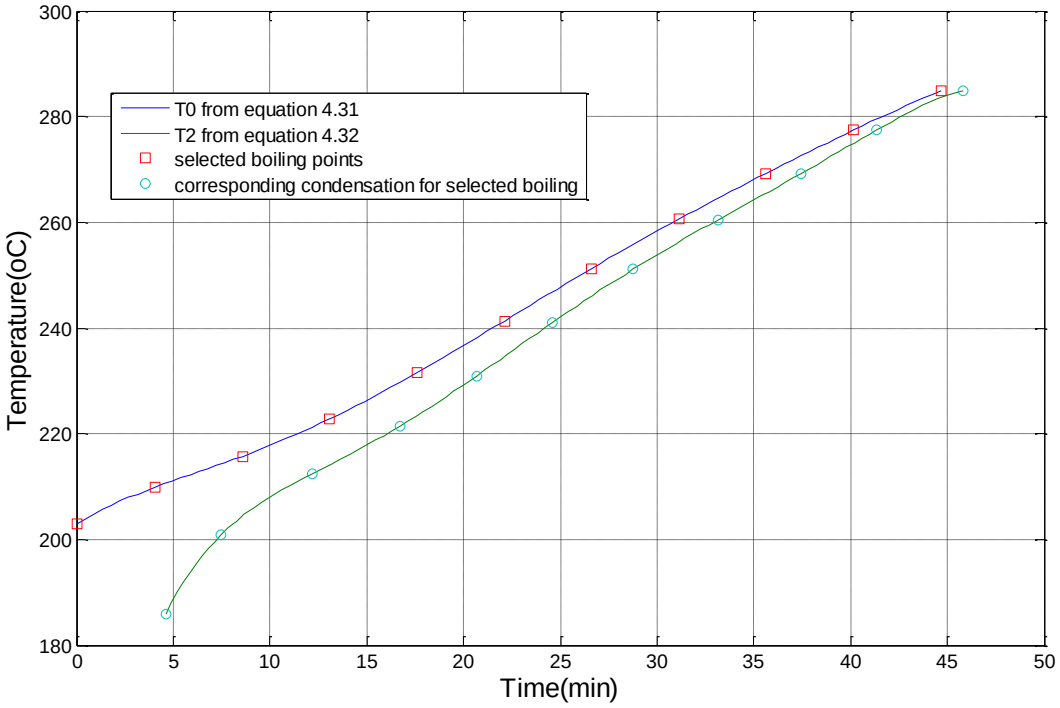

Figure 4.23 Boiling-condensation tie points for τ =5

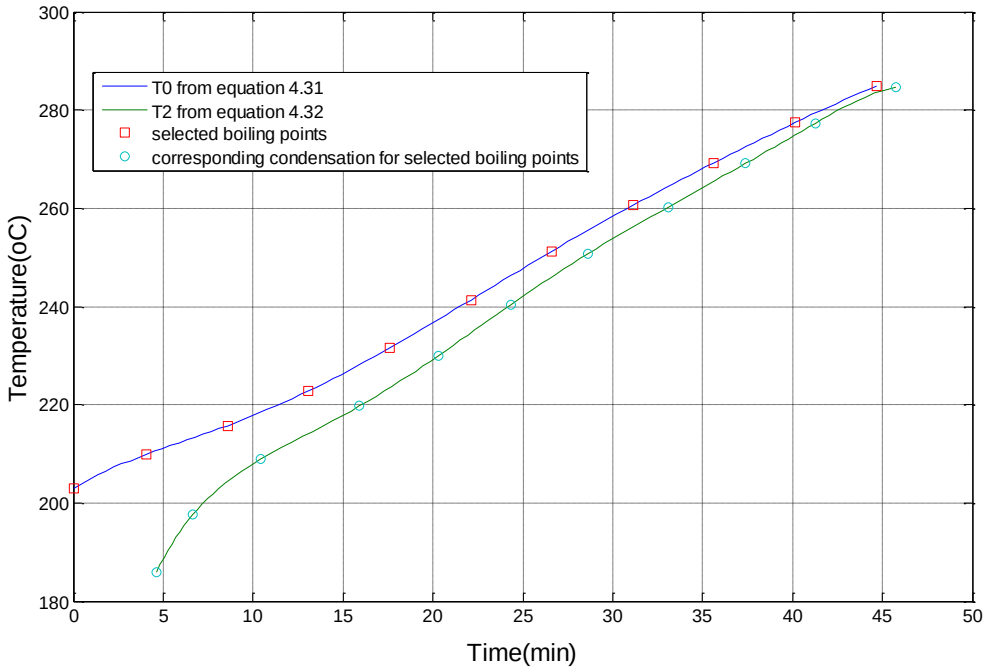

Figure 4.24 Boiling-condensation tie points for τ =7

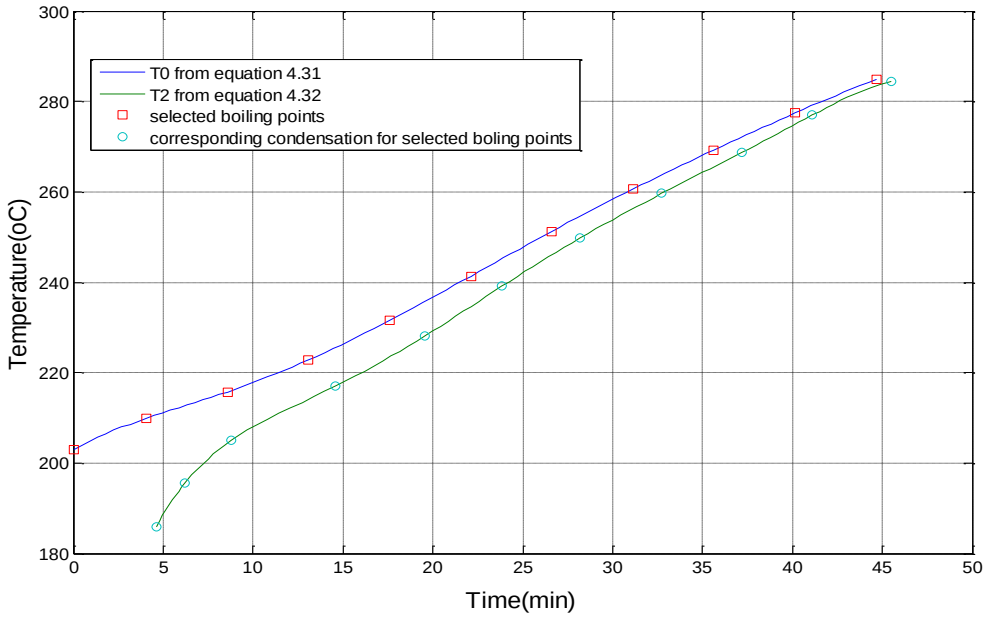

Figure 4.25 Boiling-condensation tie points for τ = 10

4.4 Effect of Removing the Waviness in Vapor Travel Time

To check if the waviness in the vapor travel time can be smoothened, a simple model was done by taking an approximate average of the travel time (t_r) from the empirical model and the values used to fit 2nd order polynomial for the travel time. The travel time results were then used to calculate for the condensation time (t_2) using equation s 4.60 and 4.61. The m.file in appendix A5 was then used to calculate for the vapor composition (yv) of the vapor.

Travel time smoothened equation is given as below.

$$tr = = \ 0.0011t^2 \ - \ 0.1311t \ + \ 4.58 \qquad (4.61)$$

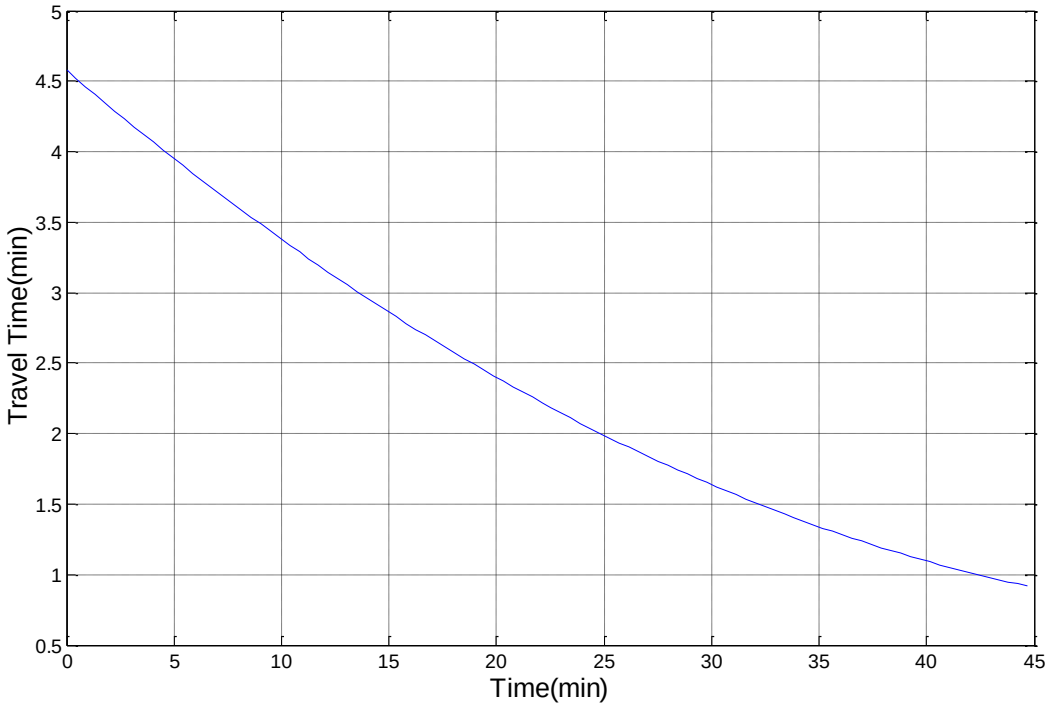

Figure 4.26 Smoothened Travel Time curve

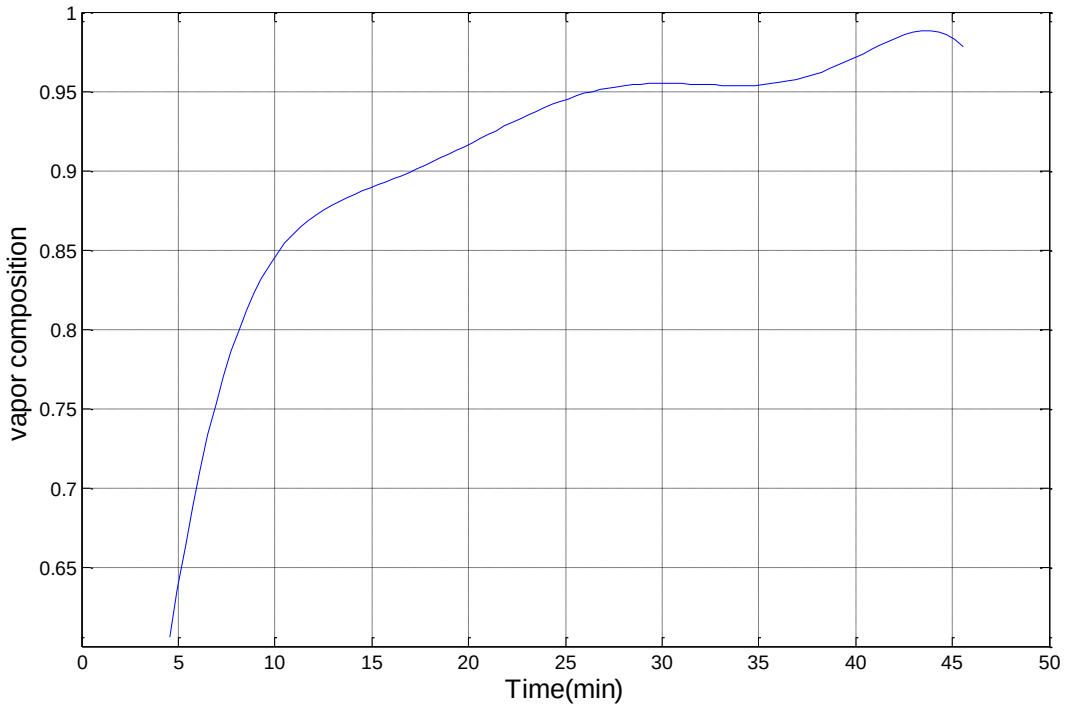

Figure 4.27 Hydrocarbon vapor composition with waviness

From figure 4.29, it notices that the exponential decay function used for the air composition does not fit the model very well if the travel time is to be smoothened. An improved function for the air decay will have to be looked into in future.

4.5 Corrected Temperature - Volume Profile

The results generated from the travel time calculation were used to correct the temperature and percent volume distilled. The correction was done in two steps. The first correction look as the time delay in the condenser and the second correction considers both the delay time and the vapor travel time. Equation 3.3 was used to calculate the percent volume correction. The new time scale used was the time for the receiver plus the summation of the delay and vapor travel time with the time being when the first vapor was observed to have started rising. Thus at time zero for the receiver, the corresponding time on the new time scale will be

(0.87 + 4.87) = 5.75 min. However 4.6min was used in calculation instead of 4.87min as explained earlier. Figure 4.28 shows the correction for the temperature- volume curve.

In the second volume correction the last travel time (1.01 min) was added to the ending time (38.82 min) of the condenser time scale to get the maximum time (39.83 min) on the time scale with reference to the vapor take off from the liquid surface. The time range from 0 min to 39.83 was then divided into 100 steps and each step of time corresponded to the travel time calculated. This 100 time steps were used with equation 3.2 to calculate the new percent volume recovery. The boiling temperature was then shifted to start from when the initial boiling started and the resulted plot is shown in figure 4.30.

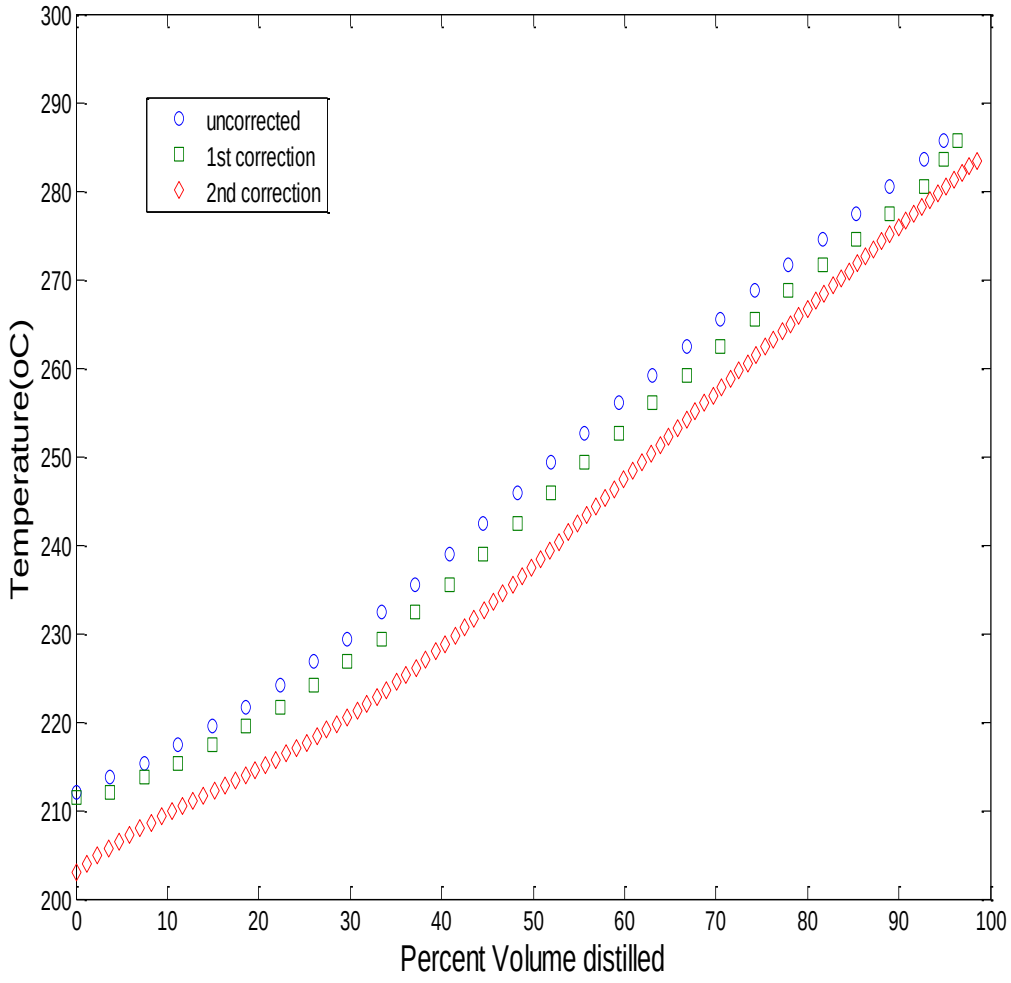

Figure 4.28 Uncorrected and corrected distillation curve for equal volume decane, dodecane, tetradecane and hexadecane for empirical model with τ =7.

4.6 Testing the Developed Empirical Model

The developed model was tested then tested with two experiments to ascertain to accuracy and reproducibility of the earlier experimental data. The first experiment done was a repetition of the four component mixture of equal 50ml volume of decane, dodecane, tetradecane and hexadecane. The room pressure recorded was 98.4mbar and the experimental data results are displayed in table

Table 4.6

Results for 2nd run Decane,Dodecane, Tetradecane and Hexadecane (Room Pressure = 98.4kPa)

Time Step (min)	Time (min)			Uncorrected Temperature (^oC)			Corrected Temperature (^oC)			Rec reading	Receiver Vol (ml)	% Uncorrected Volume Distilled
	t	t_c	t_r	T2	T1	T0	T2	T1	T0	x	V	
0.00				24.8	27.2	30.37	25.58	27.98	31.16			
5.00				24.8	28.9	35.34	25.58	29.69	36.14			
10.00				24.8	33.7	47.01	25.58	34.50	47.85			
15.00				24.9	41.0	61.13	25.68	41.82	62.00			
20.00				25.2	49.6	76.75	25.98	50.44	77.66			
25.00				25.5	59.7	92.86	26.28	60.57	93.81			
30.00				26.1	64.9	108.80	27.08	65.78	109.80			
32.00				26.3	67.7	114.90	27.48	68.59	115.91			
34.00				26.7	72.2	121.20	27.78	73.10	122.23			
36.00				27.0	75.6	128.00	28.28	76.51	129.05			
38.00				27.5	81.0	133.50	28.69	81.92	134.56			
40.00				27.9	85.9	139.50	28.69	86.84	140.58			
42.00				28.4	90.7	145.50	29.19	91.65	146.59			
44.00				28.9	95.3	151.30	29.69	96.26	152.41			
46.00				29.9	99.8	160.00	30.69	100.77	161.13			
48.00				30.2	104.8	163.00	30.99	105.79	164.14			
50.00				31.1	109.3	168.50	31.89	110.30	169.65			

Table 4.6
Cont.

52.00				32.3	115.1	176.80	33.10	116.11	177.97			
54.00				32.8	118.3	179.50	33.60	119.32	180.68			
54.33				33.1	121.2	182.20	33.90	122.23	183.39			
54.50				33.3	122.6	183.10	34.10	123.63	184.29			
55.00				33.5	123.2	183.70	34.30	124.23	184.89			
55.50				33.7	125.5	185.10	34.50	126.54	186.30			
56.00				33.8	127.4	186.40	34.60	128.45	187.59			
56.50				33.9	129.8	187.20	34.70	130.85	188.40			
57.00				34.1	132.1	189.10	34.90	133.16	190.30			
57.50				34.2	134.2	190.20	35.00	135.26	188.40			
58.00				34.3	134.5	190.80	35.10	135.56	191.41			
58.50				34.6	134.7	191.20	35.40	135.76	192.01			
59.00				34.7	134.9	191.70	35.50	135.96	192.91			
59.50				35.0	135.2	192.00	35.80	136.27	193.21			
60.00				36.0	136.1	192.50	36.81	137.17	193.71			
63.20	0.00			36.6	160.8	202.10	37.41	161.93	203.34			
64.00	0.80			38.2	172.1	204.10	39.01	173.26	205.35			
65.00	1.80			41.1	181.3	205.20	41.92	182.49	206.45			
66.00	2.80			45.3	187.1	206.10	46.13	188.30	207.35			
67.00	3.80			51.4	192.2	208.00	52.25	193.41	209.26			
68.15	4.95	0.00		184.7	196.7	210.30	185.89	197.93	211.56			
68.50	5.30	0.35		189.4	196.9	210.80	190.61	198.13	212.03			

Table 4.6
Cont.

69.03	5.83	0.88	0.00	192.6	198.7	211.50	193.82	199.93	212.76	0.0	0.00	0.0%
71.40	8.20	3.25	2.37	197.2	202.1	214.47	198.43	203.34	215.74	0.8	4.55	2.3%
72.88	9.68	4.73	3.85	201.4	208.0	216.82	202.65	209.30	218.10	1.0	7.51	3.8%
74.23	11.03	6.08	5.20	204.8	210.7	219.01	206.03	211.98	220.30	1.5	14.93	7.5%
75.65	12.45	7.50	6.62	208.1	213.3	221.37	209.39	214.54	222.66	2.0	22.34	11.2%
76.82	13.62	8.67	7.78	210.8	215.3	223.34	212.04	216.53	224.64	2.5	29.76	14.9%
78.32	15.12	10.17	9.28	214.0	217.7	225.92	215.31	219.02	227.22	3.0	37.17	18.6%
79.97	16.77	11.82	10.93	217.5	220.5	228.82	218.77	221.81	230.13	3.5	44.59	22.3%
81.72	18.52	13.57	12.68	221.1	223.6	231.96	222.35	224.89	233.27	4.0	52.00	26.0%
83.12	19.92	14.97	14.08	223.9	226.2	234.51	225.18	227.50	235.83	4.5	59.42	29.7%
83.97	20.77	15.82	14.93	225.6	227.9	236.08	226.88	229.16	237.41	5.0	66.83	33.4%
85.55	22.35	17.40	16.52	228.7	231.1	239.03	230.06	232.38	240.36	5.5	74.25	37.1%
87.25	24.05	19.10	18.22	232.2	234.7	242.24	233.49	236.03	243.59	6.0	81.66	40.8%
88.85	25.65	20.70	19.82	235.4	238.3	245.30	236.76	239.63	246.65	6.5	89.08	44.5%
90.75	27.55	22.60	21.72	239.4	242.7	248.97	240.70	244.04	250.33	7.0	96.49	48.2%
92.43	29.23	24.28	23.40	242.9	246.6	252.22	244.25	248.00	253.59	7.5	103.91	52.0%
94.25	31.05	26.10	25.22	246.8	250.9	255.75	248.17	252.27	257.13	8.0	111.32	55.7%
95.90	32.70	27.75	26.87	250.4	254.7	258.95	251.77	256.06	260.33	8.5	118.74	59.4%
97.52	34.32	29.37	28.48	254.0	258.3	262.06	255.34	259.65	263.46	9.0	126.15	63.1%
99.85	36.65	31.70	30.82	259.1	263.1	266.48	260.51	264.52	267.89	9.5	133.57	66.8%
101.25	38.05	33.10	32.22	262.2	265.8	269.09	263.60	267.25	270.50	10.0	140.98	70.5%
103.17	39.97	35.02	34.13	266.4	269.3	272.10	267.78	270.74	273.52	10.5	148.40	74.2%

Table 4.6
Cont.

105.83	42.63	37.68	36.80	271.9	273.8	277.20	273.35	275.20	278.64	11.0	155.81	77.9%
107.38	44.18	39.23	38.35	275.0	276.3	278.90	276.41	277.68	280.34	11.5	163.23	81.6%
108.00	44.80	39.85	38.97	276.2	277.2	281.60	277.59	278.68	283.05	12.0	170.64	85.3%
109.42	46.22	41.27	40.38	278.7	279.6	283.9	280.14	281.04	285.35	12.5	178.06	89.0%
110.13	46.93	41.98	41.10	279.9	280.8	285.1	281.33	282.28	286.56	13.0	185.47	92.7%
110.50	47.30	42.35	41.47	280.5	282.9	285.7	281.93	284.35	287.16	13.1	186.95	93.5%
111.35	48.15	43.20	42.32	282.1	283.7	285.9	283.55	285.15	287.36	13.2	188.44	94.2%
112.05	48.85	43.90	43.02	282.4	284.4	286.0	283.85	285.85	287.46	13.4	191.40	95.7%
113.03	49.83	44.88	44.00	282.6	285.2	286.1	284.05	286.66	287.56	13.5	192.89	96.4%
116.05	52.85	47.90	47.02	281.8	286.1	292.1	283.25	287.56	293.57	13.5	192.89	96.4%

4.6.1 Calculations for repeated four components mixture. The empirical modeling procedure as stated earlier in section 4.3 was followed to model the experimental data. Results for the calculations are shown in table 4.7 for 20 time steps. The fitted curves for T0 and T2 used in the modeling are shown in figures 4.31 and 4.32 with their corresponding equations 4.62 and 4.63. The profiles for the boiling-condensation tie points, vapor composition and travel time are shown in the figures 4.34 to 4.36 below. The parameters that changes in the m.file (iterateforyv) for this calculation are T0 fitted equation, T2 fitted equation, tau (τ) value, initial vapor composition, initial travel time and initial condensation temperature.

$$r_1 = -5.2237 \times 10^{-8};\ r_2 = 7.5290 \times 10^{-6};\ r_3 = -4.1504 \times 10^{-4}$$

$$r_4 = 1.0651 \times 10^{-2};\ r_5 = -1.1476 \times 10^{-1};\ r_6 = 1.9554;\ r_7 = 203.368$$

$$T_0 = r_1 t^6 + r_2 t^5 + r_3 t^4 + r_4 t^3 + r_5 t^2 + r_6 t + r_7 \qquad (4.62)$$

$$s_1 = -7.8255 \times 10^{-8};\quad s_2 = 1.2798 \times 10^{-5};\quad s_3 = -8.5556 \times 10^{-4};$$

$$S_4 = 2.9977 \times 10^{-2};\quad s_5 = -5.796 \times 10^{-1};\ s_6 = 7.8969;\ s_7 = 161.0893;$$

$$T_2 = s_1 t^6 + s_2 t^5 + s_3 t^{43} + s_4 t^3 + s_5 t^2 + s_6 t + s_7 \qquad (4.63)$$

The percent volume recovery fitted equation is as in equation 4.64 and the curve is shown in figure 4.33.

$$\%\, V = 0.0037\, t^2 + 2.0759\, t \qquad (4.64)$$

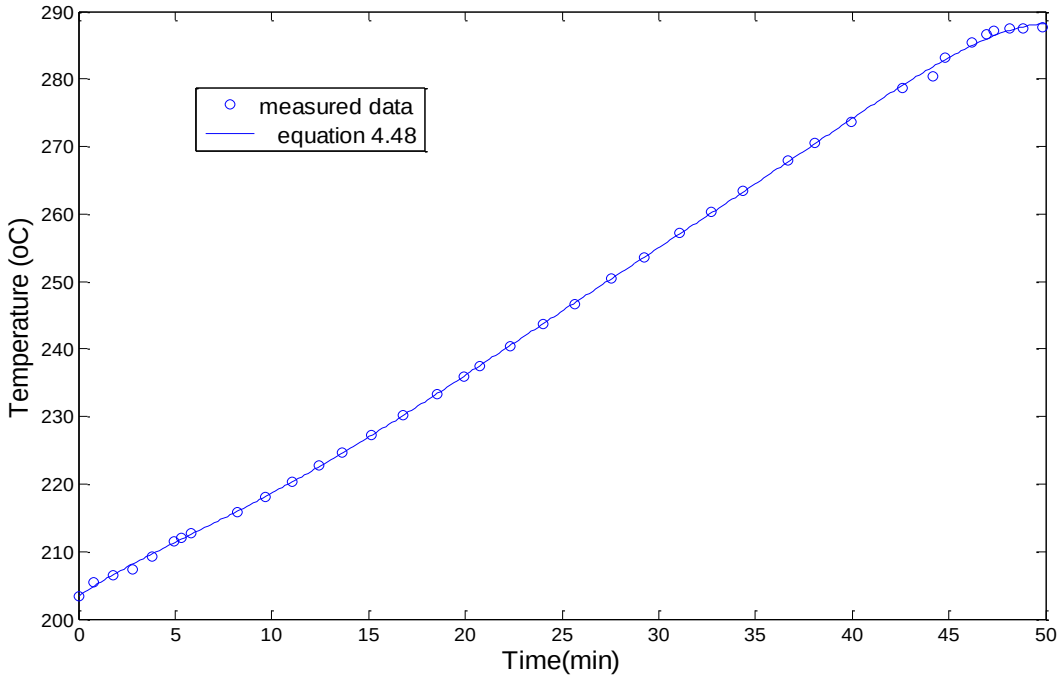

Figure 4.29 Measured T0 and T0 calculated from equation 4.62 are plotted as a function of time

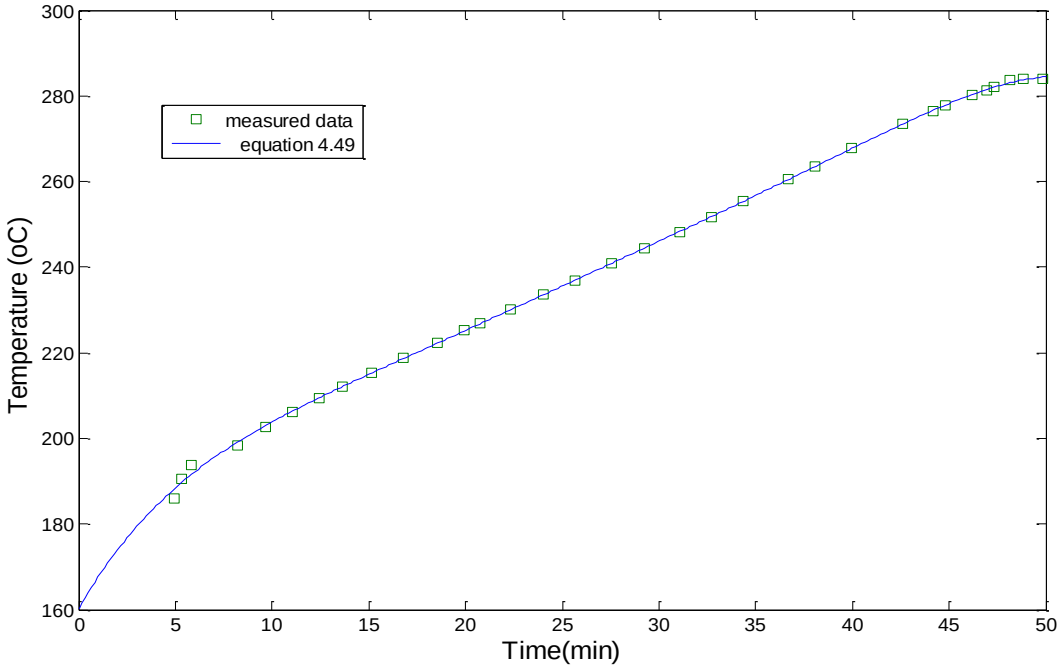

Figure 4.30 Measured T2 and T2 calculated from equation 4.63 are plotted as a function of time

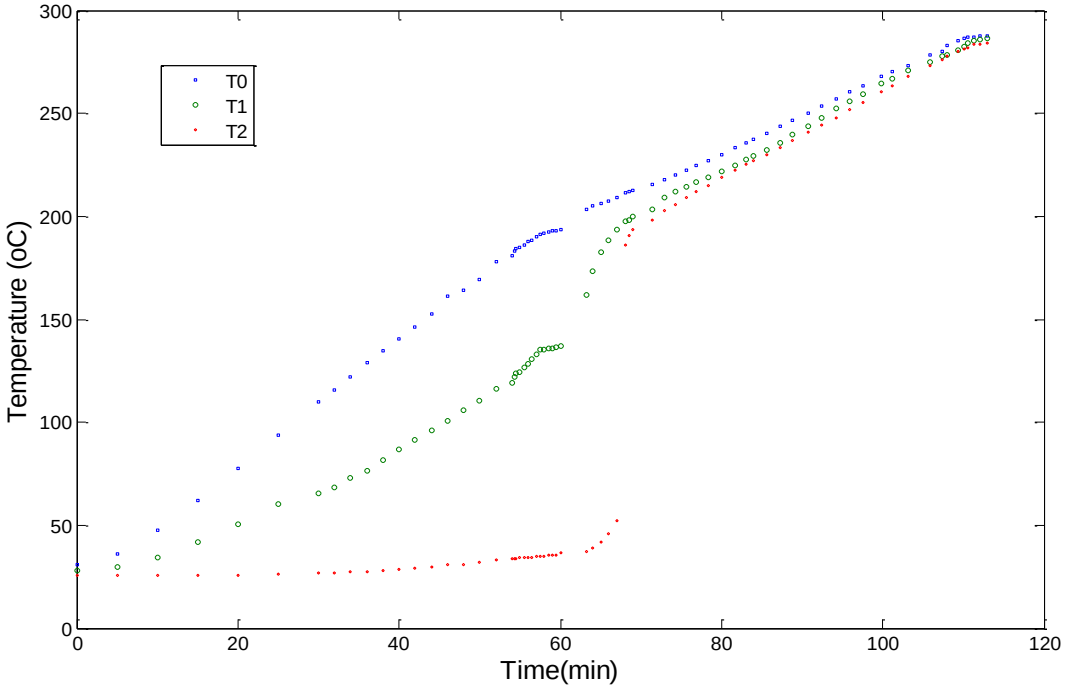

Figure 4.31 Measured for temperatures T0, T1and T2 are plotted with time

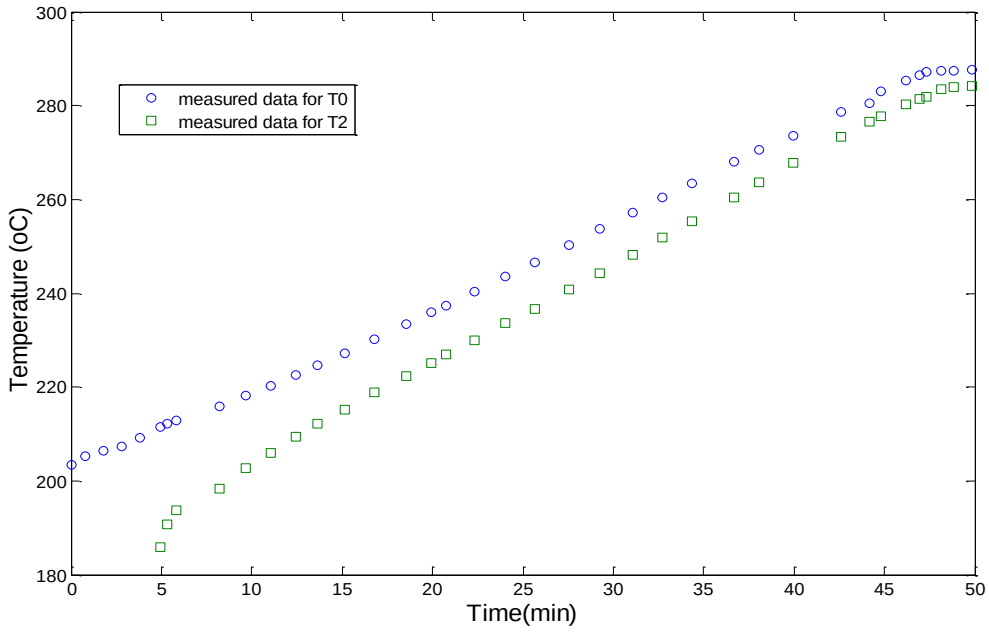

Figure 4.32 Experimental data plot for region of interest for equal volume decane, dodecane, tetradecane and hexadecane

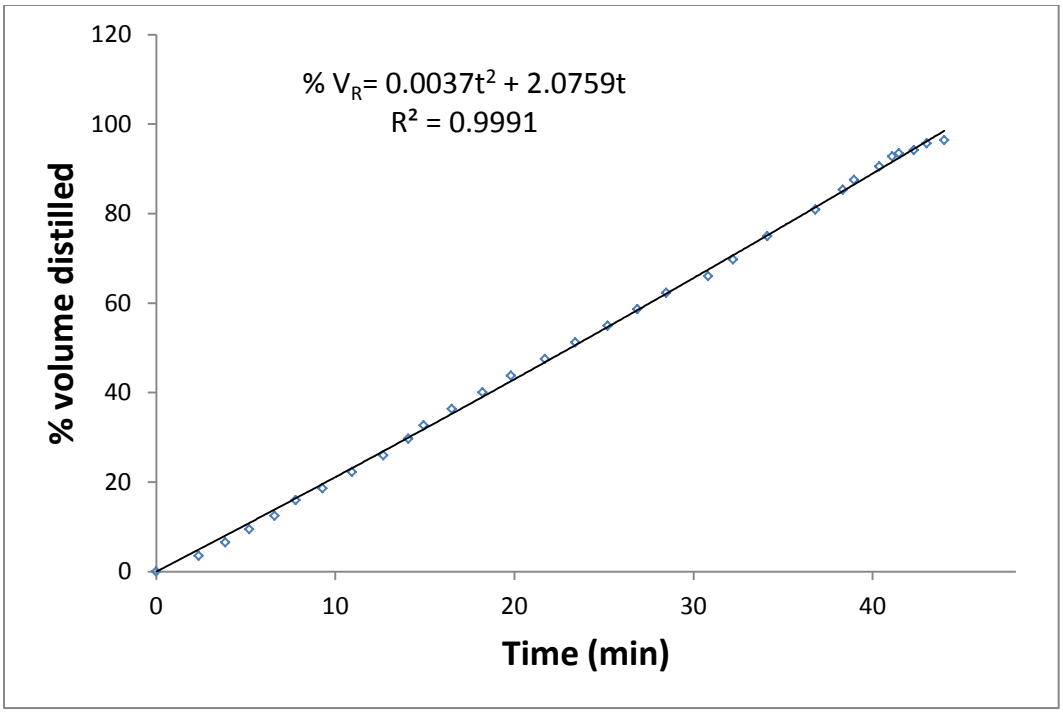

Figure 4.33 Percent volume recovery profile

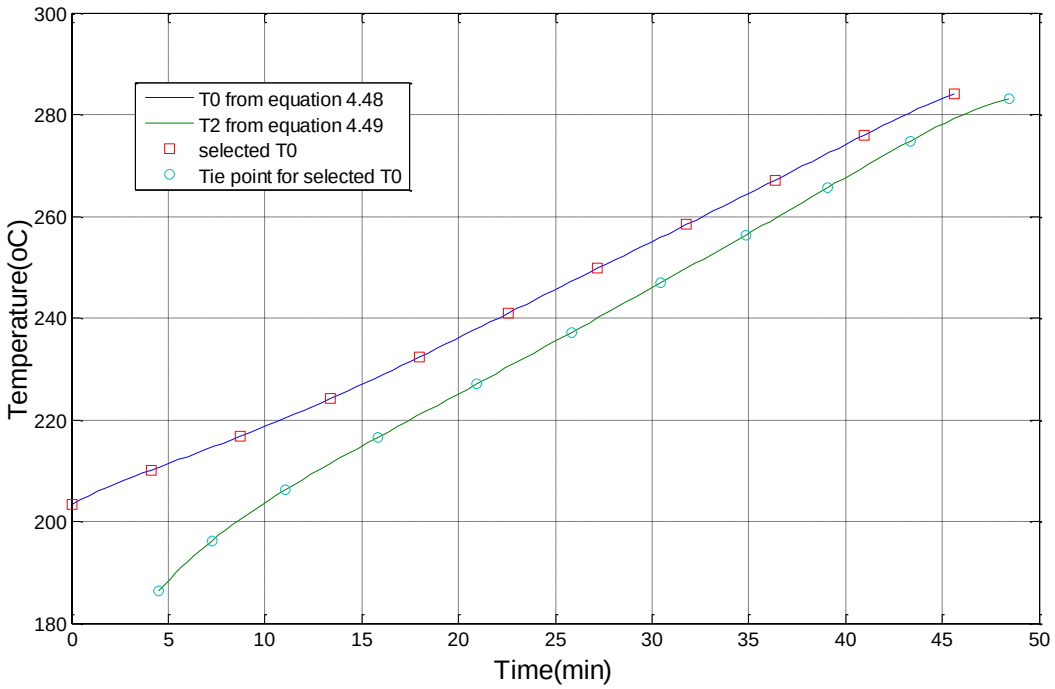

Figure 4.34 Boiling-condensation tie points of decane, dodecane, tetradecane and hexadecane for $\tau = 15$

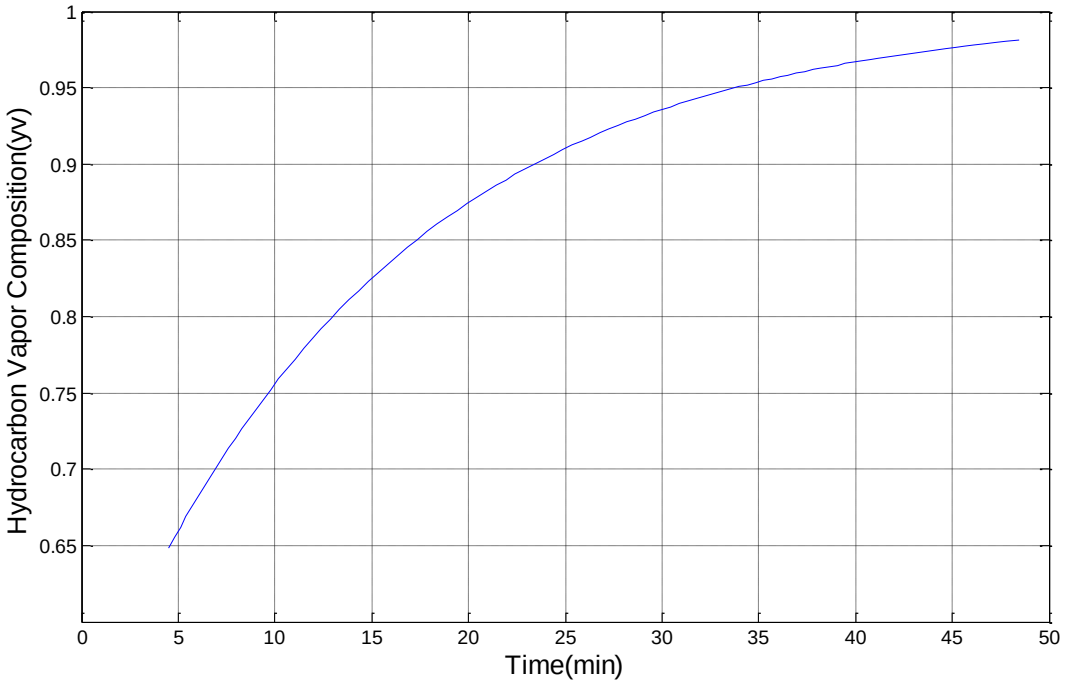

Figure 4.35 Hydrocarbon vapor composition profile of decane, dodecane, tetradecane and hexadecane for $\tau = 15$

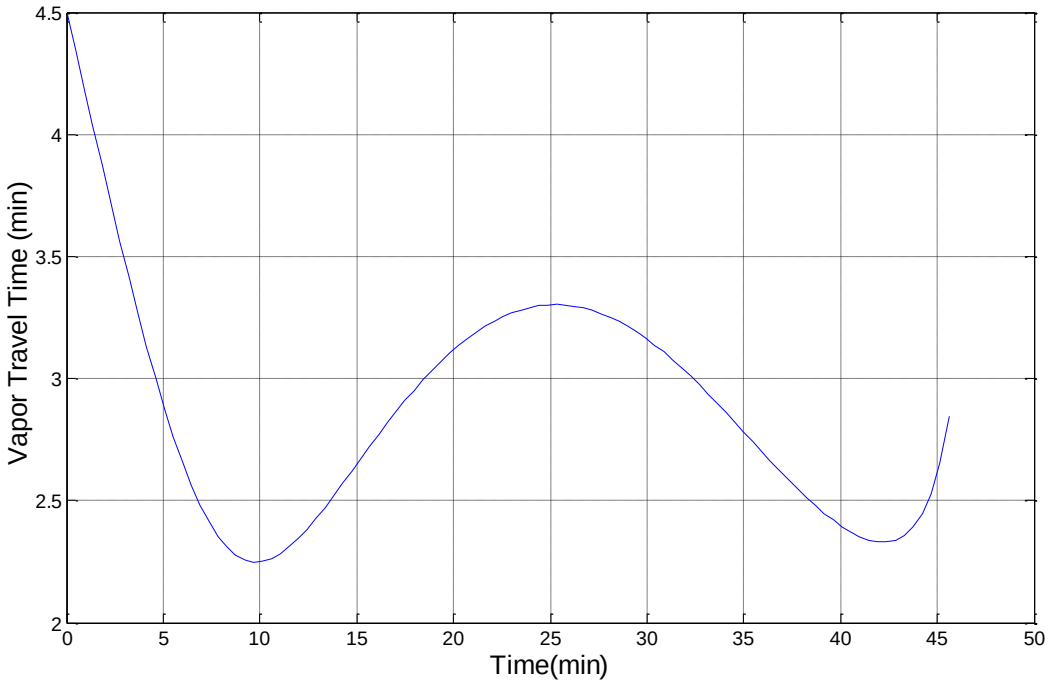

Figure 4.36 Travel time curve of decane, dodecane, tetradecane and hexadecane for $\tau = 15$

Table 4.7

Results for four components (C_{10}, C_{12}, C_{14} and C_{16}) repeated run (τ = 15)

iter	Time	Cn	T0	t2	T2	yv	Psat	tr
1	0	11.3402	203.3683	4.5	186.2861	0.648038	0.65662	4.5
2	2.4	11.5443	207.5343	6.09	192.3642	0.683366	0.69242	3.69
3	4.8	11.7204	211.0863	7.75	197.6666	0.716511	0.72601	2.95
4	7.2	11.8916	214.4966	9.64	202.8069	0.750073	0.76001	2.44
5	9.6	12.0712	218.0353	11.85	208.0661	0.784382	0.79477	2.25
6	12	12.2659	221.8242	14.35	213.4684	0.817442	0.82827	2.35
7	14.4	12.4772	225.8838	16.98	218.9286	0.846874	0.8581	2.58
8	16.8	12.7036	230.1727	19.64	224.3758	0.871731	0.88328	2.84
9	19.2	12.9418	234.6201	22.26	229.7649	0.892266	0.90409	3.06
10	21.6	13.1883	239.1512	24.81	235.0604	0.90913	0.92118	3.21
11	24	13.4398	243.7048	27.29	240.2366	0.922979	0.93521	3.29
12	26.4	13.6946	248.2445	29.69	245.2862	0.934382	0.94676	3.29
13	28.8	13.9523	252.7623	32.02	250.2243	0.943815	0.95632	3.22
14	31.2	14.2139	257.2748	34.29	255.0866	0.951681	0.96429	3.09
15	33.6	14.4815	261.8131	36.5	259.9196	0.958316	0.97101	2.9
16	36	14.757	266.4041	38.7	264.7628	0.963989	0.97676	2.7
17	38.4	15.0407	271.0461	40.9	269.6239	0.968913	0.98175	2.5
18	40.8	15.329	275.6761	43.16	274.4479	0.973259	0.98615	2.36
19	43.2	15.6116	280.1305	45.55	279.0794	0.977202	0.99015	2.35
20	45.6	15.868	284.0984	48.45	283.2291	0.981204	0.9942	2.85

4.6.2 Corrected distillation curve for repeated 4 component mixture. The figure 4.39 below shows the corrected volume profile for the four components mixture of 50ml equal volume of decane, dodecane, tetradecane and hexadecane. It can be seen that for the same volume distilled the difference in the shifted boiling temperature is significant.

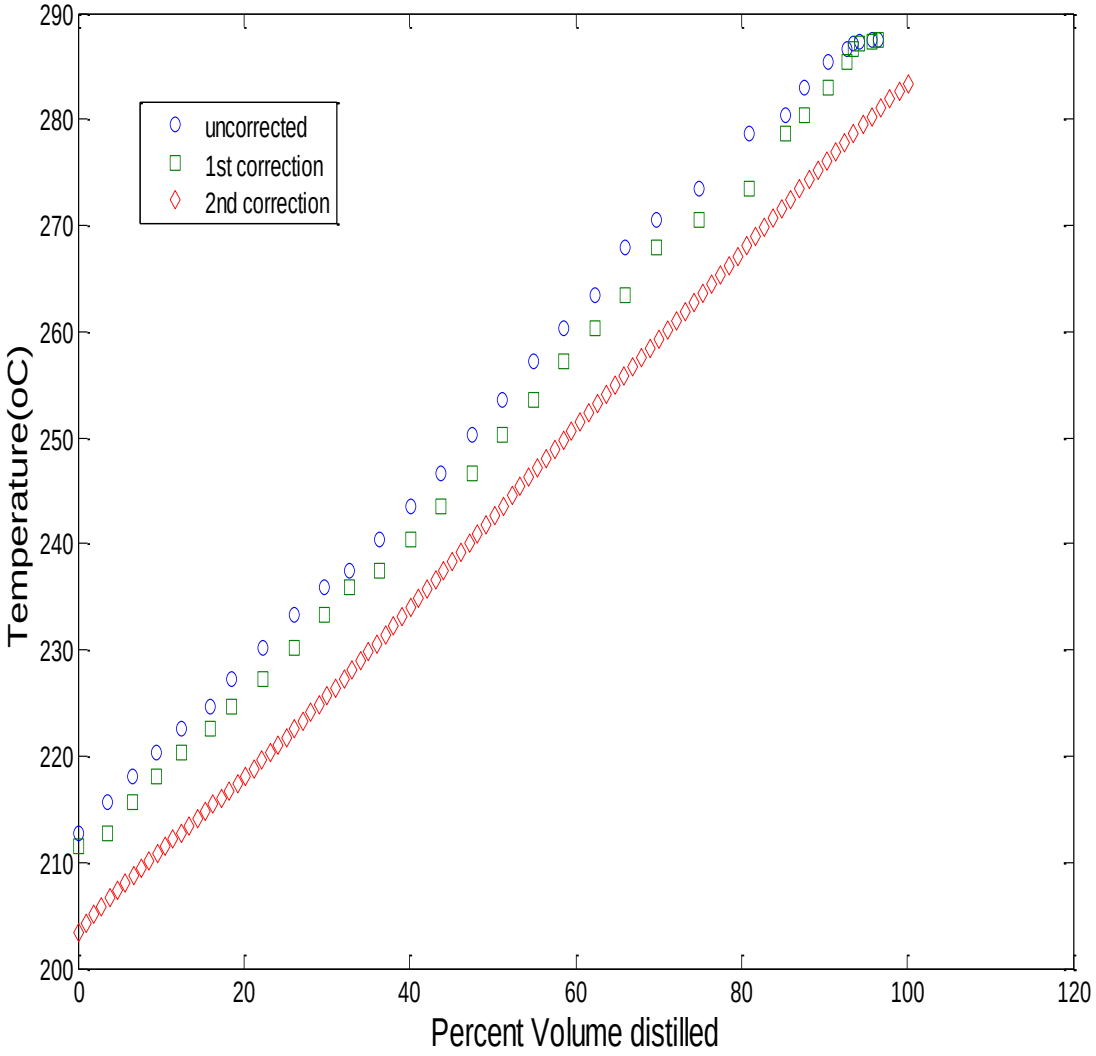

Figure 4.37 Corrected volume profile for repeated 4 components mixture

4.7 Application of the Model to 7 Components Mixture

The empirical model was again applied to a hydrocarbon mixture of seven components. The composition for the mixture is 20ml Octane, 40 ml Decane, 40 ml Dodecane, 40 ml Tetradecane, 40 ml Hexadecane, 10 ml Heptadecane and 10 ml Octadecane. The procedure for the calculation is as described for the four components repeated run. The results calculated from the experimental data in table 4.8 are given below. Figure 4.40is the profile for the experimental data and figures 4.41 and 4.42 are the plots for the fitted boiling and condensation temperatures with their corresponding equation 4.51 and 4.52 below.

$$T0 = 7.995 \times 10^{-9}t^{6} - 1.391 \times 10^{-6}t^{5} + 1.052 \times 10^{-4}t^{4} - 4.685 \times 10^{-3}t^{3} + 0.1214t^{2} + 0.6367t + 186.8 \qquad (4.65)$$

$$T2 = -4.13 \times 10^{-8}t^{6} + 9.753 \times 10^{-6}t^{5} - 9.065 \times 10^{-4}t^{4} + 4.183t^{3} - 0.9981t^{2} + 14.14t + 99.35 \qquad (4.66)$$

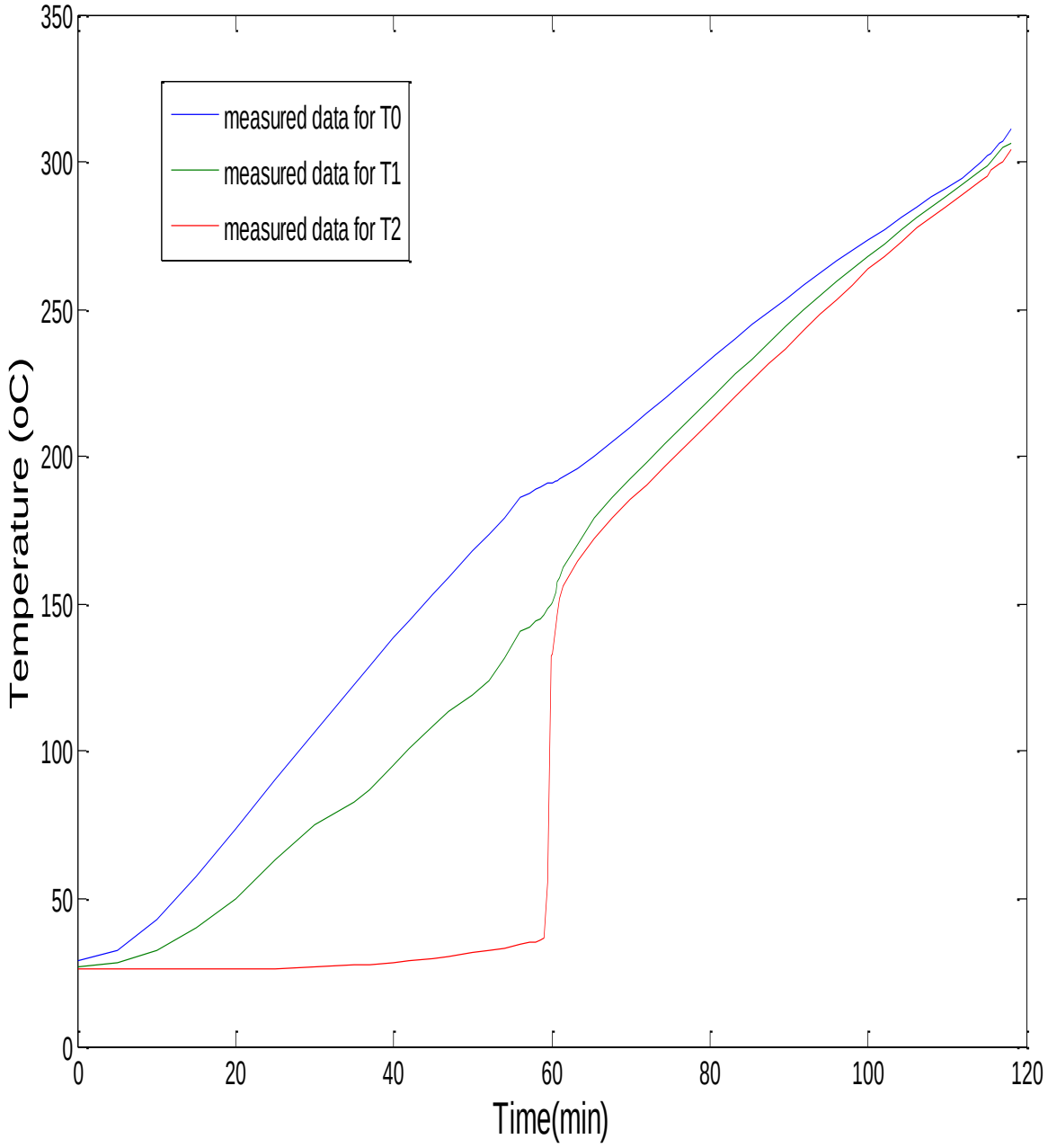

Figure 4.38 Measured temperature T0, T1 and T2 plot vs time for mixture of octane, decane, dodecane, tetradecane, hexadecane, heptadecane and octadecane

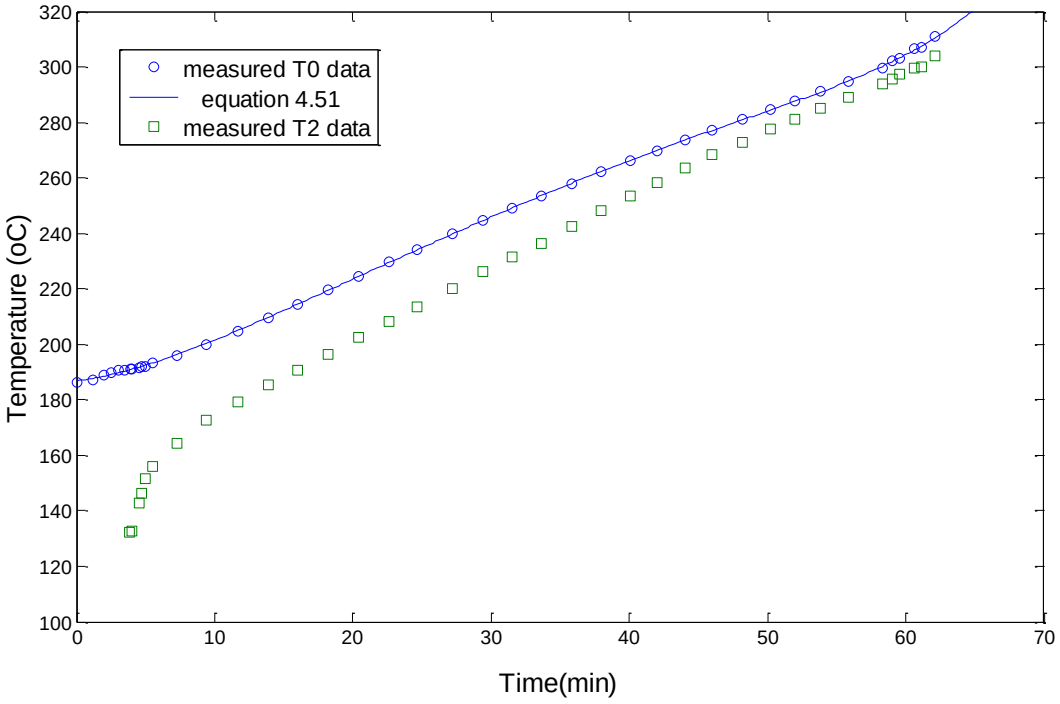

Figure 4.39 Measured T0 and T0 calculated from equation 4.65 are plotted as a function of time

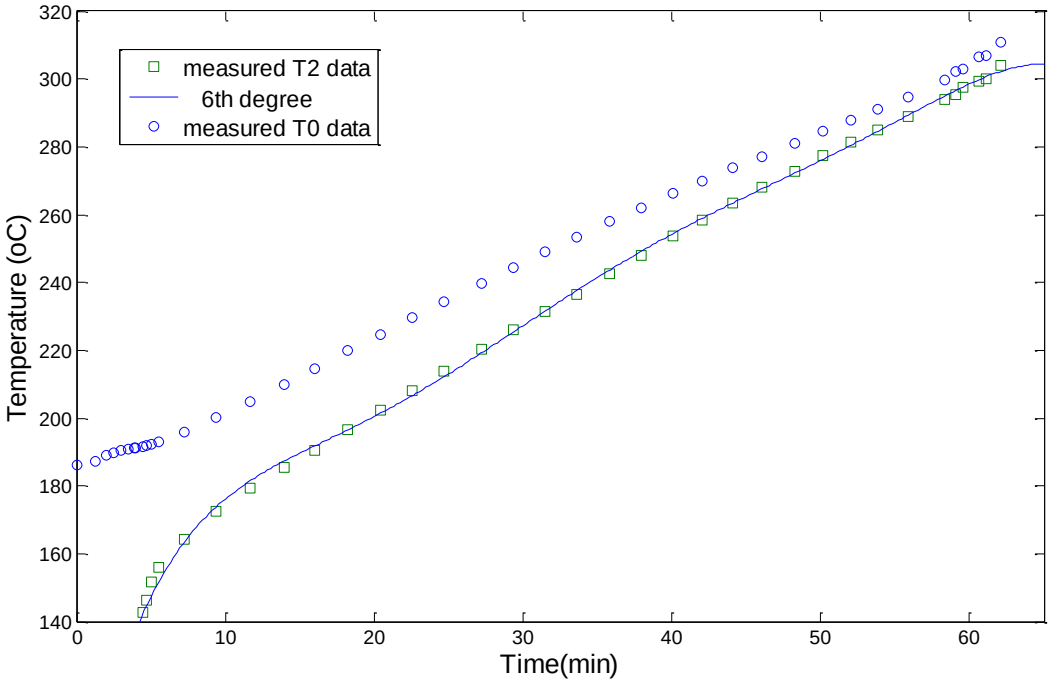

Figure 4.40 Measured T2 and T2 calculated from equation 4.66 are plotted as a function of time

Table 4.8

Experimental results for seven components (Room Pressure = 98.2 kPa)

Time Step (min)	Time (min)			Uncorrected Temp (^oC)			Corrected Temp (oC)			Receiver reading	Receiver Vol (ml)	% Uncorrected Volume Distilled
	t	t_{con}	t_{rec}	T2	T1	T0	T2	T1	T0	X	V	
0.00				25.2	26.4	28.05	26.03	27.24	28.89			
5.00				25.2	27.6	31.89	26.03	28.44	32.74			
10.00				25.2	31.8	42.20	26.03	32.65	43.08			
15.00				25.4	39.2	56.85	26.23	40.07	57.77			
20.00				25.5	48.9	72.89	26.33	49.80	73.86			
25.00				25.7	62.2	89.31	26.53	63.14	90.32			
30.00				26.2	74.1	105.60	27.04	75.07	106.66			
35.00				26.9	82.0	121.60	27.74	82.99	122.70			
37.00				27.2	86.3	127.90	28.04	87.30	129.02			
40.00				27.9	94.3	137.30	28.74	95.32	138.44			
42.00				28.4	100.3	143.20	29.24	101.34	144.36			
45.00				29.0	108.0	152.10	29.84	109.06	153.29			
47.00				29.6	112.3	158.00	30.44	113.37	159.20			
50.00				30.7	118.2	166.60	31.55	119.29	167.83			

Table 4.8

Cont.

52.00				31.5	122.7	172.20	32.35	123.80	173.44			
54.00				32.4	130.4	177.80	33.25	131.53	179.06			
56.00	0.00			33.5	139.4	184.90	34.36	140.55	186.18			
57.23	1.23			34.2	141.2	186.20	35.06	142.36	187.48			
58.00	2.00			34.6	143.0	187.80	35.46	144.16	189.09			
58.50	2.50			35.2	144.2	188.60	36.06	145.36	189.89			
59.00	3.00			35.7	145.1	189.30	36.56	146.27	190.59			
59.50	3.50			54.4	147.1	189.70	55.31	148.27	190.99			
59.85	3.85			131.3	148.8	189.90	132.43	149.98	191.19			
60.00	4.00			131.8	149.2	190.10	132.93	150.38	191.39			
60.50	4.50	0.00		141.8	153.1	190.40	142.96	154.29	191.69			
61.30	4.68	0.8	0.00	145.2	156.5	190.60	146.37	157.70	191.89	0.0	0.00	0.0%
61.50	5.00	1.65	0.20	150.7	157.7	191.00	151.88	158.90	192.29	0.6	1.58	0.8%
61.80	5.50	1.95	0.50	155.0	161.6	191.90	156.19	162.81	193.19	0.7	3.51	1.8%
63.28	7.28	3.43	1.98	163.3	169.3	194.60	164.52	170.53	195.90	1.0	7.51	3.8%
65.40	9.40	5.55	4.10	171.4	177.7	198.80	172.64	178.96	200.12	1.5	14.93	7.5%
67.67	11.67	7.82	6.37	178.1	184.8	203.50	179.36	186.08	204.83	2.0	22.34	11.2%

Table 4.8

Cont.

69.92	13.92	10.07	9.23	184.1	191.1	208.50	185.38	192.39	209.84	2.5	29.76	14.9%
72.00	16.00	12.15	11.32	189.4	196.7	213.30	190.69	198.01	214.66	3.0	37.17	18.6%
74.23	18.23	14.38	13.55	195.4	202.8	218.50	196.71	204.13	219.87	3.5	44.59	22.3%
76.40	20.40	16.55	15.72	201.1	208.8	223.40	202.42	210.14	224.78	4.0	52.00	26.0%
78.57	22.57	18.72	17.88	206.8	214.1	228.30	208.14	215.46	229.70	4.5	59.42	29.7%
80.67	24.67	20.82	19.98	212.4	219.7	233.00	213.75	221.07	234.41	5.0	66.83	33.4%
83.18	27.18	23.33	22.50	219.0	226.5	238.40	220.37	227.89	239.83	5.5	74.25	37.1%
85.37	29.37	25.52	24.68	224.9	231.9	243.20	226.29	233.31	244.64	6.0	81.66	40.8%
87.50	31.50	27.65	26.82	230.0	237.1	247.70	231.40	238.52	249.15	6.5	89.08	44.5%
89.62	33.62	29.77	28.93	235.2	242.6	252.10	236.62	244.04	253.57	7.0	96.49	48.2%
91.85	35.85	32.00	31.17	241.3	248.1	256.60	242.73	249.55	258.08	7.5	103.91	52.0%
93.95	37.95	34.10	33.27	246.7	253.2	260.70	248.15	254.67	262.19	8.0	111.32	55.7%
96.05	40.05	36.20	35.37	252.2	257.9	264.80	253.67	259.38	266.30	8.5	118.74	59.4%
98.03	42.03	38.18	37.35	257.1	262.1	268.50	258.58	263.59	270.01	9.0	126.15	63.1%
100.05	44.05	40.20	39.37	262.1	266.8	272.30	263.59	268.31	273.82	9.5	133.57	66.8%
102.02	46.02	42.17	41.33	266.8	270.6	275.80	268.31	272.12	277.33	10.0	140.98	70.5%
104.22	48.22	44.37	43.53	271.3	275.5	279.70	272.82	277.03	281.24	10.5	148.40	74.2%

Table 4.8

Cont.

106.17	50.17	46.32	45.48	276.0	279.5	283.20	277.53	281.04	284.75	11.0	155.81	77.9%
108.00	52.00	48.15	47.32	279.9	283.2	286.40	281.44	284.75	287.96	11.5	163.23	81.6%
109.83	53.83	49.98	49.15	283.5	287.0	289.60	285.05	288.56	291.17	12.0	170.64	85.3%
111.87	55.87	52.02	51.18	287.5	290.8	293.20	289.06	292.37	294.78	12.5	178.06	89.0%
114.32	58.32	54.47	53.63	292.5	295.8	298.30	294.08	297.39	299.89	13.0	185.47	92.7%
115.05	59.05	55.20	54.37	294.0	297.5	300.70	295.59	299.09	302.30	13.1	186.95	93.5%
115.58	59.58	55.73	54.90	295.9	298.9	301.50	297.49	300.50	303.10	13.2	188.44	94.2%
116.63	60.63	56.78	55.95	298.0	301.8	304.90	299.59	303.40	306.51	13.3	189.92	95.0%
117.10	61.10	57.25	56.42	298.6	303.1	305.50	300.21	304.71	307.11	13.4	191.40	95.7%
118.12	62.12	58.27	57.43	302.6	305.1	309.40	304.21	306.71	311.02	13.5	192.89	96.4%

The volume distilled profile is shown in figure 4.41, figures 4.42, 4.43 and 4.44 are the model results for the vapor travel time, hydrocarbon vapor composition and the boiling – condensation tie points profile and respectively. The boiling-condensation has been done for only τ=16.5.

The results for the seven components were used to calculate for a time constant of τ = 10 to see the behavior of the travel time. Figure 4.44 shows the plot of travel time vs time.

From figure 4.44, it can be seen that the time constant plays a critical role in the travel time curve. The observation was that, when you increase the time constant beyond 17, the travel time curve overlaps the zero line and moves to negative travel time which is impractical. The travel time can never be a negative value, boiling must take place before condensation.

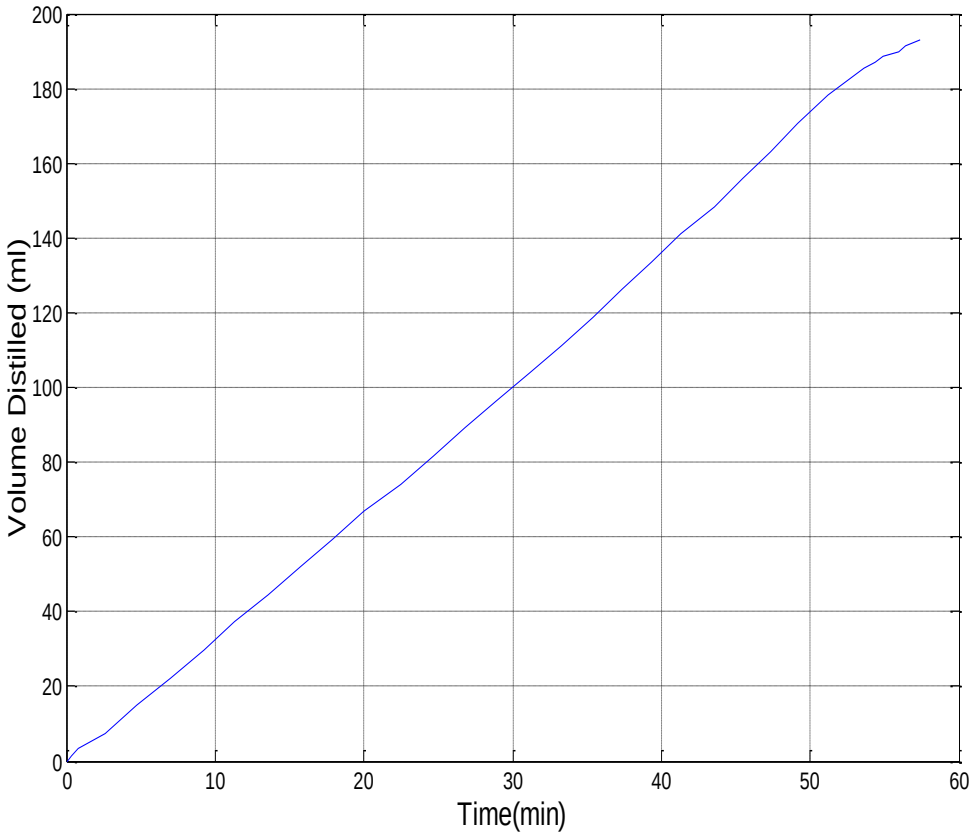

Figure 4.41 Volume –time profile for 7 components mixture

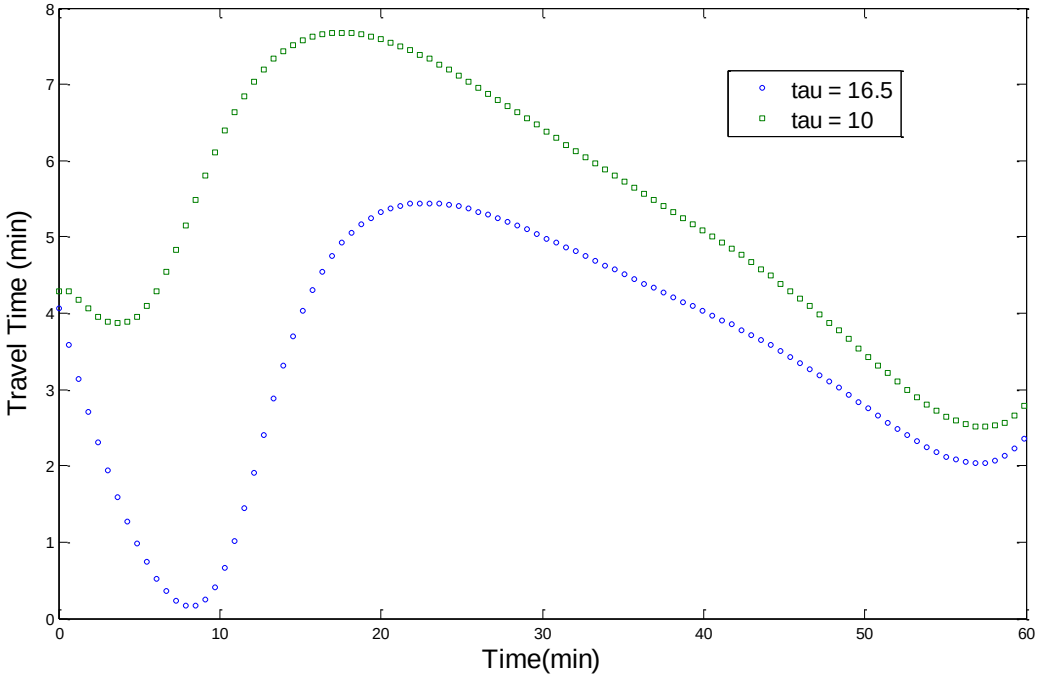

Figure 4.42 Hydrocarbon Vapor Travel Time for 7 components mixture

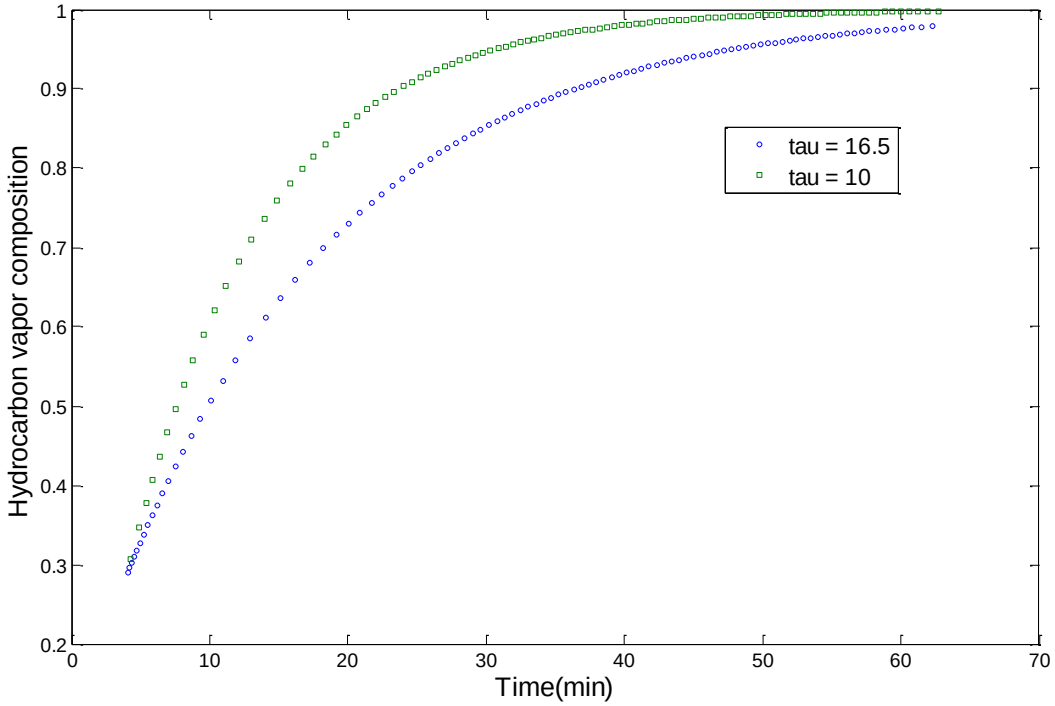

Figure 4.43 Hydrocarbon Vapor Composition for 7 component mixture

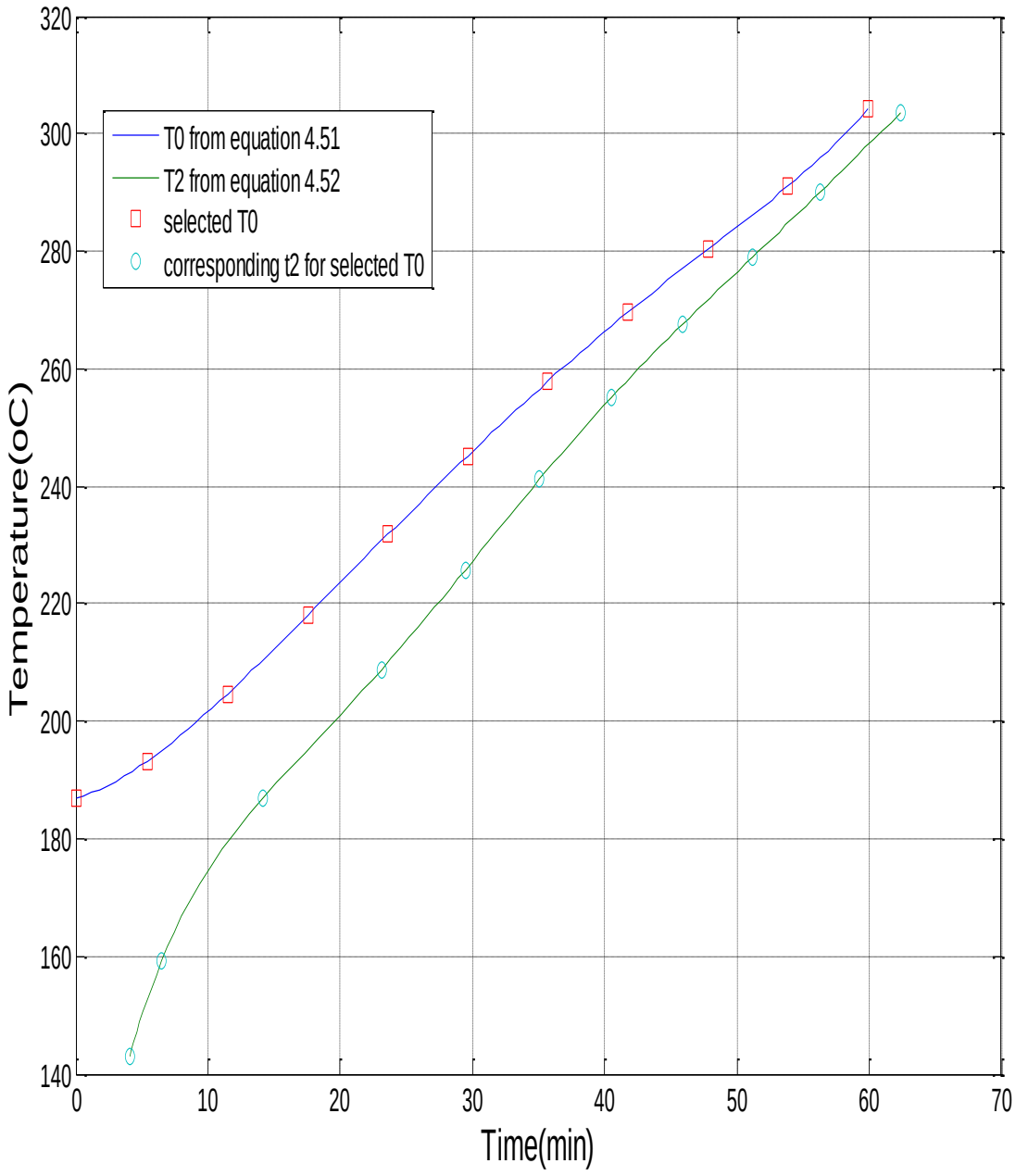

Figure 4.44 Boiling-condensation tie points of decane, dodecane, tetradecane and hexadecane for $\tau = 16.5$

Table 4.9

Modeling results for 7 components mixture

iter	Time	Cn	T0	t2	T2	yv	Psat	tr
1	0	10.5594	186.8668	4.07	142.9909	0.290201	0.29405	4.07
2	3.15	10.7018	189.9442	5.01	149.8949	0.329488	0.33385	1.86
3	6.31	10.9241	194.687	6.75	160.4654	0.396573	0.40183	0.45
4	9.46	11.2027	200.5276	9.8	173.9216	0.498201	0.5048	0.34
5	12.61	11.5207	207.0561	14.94	188.9662	0.632603	0.64098	2.33
6	15.76	11.8656	213.9825	20.09	201.2919	0.731055	0.74074	4.32
7	18.92	12.2287	221.104	24.11	211.3358	0.789187	0.79964	5.19
8	22.07	12.6033	228.2793	27.51	220.3954	0.828462	0.83944	5.44
9	25.22	12.9844	235.4068	30.6	228.8909	0.85775	0.86912	5.38
10	28.37	13.3679	242.4099	33.53	236.9585	0.880901	0.89257	5.15
11	31.53	13.7503	249.2272	36.39	244.6398	0.899857	0.91178	4.86
12	34.68	14.1284	255.8083	39.23	251.9398	0.915697	0.92783	4.55
13	37.83	14.4996	262.116	42.07	258.8522	0.929042	0.94135	4.24
14	40.98	14.8621	268.1334	44.91	265.3779	0.940261	0.95272	3.93
15	44.14	15.2162	273.8766	47.72	271.5447	0.949608	0.96219	3.58
16	47.29	15.5658	279.4138	50.47	277.4324	0.957333	0.97002	3.18
17	50.44	15.9196	284.8893	53.16	283.1994	0.963755	0.97652	2.71
18	53.59	16.2947	290.5538	55.87	289.1137	0.969253	0.9821	2.28
19	56.75	16.7192	296.7995	58.78	295.5859	0.974229	0.98714	2.04
20	59.9	17.2377	304.2017	62.26	303.2121	0.979127	0.9921	2.36

4.8 Volume Correction for 7 Components Mixture. The percent volume recovery profile is shown in figure 4.45 and the fitted equation 4.67 was used to correct the volume after the travel time calculation.

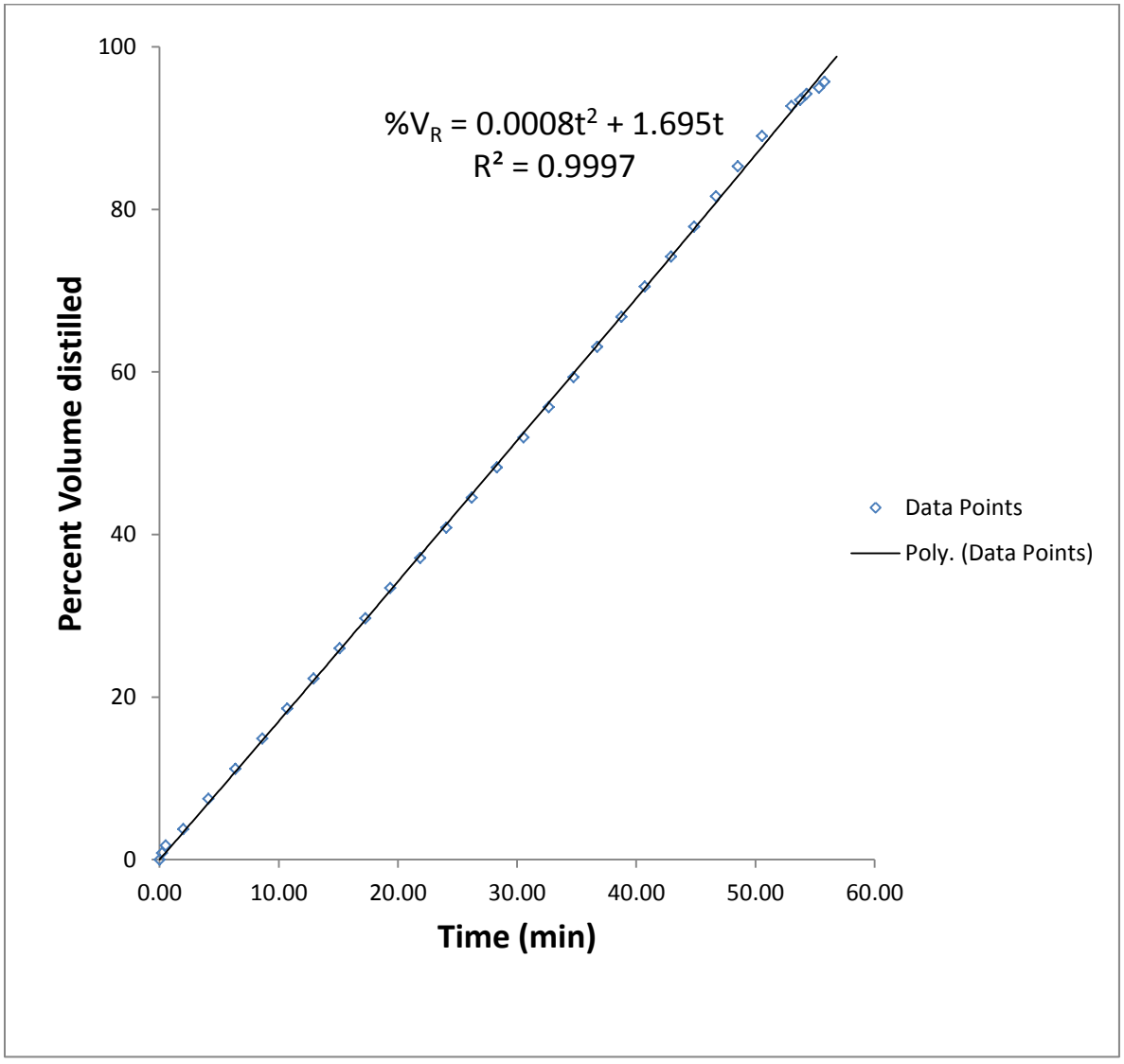

Figure 4.45 Percent volume recovery plot for 7 components mixture

$$V_R = 0.0008\,t^2 + 1.695\,t \qquad (4.67)$$

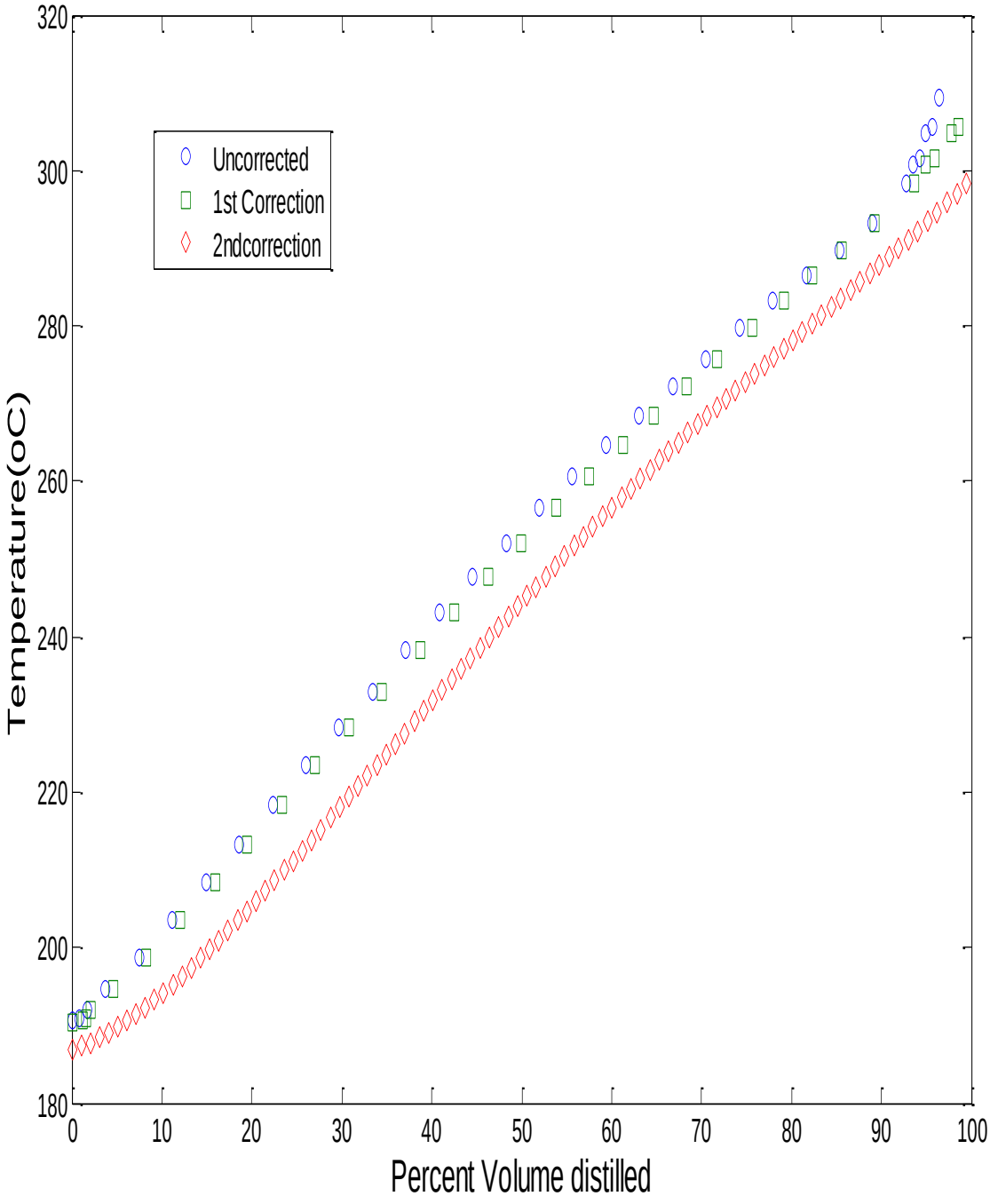

Figure 4.46 Corrected Volume profile for 7 components mixture

CHAPTER 5

Results Discussion and Conclusion

In the measurement of the advanced distillation curve (ADC) as proposed by Bruno[3], the boiling temperature (T0) and the % volume recovered (%V) are taken concurrently. In representing the % volume recovered (%V) or the boiling temperature as a function of time, this approach has some error as it fails to account for the actual boiling temperature for every % volume recorded as a result of the time (delay time) that the distillate travels in the condenser as well as the travel time of the vapor in the distillation flask from the boiling temperature (T0) to the condensation temperature (T2).

The distillate delay time and the vapor travel time plays very important role in predicting the correct boiling temperature for every fraction of the volume distilled. In the ADC procedure by Bruno, the receiver is taken as the zero volume reference at the start of the distillate recordings. Thus only the distillate in the receiver is recorded without taking account of the distillate in the condenser as well as the vapor in the flask. However as corrected by Laya[5] in his thesis, this zero volume reference should start from the condenser intake to take care of the delay time. To further improve the ADC the zero volume reference has been considered to start from just after the liquid surface or when the vapor take off and this helps to estimate the vapor travel time. The summation of the delay time and the travel time are added to the experimentally recorded time. The overall time is used with equation 3.3 to calculate the adjusted % volume ($\%V_2$). Tables 4.2 and 4.4 shows detail results of calculations for plug flow and complete mixing.

To illustrate the improvement of advanced distillation curve as just mentioned above, a four component hydrocarbon mixture of equal volume of n-decane, n-dodecane, n-tetradecane

and n-hexadecane was used to run a batch distillation and the boiling point and volume distilled curves were generated as in figures 3.8 and 3.9. The delay time was observed to be 0.78 min.

As a way of calculating the vapor travel time, the results were modeled as (1) a plug flow process, (2) complete mixing process and (3) empirical. Travel times for both plug flow and complete mixing calculated to be seen in figure 4.4 and figure 4.12 respectively. The travel time for the plug flow was in the range of 0.4min to 0.55 min and showed an increasing trend with respect to the boiling temperature and the liquid height. This time range did not satisfy the experimental data in the sense that the plug plow predicts 0.4min for the first vapor that rises to reach the condenser and condenses whiles the experimental value was 4.87 min. Detail calculations can be seen in section 4.1. The complete mixing model also gave similar trend as the plug flow. For the first 1.4 min in the complete mixing model, the travel time is seen to decrease with time explaining the presence of air in the control volume. The initial time that the first drop of distillate should appear at the condenser intake was calculated as 0.43 min and slowly went down as the air was displaced from the control volume until 1.4 min when the travel time is seen to start to increase. Again it was clear that this model did not predict anywhere close to the experimental initial travel time of 4.87 min. Detail calculations can be seen in section 4.2.

The empirical model was then developed to predict the actual behavior of the experimental data. Here the basic assumption was that, with no heat loss or negligible heat loss to the surrounding, the vapor temperature (T2) at the head of the distillation flask gradually approaches the liquid temperature (T0) as a result of the exponential decay of air in the control volume. The hydrocarbon being distilled condenses at a temperature when its composition in the air-vapor mixture increases, then the vapor pressure also increase until its higher than that of air. At this point, the hydrocarbon reaches its dew point and then condenses.

The actual mean residence time distribution of the vapor wasn't known, hence a range was assumed to satisfy the results as seen in the calculations in chapter 4.3. The empirical model predicted well the experimental data for the head temperature (T2). One observation found was the curvy or wavy nature of the travel time. This was actually as a result of the combine effect of the experimental data and the fitting of the data for T0 and T2. In an attempt to smoothen the travel time curve, the wavy nature was seen in the vapor composition curve. This confirmed the effect of the experimental data used.

From the empirical model, using the four component mixture of decane, dodecane, tetradecane and tetradecane, it was observed that a range of time constant (τ) ($5 \leq \tau \leq 10$) satisfy the experimental data. A time constant of $\tau = 7$ was however used to model since it's somewhere within the mid-range and also satisfy the experimental data closely.

The repeated run for the same composition of mixture was however modeled with tau (τ) = 15. This is because the temperatures at the end of the experiment were about 4^{o}C apart and the model gave 2^{o}C. The difference in the temperatures is as a result of the constant interaction of the air in the condenser with the thermocouple (T2) placed at the flask head. This eventually affects the control volume under discussion.

The same explanation can be said for the seven components mixture. Though the end point temperatures obtained from the model gave a difference of about 1oC as compared to the experimental results of about 6oC, it can still be said that the empirical model developed predicts closely the behavior of the temperature profile in the control volume and the travel time can be used to correct the boiling curve for fuels.

References

1. Smith, B.L. and T.J. Bruno, *Advanced Distillation Curve Measurement with a Model Predictive Temperature Controller.* International Journal of Thermophysics, 2006. **27**(5): p. 1419 - 1434.
2. Randolph, J. and G.M. Masters, *Energy for Sustainability*. 2008: Island Press.
3. Bruno, T.J., *Improvements in the Measurement of Distillation Curves. 1. A Composition-Explicit Approach.* American Chemical Society, 2006. **45**(12): p. 4371-4380.
4. *Standard Test Method for Distillation of Petroleum Products at Atmospheric Pressure, ASTM standard D86-04.* 2010. **9**.
5. Laya, B., *Distillation Curve Measurements of Alternative Aviation Fuels*. 2012, North Coralina A&T State University. p. 43-49.
6. Seader, J.D., E.J. Henley, and D.K. Roper, *Separation Process Principles* 3ed. 2011: John Wiley & Sons, Inc.
7. Leffler, W.L., *Petroleum Refining in Nontechnical Language, PennWell, Tulsa*. 2000: Oklahoma.
8. Shin, Y.G., *volatility of commercial gasoline based on major hydrocarbon species.* KSME Int. J, 1997. **11**(6): p. 714-725.
9. *Orbital Engine Company, Market barriers to the uptake of biofuels study: A testing based assessment to determine the impacts of a 20% ethanol gasoline fuel blend on the Australian passenger fleet. Report to Environment Australia; Australian Government, Department of the Environment and Heritage.* Parkes, Australia, 2003.
10. *Orbital Engine Company, A literature review based assessment on the impacts of a 20% ethanol gasoline fuel blend on the Australian vehicle fleet. Report to Environment*

Australia; Australian Government, Department of the Environment and Heritage. Parkes, Australia, 2002.

11. Visser, B., *Autogas vs avgas: The differences can be major if not properly managed.* Gen. AViat. News, 2004.
12. Hallett, W.L. and H. Ricard, *Calculations of the auto-ignition of liquid hydrocarbon mixtures as single droplets.* Fuel, 1991. **71**(2): p. 225-229.
13. Emel'yanov, V.E., V.P. Grebenshchikov, V.F. Golosova, and G.N. Baranova, *Influence of gasoline distillation curve on carburetor icing.* Khim. Tekhnol. Topl. Masel 1982. **11**: p. 22-23.
14. Huber, M.L., B.L. Smith, O.S. Lisa, and T.J. Bruno, *Surrogate Mixture Model for the Thermophysical Properties of Synthetic Aviation Fuel S-8: Explicit Application of the Advanced Distillation Curve.* American Chemical Society, 2008. **22**: p. 1104–1114.
15. Otta, L.S., B.L. Smith, and T.J. Bruno, *Experimental test of the Sydney Young equation for the presentation of distillation curves.* Elsevier Ltd, 2008. **40**: p. 1352–1357.
16. Young, S., *Fractional distillation*. 1903, Macmillan and Co. Ltd, London.
17. Young, S., *Distillation principles and processes*. 1922, Macmillan and Co. Ltd, London.
18. Smith, B.L. and T.J. Bruno, *Composition-Explicit Distillation Curves of Aviation Fuel JP-8 and a Coal-Based Jet Fuel.* Energy & Fuels, 2007. **21**(5): p. 2853-2862.
19. Poling, B.E., J.M. Prausnitz, and J.P. Oconnel, *The Properties of Gases and Liquids* Vol. 5. 2001: McGRAW-HILL.
20. Smith, J.M., H.C.V. Ness, and M.M. Abbott, *Introduction to Chemical Engineering Thermodynamics*. 7th ed. 2005: McGraw Hill.

21. Chapra, S.C., *Applied Numerical Methods with Matlab for Engineers and Scientists*, ed. 3rd. 2012: McGraw-Hill Companies, Inc.

22. Ambrose, D. and J. Walton, *Vapour pressures up to their critical temperatures of normal alkanes and I-alkanols.* Pure & Applied Chemistry, 1989. **61**(8): p. 1395-1403.

Appendix A

List of M.files used for calculation

Appendix A1: M.file to calculate the liquid level or height

```
function liqlevel
% calculating the liquid in flask height
% Liquid height or level hl in m
% Liquid Volumetric flow rate Ql in mm3/min
% % Radius of flask Rf in mm
%function to calculate the roots(hl)
% f(hl)= pi*hl^3 - 3*pi*Rf*hl^2 + 3Vlo - 3*Ql*t = 0
%Vector for roots, liqlevel= roots([q r s u])
Vlo=200000; Ql=4730;
Rf=49.2;
t=[0 4.87 5.6 7.15 8.42 9.77 11.07 12.40 13.77 15.08 16.40 17.87 19.38 20.95
22.53 24.08 25.72 27.27 28.90 30.43 31.93 33.57 35.15 36.80 38.45 40.12 41.98
43.68 45.12 46.38];
 for i=1:length(t)
    q=pi;
    r=-3*pi*Rf;
    s=0;
    u=3*Vlo-3*Ql*t(i);
    liqlevel=roots([q r s u]);
    x=real(liqlevel);
    x(2);
    hl=x(2)
 end
end
```

Appendix A2: M.file used to calculate the travel time

```
function traveltime
%Experimental Data for t in min
t=[0 4.87 5.6 7.15 8.42 9.77 11.07 12.40 13.77 15.08 16.40 17.87 19.38 20.95
22.53 24.08 25.72 27.27 28.90 30.43 31.93 33.57 35.15 36.80 38.45 40.12
41.98];% 43.68 45.12 46.38];


%Calculated hl values from appendix A.1
hl=[42.6611 39.5467 39.0735 38.0622 37.2261 36.3292 35.4568 34.5544 33.6135
32.7017 31.7699 30.7150 29.6103 28.4363 27.2250 26.0034 24.6695 23.3630
21.9324 20.5262 19.0749 17.3851 15.6248 13.5949 11.2695 8.3776 3.0788];


%Constants
    a=0.0039; % Constant to Calculate Temperature
    b=1.7495; % Constant to Calculate Temperature
    c=200.99; % Constant to Calculate Temperature
    cc=c+273.15; % Constant to Calculate Temperature
    P=101325; %Pressure in Pa
    R=8.314; % Gas Constant in J/mol/K
    Ql=4730; % mm3/min
    Rf=49.2; %Radius of Flask in mm
    ld=0.749*10^6;% Density of distillate using Dodecane in g/m3
    M=170.41; % Molecular weight of Dodecane in g/mol
    hs=89.7;%Height of Spherical part of Flask in mm
    hc=62.0; %Height of cylindrical part of flask in mm
    rc=13.0; %Radius of cylindrical part of flask in mm
 %Deducted variables for calculation
```

```
    K1=P*M/R;
    m=ld*Ql;
    K2=m/K1;
%For the cylindrical Portion, travel time is trc=pi/Qv*rc^2*hc;
      i=1;
   tr(i)=0;
   Qv(i)=0;
%calculating the travel time
for i=1:length(t)
    Qv(i)=K2*(a*t(i).^2+b*t(i)+cc);
    trc=pi/Qv(i)*rc^2*hc;
    tr(i)=(pi/Qv(i))*(Rf*(hs.^2-hl(i).^2)-1/3*(hs.^3-hl(i)^3))+trc;
end
    z=[t;hl;tr];
    fprintf(' t(min)        hl(mm)        tr(min)\n');
    fprintf('%1.1f %15.2f %15.4f\n',z);
    plot(t,tr,'-o');
    xlabel('Experimental Time (min)');
    ylabel('Travel Time (min)');
end
```

Appendix A3: M.file for calculating T2 and yv complete mixing modeling

```
function dmdt=compmix(t,m)

% Solve the Complete mixing model
dmdt = zeros(size(m));
T= m(1);
Yv = m(2);

% Input variables
P = 101325; %Pa
Vs = 0.0003; % m3 =(300 ml)
Vc = 32.918*10^-6; %m3 = (32.916 ml)
Vo = Vs + Vc; %m3
Ql = 4.73e-6; % m3/min = (4.73 ml/min)
ld = 0.749*10^6;% Density of distillate using Dodecane in g/m3
M = 170.41;% Molecular weight of Dodecane in g/mol
Fvo = Ql*ld/M; % Molar flow rate mol/min
R = 8.314;% Gas Constant in J/mol/K
a = 0.0039;
b = 1.7495;
c = 200.99+273.15;
To = a*t^2 + b*t + c ; % K
N = P*(Vo + Ql*t)/(R*T);

% Heat capacities
CpA = R*(3.359 - 0.261*10^-3*T + 0.007*10^-5*T^2 + 0.157*10^-8*T^3 -
0.099*10^-11*T^4);
Cpv = R*(17.229 - 7.242*10^-3*T + 31.922*10^-5*T^2 - 42.322*10^-8*T^3 +
17.022*10^-11*T^4);
Cpvo = R*(17.229 - 7.242*10^-3*To + 31.922*10^-5*To^2 - 42.322*10^-8*To^3 +
17.022*10^-11*To^4);
Cvv = Cpv - R;
CvA = CpA - R;
% Solving ODE for Temperature and Mole fraction

dmdt(1)=(P*Ql + Fvo*(Cpvo*To - CpA*T - T*(Cvv - CvA)))/(N*(R + (CvA + yv*(Cvv
- CvA))));
dmdt(2)=(Fvo/N)*(1-yv);

end
```

Appendix A4: M.file for Empirical modeling

```
function iterateforyv
     global Tc r Psat Pc w t T0
     xl = 0;
     xu = 30;
     es = 0.00001;
     maxit = 50;
     AllCn =  bisect2(@calCn,xl,xu,es,maxit);
     NumOfCn = length(AllCn);
     Temp = zeros(NumOfCn,1);
     Time = zeros(NumOfCn,1);
     YV = zeros(NumOfCn,1);
     PSAT = zeros(NumOfCn,1);
     iterCounts = 1:NumOfCn;
     for i=1:NumOfCn
         yv= 6.476286713904853e-001;
         yo=1-yv;
         er =2;
         Tinit = 250;
         Cn = AllCn(i);
         P=1.01325; %bar
         Psat=yv*P;
while er>=0.000001;

    % calculating Omega (fitted from publication paper)
    a1 = 5.9254e-007;  a2 = -4.5176e-005;  a3 = 0.0014037;  a4 = -0.022724;
    a5 = 0.20133;  a6 = -0.87663;  a7 = 1.7351;
    w = a1*Cn^6 + a2*Cn^5 + a3*Cn^4 + a4*Cn^3 + a5*Cn^2 + a6*Cn + a7 ;

    Tc =960 - exp(6.8162 - 0.2115.*(Cn.^(2/3)));% (from publication paper)

    % Molecular weight (accepted) fitted from Properties of gases and Liquids
    m1 = -7.3272e-007;  m2 = 4.1367e-005;  m3 = -0.00083372;  m4 = 14.034;
m5 = 1.9947;
    M = m1*Cn^4 + m2*Cn^3 + m3*Cn^2 + m4*Cn + m5 ;

    Pc= M./((0.339 + 0.226*Cn).^2); % bar


    a=[-5.97616 -5.03365 -0.64771];% (from publication paper)
    b=[1.29874 1.11505 2.41539];% (from publication paper)
    c=[-0.60394 -5.41217 -4.26979];% (from publication paper)
    d=[-1.06841 -7.46628 3.25259];% (from publication paper)
    r=[a;b;c;d];

    Tsat = fsolve(@hFunc,Tinit, optimset('Display','off'));

    % Coefficients for Temperature T2 from fitting
    n=[-3.974646421593612e-007 6.526331821144027e-005 -4.246735561770674e-
003...
    1.383799928679778e-001 -2.346492772153197e+000 2.162750038425736e+001
1.243165796285932e+002];
```

```
    % Calculating the roots(time t2) from Tsat
    m1 = (roots([n(1:end-1), n(end)-Tsat+273.15]));

    reals=m1(find(imag(m1)==0));
    m2=reals;
    t2=min(m2);

    tau=10;
    yvnew = 1 - yo*exp(-(t2-4.6)/tau);
    er = abs(((yvnew - yv)/yvnew)*100);
    yv=yvnew;
    Psat=yv*P;
end
Temp(i)=Tsat-273.15;
Time(i) = t2;
YV(i) = yv;
PSAT(i) = Psat;
     end
allResults =[iterCounts',t',AllCn, T0', Time, Temp, YV, PSAT, Time-t']';
fprintf('%1.0f %10.2f  %10.4f %10.4f  %10.2f  %12.4f %10.6f %10.5f
%10.2f\n',allResults)
Title = {'iter','t','Cn', 'T0', 't2', 'T2', 'yv', 'Psat', 'tr'};
xlswrite('Result', Title, 'A1:H1');
xlswrite('Result', allResults,'A2:H101');

% Selected Tie Line for Plotting
Toti=[T0(1) T0(10) T0(20) T0(30) T0(40) T0(50) T0(60) T0(70) T0(70) T0(80)
T0(90) T0(100)];
tti=[t(1) t(10) t(20) t(30) t(40) t(50) t(60) t(70) t(70) t(80) t(90)
t(100)];

T2ti=[Temp(1) Temp(10) Temp(20) Temp(30) Temp(40) Temp(50) Temp(60) Temp(70)
Temp(70) Temp(80) Temp(90) Temp(100)];
t2ti=[Time(1) Time(10) Time(20) Time(30) Time(40) Time(50) Time(60) Time(70)
Time(70) Time(80) Time(90) Time(100)];

figure(1)
plot(t,T0,Time,Temp,tti,Toti,'s',t2ti,T2ti,'o')
xlabel('Time(min)')
ylabel('Temperature(oC)')
grid

figure(2)
plot(t,(Time-t'))
xlabel('Time(min)')
ylabel('Vapor Travel Time (min)')
grid

figure(3)
plot(t,YV)
xlabel('Time(min)')
ylabel('Hydrocarbon Vapor Composition(yv)')
grid
end
```

```
%%%%%%% sub-functions

function h = hFunc(T)
    global Tc r Psat Pc w
    Tr=T./Tc;
    z = 1-Tr; % z = (from publication paper)

    % Calculating ln(Pr)= ln(Pr0) + ln(Pr1) + ln(Pr2). (from publication
paper)
    e =(r(1,1)*z + r(2,1)*(z^1.5) + r(3,1)*(z^2.5) + r(4,1)*(z^5))/(Tr);
    f =(r(1,2)*z + r(2,2)*(z^1.5) + r(3,2)*(z^2.5) + r(4,2)*(z^5))/(Tr);
    g =(r(1,3)*z + r(2,3)*(z^1.5) + r(3,3)*(z^2.5) + r(4,3)*(z^5))/(Tr);
    b =log(Psat./Pc);

    h = b - (e + w*f + (w^2).*g);
end


%%%%%%% Function for Calculating Carbon Numbers
 function f = calCn(Cn)
global t T0
t=linspace(0,44.66,100); % T0 time scale

% 6th order fit for corrected T0
p=[-7.007378635848691e-008 1.096576499276833e-005 -6.571917732049750e-004
1.808031759100679e-002...
   -2.046915777527842e-001 2.278582177022307e+000 2.029442137139240e+002];

T0 = p(1)*(t.^6) + p(2)*(t.^5) + p(3)*(t.^4) + p(4)*(t.^3) + p(5)*(t.^2) +
p(6)*t +  p(7); % 6th order fit for To

T0k=T0+273.15;% To in Kelvin

Psat = 1.01325; % bar

% calculating Omega (Fitted from publication paper)
a1 = 5.9254e-007;  a2 = -4.5176e-005;  a3 = 0.0014037;  a4 = -0.022724;
a5 = 0.20133;  a6 = -0.87663;  a7 = 1.7351;
w = a1*Cn.^6 + a2*Cn.^5 + a3*Cn.^4 + a4*Cn.^3 + a5*Cn.^2 + a6*Cn + a7 ;

Tc =960 - exp(6.8162 - 0.2115.*(Cn.^(2/3)));% (from publication paper)

% Molecular weight (accepted) fitted from Prperties of Gases and Liquids
m1 = -7.3272e-007;  m2 = 4.1367e-005;  m3 = -0.00083372;  m4 = 14.034;  m5 =
1.9947;
M = m1*Cn.^4 + m2*Cn.^3 + m3*Cn.^2 + m4*Cn + m5 ;

Pc= M./((0.339 + 0.226*Cn).^2); % bar

a=[-5.97616 -5.03365 -0.64771];% (from publication paper)
```

```
b=[1.29874 1.11505 2.41539];% (from publication paper)
c=[-0.60394 -5.41217 -4.26979];% (from publication paper)
d=[-1.06841 -7.46628 3.25259];% (from publication paper)
r=[a;b;c;d];

Tr=T0k./Tc;
z = 1-Tr; % z = (from publication paper)

% Calculating ln(Pr)= ln(Pr0) + ln(Pr1) + ln(Pr2). (from publication paper)
e =(r(1,1)*z + r(2,1)*(z.^1.5) + r(3,1)*(z.^2.5) + r(4,1)*(z.^5))./Tr;
f =(r(1,2)*z + r(2,2)*(z.^1.5) + r(3,2)*(z.^2.5) + r(4,2)*(z.^5))./Tr;
g =(r(1,3)*z + r(2,3)*(z.^1.5) + r(3,3)*(z.^2.5) + r(4,3)*(z.^5))./Tr;
b=log(Psat/Pc);% b = e + w.*f + (w.^2).*g; % b=log(Pr)

% Calculating for carbon no
f = b-(e + w.*f + (w.^2).*g);

 end


 %%%%%%% Function for iteration for Carbon Numbers
 function [root,fx,ea,iter]=bisect2(func,xl,xu,es,maxit,varargin)
% bisect: root location zeroes
    % [root,fx,ea,iter]=bisect(func,xl,xu,es,maxit,p1,p2,...):
    % uses bisection method to find the root of func
% input:
    % func = name of function
    % xl, xu = lower and upper guesses
    % es = desired relative error (default = 0.0001%)
    % maxit = maximum allowable iterations (default = 50)
    % p1,p2,... = additional parameters used by func
% output:
    % root = real root
    % fx = function value at root
    % ea = approximate relative error (%)
    % iter = number of iterations

if nargin<3,error('at least 3 input arguments required'),end
test = func(xl,varargin{:}).*func(xu,varargin{:});
if test>0,error('no sign change'),end
if nargin<4||isempty(es), es=0.0001;end
if nargin<5||isempty(maxit), maxit=50;end

root = zeros(length(test), 1);
fx = zeros(length(test), 1);
x1org = xl;
xuorg = xu;
for k=1:length(test)
    xl = x1org;
    xu = xuorg;
    iter = 0; xr = xl; ea = 100;
while (1)
    xrold = xr;
    xr = (xl + xu)/2;
    iter = iter + 1;
```

```
    if xr ~= 0,ea = abs((xr - xrold)/xr) * 100;end
    test = func(xl,varargin{:}).*func(xr,varargin{:});

    if test(k) < 0
    xu = xr;
    elseif test(k) > 0
    xl = xr;
    else
    ea = 0;
    end
    if ea <= es || iter >= maxit,break,end

end
root(k) = xr; fx = func(xr, varargin{:});
end
 end
```

Appendix A5: M.file for smoothened travel time calculation

```
function Testempiricalmodel

global t

ao = 0.0011; a1=- 0.1311;  a2=4.58;
tr=ao*(t.^2)+ a1*t + a2;
t2=tr+t;

% 6th order polynomial for T2
n=[-3.974646421593612e-007 6.526331821144027e-005 -4.246735561770674e-003...
    1.383799928679778e-001 -2.346492772153197e+000 2.162750038425736e+001
1.243165796285932e+002];

T2 = n(1)*(t2.^6) + n(2)*(t2.^5) + n(3)*(t2.^4) + n(4)*(t2.^3) + n(5)*(t2.^2)
+ n(6)*t2 +  n(7);
T2k=T2+271.15;

%Calculating carbon no for To
     xl = 0;
     xu = 30;
     es = 0.00001;
     maxit = 50;
     Cn =  bisect2(@calCn,xl,xu,es,maxit);

P=1.01325;% bar

p1 = -6.6772e-006; p2 = 0.00044508; p3 = -0.011442; p4 = 0.14075; p5 = -
0.78193; p6 = 1.8968; % Constants for omega
w = p1*(Cn.^5) + p2*(Cn.^4) + p3*(Cn.^3) + p4*(Cn.^2) + p5*Cn + p6; % fitted
from Txt bk data
Tc =960 - exp(6.8162 - 0.2115.*(Cn.^(2/3)));% from refence article
M = (14.03*Cn + 2.016); % Molecular wt for C7 to C20 in kg/mol from fitted
data
Pc= M./((0.339 + 0.226*Cn).^2); % bar

a=[-5.97616 -5.03365 -0.64771];% from refence article
b=[1.29874 1.11505 2.41539];% from refence article
c=[-0.60394 -5.41217 -4.26979];% from refence article
d=[-1.06841 -7.46628 3.25259];% from refence article
r=[a;b;c;d];

Tr=T2k'./Tc;
z = 1-Tr; % z = Thao from refence article

% Calculating ln(Pr)= ln(Pr0) + ln(Pr1) + ln(Pr2).
e =(r(1,1)*z + r(2,1)*(z.^1.5) + r(3,1)*(z.^2.5) + r(4,1)*(z.^5))./Tr;% e =
log(Pr0) from refence article
f =(r(1,2)*z + r(2,2)*(z.^1.5) + r(3,2)*(z.^2.5) + r(4,2)*(z.^5))./Tr;% f =
log(Pr1) from refence article
g =(r(1,3)*z + r(2,3)*(z.^1.5) + r(3,3)*(z.^2.5) + r(4,3)*(z.^5))./Tr;% g =
log(Pr2) from refence article
b = e + w.*f + (w.^2).*g; % b=log(Pr) % from refence article
```

```
% Calculating for Psat

Psat=Pc.*exp(b); %bar

yv=Psat./P;

figure(1)
plot(t,tr)
xlabel('Time(min)')
ylabel('Travel Time(min)')
grid

figure(2)
plot(t2,yv)
xlabel('Time(min)')
ylabel('vapor composition')
grid
end




%%%%%%% Function for Calculating Carbon Numbers
 function f = calCn(Cn)
global t T0
t=linspace(0,44.66,100); % T0 time scale

% 6th order fit for corrected T0
p=[-7.007378635848691e-008 1.096576499276833e-005 -6.571917732049750e-004
1.808031759100679e-002...
   -2.046915777527842e-001 2.278582177022307e+000 2.029442137139240e+002];

T0 = p(1)*(t.^6) + p(2)*(t.^5) + p(3)*(t.^4) + p(4)*(t.^3) + p(5)*(t.^2) +
p(6)*t +  p(7); % 6th order fit for To

T0k=T0+273.15;% To in Kelvin

Psat = 1.01325; % bar

% calculating Omega (Fitted from publication paper)
a1 = 5.9254e-007;  a2 = -4.5176e-005;  a3 = 0.0014037;  a4 = -0.022724;
a5 = 0.20133;  a6 = -0.87663;  a7 = 1.7351;
w = a1*Cn.^6 + a2*Cn.^5 + a3*Cn.^4 + a4*Cn.^3 + a5*Cn.^2 + a6*Cn + a7 ;

Tc =960 - exp(6.8162 - 0.2115.*(Cn.^(2/3)));% (from publication paper)

% Molecular weight (accepted) fitted from Prperties of Gases and Liquids
m1 = -7.3272e-007;  m2 = 4.1367e-005;  m3 = -0.00083372;  m4 = 14.034;  m5 =
1.9947;
M = m1*Cn.^4 + m2*Cn.^3 + m3*Cn.^2 + m4*Cn + m5 ;

Pc= M./((0.339 + 0.226*Cn).^2); % bar
```

```
a=[-5.97616 -5.03365 -0.64771];% (from publication paper)
b=[1.29874 1.11505 2.41539];% (from publication paper)
c=[-0.60394 -5.41217 -4.26979];% (from publication paper)
d=[-1.06841 -7.46628 3.25259];% (from publication paper)
r=[a;b;c;d];

Tr=T0k./Tc;
z = 1-Tr; % z = (from publication paper)

% Calculating ln(Pr)= ln(Pr0) + ln(Pr1) + ln(Pr2). (from publication paper)
e =(r(1,1)*z + r(2,1)*(z.^1.5) + r(3,1)*(z.^2.5) + r(4,1)*(z.^5))./Tr;
f =(r(1,2)*z + r(2,2)*(z.^1.5) + r(3,2)*(z.^2.5) + r(4,2)*(z.^5))./Tr;
g =(r(1,3)*z + r(2,3)*(z.^1.5) + r(3,3)*(z.^2.5) + r(4,3)*(z.^5))./Tr;
b=log(Psat/Pc);% b = e + w.*f + (w.^2).*g; % b=log(Pr)

% Calculating for carbon no
f = b-(e + w.*f + (w.^2).*g);

 end


 %%%%%%% Function for iteration for Carbon Numbers
 function [root,fx,ea,iter]=bisect2(func,xl,xu,es,maxit,varargin)
% bisect: root location zeroes
    % [root,fx,ea,iter]=bisect(func,xl,xu,es,maxit,p1,p2,...):
    % uses bisection method to find the root of func
% input:
    % func = name of function
    % xl, xu = lower and upper guesses
    % es = desired relative error (default = 0.0001%)
    % maxit = maximum allowable iterations (default = 50)
    % p1,p2,... = additional parameters used by func
% output:
    % root = real root
    % fx = function value at root
    % ea = approximate relative error (%)
    % iter = number of iterations

if nargin<3,error('at least 3 input arguments required'),end
test = func(xl,varargin{:}).*func(xu,varargin{:});
if test>0,error('no sign change'),end
if nargin<4||isempty(es), es=0.0001;end
if nargin<5||isempty(maxit), maxit=50;end

root = zeros(length(test), 1);
fx = zeros(length(test), 1);
x1org = xl;
xuorg = xu;
for k=1:length(test)
    xl = x1org;
    xu = xuorg;
    iter = 0; xr = xl; ea = 100;
while (1)
    xrold = xr;
```

```
    xr = (xl + xu)/2;
    iter = iter + 1;
    if xr ~= 0,ea = abs((xr - xrold)/xr) * 100;end
    test = func(xl,varargin{:}).*func(xr,varargin{:});

    if test(k) < 0
    xu = xr;
    elseif test(k) > 0
    xl = xr;
    else
    ea = 0;
    end
    if ea <= es || iter >= maxit,break,end

end
root(k) = xr; fx = func(xr, varargin{:});
end
 end
```

Appendix B

Calculated Results Table

Table B1: Results of equations 4.39 and 4.40 for Complete mixing model

No	time t (min)	Exit TempT2 (K)	Exit Temp T2 (^oC)	Exit Vap. Composition(y_v)	time at $T_0=T_2$ $t_{T0=T2}$	$t_r = t_{T0=T2} - t$
1	0.0000	293.1500	20.0000	0.0000	0.4188	0.4188
2	0.0000	293.3549	20.2049	0.0001	0.4188	0.4188
3	0.0001	293.5596	20.4096	0.0001	0.4188	0.4187
4	0.0001	293.7642	20.6142	0.0002	0.4188	0.4187
5	0.0001	293.9687	20.8187	0.0002	0.4188	0.4187
6	0.0003	294.9890	21.8390	0.0005	0.4189	0.4186
7	0.0005	296.0058	22.8558	0.0007	0.4190	0.4185
8	0.0006	297.0193	23.8693	0.0010	0.4190	0.4184
9	0.0008	298.0292	24.8792	0.0012	0.4191	0.4183
10	0.0016	303.0245	29.8745	0.0025	0.4194	0.4178
11	0.0025	307.9254	34.7754	0.0038	0.4197	0.4173
12	0.0033	312.7271	39.5771	0.0051	0.4200	0.4167
13	0.0041	317.4254	44.2754	0.0065	0.4204	0.4162
14	0.0083	339.2528	66.1028	0.0134	0.4220	0.4136
15	0.0125	358.2328	85.0828	0.0208	0.4236	0.4110
16	0.0167	374.4260	101.2760	0.0284	0.4252	0.4085
17	0.0209	388.0722	114.9222	0.0363	0.4267	0.4059
18	0.0288	408.2958	135.1458	0.0519	0.4298	0.4009
19	0.0368	422.8407	149.6907	0.0679	0.4328	0.3960
20	0.0448	433.5168	160.3668	0.0841	0.4359	0.3911
21	0.0528	441.4037	168.2537	0.1003	0.4389	0.3861
22	0.0619	447.9706	174.8206	0.1188	0.4424	0.3805
23	0.0711	452.8376	179.6876	0.1372	0.4459	0.3748
24	0.0802	456.5350	183.3850	0.1554	0.4494	0.3692
25	0.0893	459.4084	186.2584	0.1733	0.4529	0.3635
26	0.1045	462.9253	189.7753	0.2024	0.4587	0.3542
27	0.1197	465.3866	192.2366	0.2307	0.4645	0.3448
28	0.1349	467.1718	194.0218	0.2580	0.4703	0.3354
29	0.1501	468.5162	195.3662	0.2845	0.4761	0.3260
30	0.1744	470.0604	196.9104	0.3250	0.4876	0.3132
31	0.1987	471.1160	197.9660	0.3633	0.5004	0.3017
32	0.2230	471.8639	198.7139	0.3995	0.5133	0.2903
33	0.2472	472.4222	199.2722	0.4336	0.5261	0.2789
34	0.2881	473.0991	199.9491	0.4868	0.5478	0.2597

Table B1

Conti

35	0.3290	473.5526	200.4026	0.5351	0.5771	0.2481
36	0.3699	473.8657	200.7157	0.5788	0.6067	0.2368
37	0.4108	474.1034	200.9534	0.6184	0.6390	0.2282
38	0.4797	474.4193	201.2693	0.6769	0.6962	0.2165
39	0.5486	474.6471	201.4971	0.7265	0.7535	0.2049
40	0.6175	474.8139	201.6639	0.7683	0.8140	0.1965
41	0.6864	474.9596	201.8096	0.8038	0.8779	0.1915
42	0.7830	475.1633	202.0133	0.8446	0.9768	0.1937
43	0.8796	475.3460	202.1960	0.8769	1.0770	0.1974
44	0.9762	475.5114	202.3614	0.9024	1.1737	0.1975
45	1.0728	475.6746	202.5246	0.9225	1.2717	0.1988
46	1.1831	475.8681	202.7181	0.9406	1.3850	0.2019
47	1.2934	476.0590	202.9090	0.9544	1.4983	0.2050
48	1.4036	476.2472	203.0972	0.9649	1.6118	0.2081
49	1.5139	476.4359	203.2859	0.9730	1.7224	0.2085
50	1.6474	476.6677	203.5177	0.9804	1.8564	0.2090
51	1.7809	476.8997	203.7497	0.9858	1.9903	0.2094
52	1.9144	477.1313	203.9813	0.9896	2.1243	0.2099
53	2.0479	477.3637	204.2137	0.9924	2.2582	0.2103
54	2.2118	477.6510	204.5010	0.9949	2.4227	0.2109
55	2.3757	477.9386	204.7886	0.9966	2.5872	0.2114
56	2.5397	478.2264	205.0764	0.9976	2.7516	0.2120
57	2.7036	478.5146	205.3646	0.9983	2.9161	0.2125
58	2.9123	478.8827	205.7327	0.9990	3.1256	0.2132
59	3.1211	479.2512	206.1012	0.9995	3.3350	0.2139
60	3.3299	479.6204	206.4704	0.9996	3.5445	0.2146
61	3.5387	479.9900	206.8400	0.9997	3.7539	0.2153
62	3.8165	480.4778	207.3278	0.9999	4.0327	0.2162
63	4.0944	480.9696	207.8196	1.0000	4.3114	0.2171
64	4.3722	481.4701	208.3201	1.0000	4.5902	0.2180
65	4.6501	481.9678	208.8178	0.9999	4.8689	0.2188
66	5.0339	482.3589	209.2089	1.0001	5.2539	0.2200
67	5.4177	482.9937	209.8437	1.0001	5.6390	0.2213
68	5.8015	484.1893	211.0393	1.0000	6.0240	0.2225
69	6.1853	485.0642	211.9142	0.9999	6.4090	0.2237
70	6.3505	485.1019	211.9519	0.9999	6.5747	0.2242
71	6.5156	485.2778	212.1278	0.9999	6.7404	0.2248
72	6.6807	485.6472	212.4972	1.0000	6.9060	0.2253

Table B1

Conti

73	6.8459	486.0051	212.8551	1.0000	7.0717	0.2258
74	7.0110	486.2194	213.0694	1.0000	7.2373	0.2263
75	7.1762	486.4777	213.3277	1.0000	7.4029	0.2268
76	7.3413	486.7972	213.6472	1.0000	7.5686	0.2273
77	7.5064	487.1135	213.9635	1.0000	7.7342	0.2278
78	7.7348	487.4464	214.2964	1.0000	7.9633	0.2285
79	7.9632	487.8323	214.6823	1.0000	8.1924	0.2292
80	8.1916	488.3311	215.1811	1.0000	8.4215	0.2299
81	8.4200	488.7965	215.6465	1.0000	8.6506	0.2305
82	8.6951	488.9241	215.7741	1.0000	8.9264	0.2313
83	8.9701	489.3217	216.1717	1.0000	9.2022	0.2321
84	9.2451	490.3475	217.1975	1.0000	9.4781	0.2329
85	9.5202	491.1273	217.9773	1.0000	9.7539	0.2337
86	9.6951	491.1360	217.9860	1.0000	9.9294	0.2342
87	9.8701	491.3138	218.1638	1.0000	10.1049	0.2348
88	10.0451	491.7383	218.5883	1.0000	10.2804	0.2353
89	10.2201	492.1419	218.9919	1.0000	10.4558	0.2358
90	10.3950	492.3503	219.2003	1.0000	10.6313	0.2363
91	10.5700	492.6189	219.4689	1.0000	10.8068	0.2368
92	10.7450	492.9749	219.8249	1.0000	10.9822	0.2372
93	10.9200	493.3241	220.1741	1.0000	11.1577	0.2377
94	11.1450	493.6458	220.4958	1.0000	11.3834	0.2384
95	11.3701	494.0263	220.8763	1.0000	11.6091	0.2390
96	11.5951	494.5266	221.3766	1.0000	11.8347	0.2396
97	11.8202	494.9949	221.8449	1.0000	12.0604	0.2402
98	12.0884	495.2027	222.0527	1.0000	12.3293	0.2410
99	12.3566	495.6132	222.4632	1.0000	12.5983	0.2417
100	12.6248	496.4861	223.3361	1.0000	12.8672	0.2424
101	12.8930	497.1913	224.0413	1.0000	13.1362	0.2432
102	13.0852	497.2776	224.1276	1.0000	13.3288	0.2437
103	13.2773	497.5181	224.3681	1.0000	13.5215	0.2442
104	13.4695	498.0075	224.8575	1.0000	13.7142	0.2447
105	13.6617	498.4617	225.3117	1.0000	13.9069	0.2452
106	13.8539	498.6860	225.5360	1.0000	14.0996	0.2457
107	14.0460	498.9855	225.8355	1.0000	14.2923	0.2462
108	14.2382	499.4054	226.2554	1.0000	14.4849	0.2467
109	14.4304	499.8091	226.6591	1.0000	14.6776	0.2472
110	14.6611	500.1182	226.9682	1.0000	14.9089	0.2478

Table B1

Cont.

111	14.8917	500.5048	227.3548	1.0000	15.1402	0.2484
112	15.1224	501.0479	227.8979	1.0000	15.3715	0.2490
113	15.3531	501.5499	228.3999	1.0000	15.6028	0.2496
114	15.6144	501.7620	228.6120	1.0000	15.8647	0.2503
115	15.8756	502.1643	229.0143	1.0000	16.1265	0.2510
116	16.1368	502.9879	229.8379	1.0000	16.3884	0.2516
117	16.3981	503.6718	230.5218	1.0000	16.6503	0.2523
118	16.6416	503.6108	230.4608	1.0000	16.8944	0.2529
119	16.8851	503.8921	230.7421	1.0000	17.1385	0.2535
120	17.1286	504.8859	231.7359	1.0000	17.3826	0.2541
121	17.3721	505.6747	232.5247	1.0000	17.6267	0.2546
122	17.5761	505.6325	232.4825	1.0000	17.8312	0.2551
123	17.7801	505.8389	232.6889	1.0000	18.0357	0.2556
124	17.9841	506.4581	233.3081	1.0000	18.2402	0.2561
125	18.1881	507.0117	233.8617	1.0000	18.4447	0.2566
126	18.3796	507.1791	234.0291	1.0000	18.6367	0.2571
127	18.5712	507.4535	234.3035	1.0000	18.8287	0.2575
128	18.7628	507.8879	234.7379	1.0000	19.0207	0.2580
129	18.9543	508.3070	235.1570	1.0000	19.2128	0.2584
130	19.1734	508.6101	235.4601	1.0000	19.4323	0.2589
131	19.3924	508.9812	235.8312	1.0000	19.6518	0.2595
132	19.6114	509.4758	236.3258	1.0000	19.8714	0.2600
133	19.8304	509.9456	236.7956	1.0000	20.0909	0.2605
134	20.0917	510.2654	237.1154	1.0000	20.3528	0.2611
135	20.3530	510.7051	237.5551	1.0000	20.6147	0.2617
136	20.6143	511.4037	238.2537	1.0000	20.8766	0.2623
137	20.8756	512.0220	238.8720	1.0000	21.1384	0.2629
138	21.1446	512.1118	238.9618	1.0000	21.4081	0.2635
139	21.4137	512.4918	239.3418	1.0000	21.6777	0.2641
140	21.6827	513.5065	240.3565	1.0000	21.9474	0.2647
141	21.9518	514.3164	241.1664	1.0000	22.2170	0.2652
142	22.1836	514.2376	241.0876	1.0000	22.4494	0.2657
143	22.4155	514.4849	241.3349	1.0000	22.6817	0.2662
144	22.6473	515.3447	242.1947	1.0000	22.9141	0.2667
145	22.8792	516.0655	242.9155	1.0000	23.1464	0.2672
146	23.0802	516.1514	243.0014	1.0000	23.3479	0.2677
147	23.2813	516.4047	243.2547	1.0000	23.5494	0.2681
148	23.4824	516.9114	243.7614	1.0000	23.7509	0.2685

Table B1

Cont.

149	23.6834	517.3914	244.2414	1.0000	23.9523	0.2689
150	23.8936	517.6609	244.5109	1.0000	24.1630	0.2694
151	24.1038	518.0085	244.8585	1.0000	24.3736	0.2698
152	24.3139	518.4822	245.3322	1.0000	24.5842	0.2702
153	24.5241	518.9386	245.7886	1.0000	24.7948	0.2707
154	24.7759	519.2991	246.1491	1.0000	25.0471	0.2712
155	25.0276	519.7422	246.5922	1.0000	25.2993	0.2717
156	25.2794	520.3526	247.2026	1.0000	25.5516	0.2722
157	25.5311	520.9187	247.7687	1.0000	25.8038	0.2727
158	25.8146	521.1785	248.0285	1.0000	26.0879	0.2733
159	26.0981	521.6397	248.4897	1.0000	26.3719	0.2739
160	26.3815	522.5461	249.3961	1.0000	26.6560	0.2744
161	26.6650	523.3054	250.1554	1.0000	26.9400	0.2750
162	26.9284	523.2854	250.1354	1.0000	27.2038	0.2755
163	27.1917	523.6181	250.4681	1.0000	27.4677	0.2760
164	27.4550	524.6818	251.5318	1.0000	27.7315	0.2765
165	27.7184	525.5373	252.3873	1.0000	27.9953	0.2770
166	27.9395	525.5375	252.3875	1.0000	28.2169	0.2774
167	28.1607	525.7904	252.6404	1.0000	28.4385	0.2778
168	28.3819	526.4618	253.3118	1.0000	28.6601	0.2782
169	28.6031	527.0675	253.9175	1.0000	28.8817	0.2786
170	28.8119	527.2799	254.1299	1.0000	29.0909	0.2790
171	29.0206	527.6021	254.4521	1.0000	29.3000	0.2794
172	29.2294	528.0894	254.9394	1.0000	29.5092	0.2798
173	29.4382	528.5604	255.4104	1.0000	29.7183	0.2802
174	29.6772	528.9152	255.7652	1.0000	29.9578	0.2806
175	29.9161	529.3418	256.1918	1.0000	30.1972	0.2810
176	30.1551	529.8993	256.7493	1.0000	30.4366	0.2815
177	30.3941	530.4302	257.2802	1.0000	30.6760	0.2819
178	30.6781	530.8043	257.6543	1.0000	30.9604	0.2824
179	30.9620	531.3066	258.1566	1.0000	31.2449	0.2829
180	31.2459	532.0861	258.9361	1.0000	31.5293	0.2834
181	31.5299	532.7796	259.6296	1.0000	31.8137	0.2839
182	31.8206	532.9137	259.7637	1.0000	32.1049	0.2844
183	32.1113	533.3519	260.2019	1.0000	32.3962	0.2849
184	32.4020	534.4537	261.3037	1.0000	32.6874	0.2853
185	32.6928	535.3428	262.1928	1.0000	32.9786	0.2858
186	32.9431	535.3062	262.1562	1.0000	33.2293	0.2862

Table B1

Cont.

187	33.1933	535.6034	262.4534	1.0000	33.4800	0.2866
188	33.4436	536.5244	263.3744	1.0000	33.7307	0.2870
189	33.6939	537.3058	264.1558	1.0000	33.9814	0.2874
190	33.9120	537.4374	264.2874	1.0000	34.1997	0.2878
191	34.1300	537.7394	264.5894	1.0000	34.4181	0.2881
192	34.3480	538.2997	265.1497	1.0000	34.6365	0.2885
193	34.5661	538.8326	265.6826	1.0000	34.8549	0.2888
194	34.7950	539.1530	266.0030	1.0000	35.0842	0.2892
195	35.0239	539.5546	266.4046	1.0000	35.3135	0.2895
196	35.2528	540.0882	266.9382	1.0000	35.5427	0.2899
197	35.4818	540.6031	267.4531	1.0000	35.7720	0.2903
198	35.7556	541.0215	267.8715	1.0000	36.0463	0.2907
199	36.0294	541.5281	268.3781	1.0000	36.3205	0.2911
200	36.3032	542.2141	269.0641	1.0000	36.5947	0.2915
201	36.5771	542.8523	269.7023	1.0000	36.8690	0.2919
202	36.8837	543.1642	270.0142	1.0000	37.1760	0.2924
203	37.1903	543.6906	270.5406	1.0000	37.4831	0.2928
204	37.4969	544.6912	271.5412	1.0000	37.7901	0.2932
205	37.8035	545.5355	272.3855	1.0000	38.0972	0.2937
206	38.0871	545.5583	272.4083	1.0000	38.3812	0.2941
207	38.3707	545.9467	272.7967	1.0000	38.6652	0.2945
208	38.6543	547.0897	273.9397	1.0000	38.9491	0.2949
209	38.9379	548.0204	274.8704	1.0000	39.2331	0.2953
210	39.1765	548.0663	274.9163	1.0000	39.4721	0.2956
211	39.4152	548.3699	275.2199	1.0000	39.7111	0.2959
212	39.6539	549.0983	275.9483	1.0000	39.9501	0.2962
213	39.8925	549.7612	276.6112	1.0000	40.1891	0.2966
214	40.1191	550.0240	276.8740	1.0000	40.4160	0.2969
215	40.3457	550.3994	277.2494	1.0000	40.6428	0.2972
216	40.5722	550.9450	277.7950	1.0000	40.8697	0.2975
217	40.7988	551.4734	278.3234	1.0000	41.0966	0.2978
218	41.0587	551.8865	278.7365	1.0000	41.3568	0.2981
219	41.3185	552.3753	279.2253	1.0000	41.6170	0.2984
220	41.5784	553.0035	279.8535	1.0000	41.8772	0.2988
221	41.8383	553.6027	280.4527	1.0000	42.1374	0.2991
222	42.1459	554.0371	280.8871	1.0000	42.4454	0.2995
223	42.4535	554.6094	281.4594	1.0000	42.7533	0.2999

Table B1

Cont.

224	42.7611	555.4804	282.3304	1.0000	43.0613	0.3002
225	43.0687	556.2584	283.1084	1.0000	43.3693	0.3006
226	43.3817	556.4395	283.2895	1.0000	43.6827	0.3010
227	43.6947	556.9415	283.7915	1.0000	43.9960	0.3013
228	44.0077	558.1421	284.9921	1.0000	44.3094	0.3017
229	44.3207	559.1203	285.9703	1.0000	44.6228	0.3021
230	44.4905	559.2782	286.1282	1.0000	44.7928	0.3023
231	44.6604	559.5189	286.3689	1.0000	44.9628	0.3025
232	44.8302	559.8372	286.6872	1.0000	NaN	NaN
233	45.0000	560.1757	287.0257	1.0000	NaN	NaN

Table B2: Results for Empirical modeling for $\tau = 7$

iter	t	Cn	T0	t2	T2	y_v	P^{sat}	tr
1	0	11.3196	202.9442	4.6	185.8492	0.647624	0.65621	4.6
2	0.45	11.3677	203.9321	4.83	187.459	0.658842	0.66757	4.38
3	0.9	11.4123	204.8462	5.05	188.9629	0.669579	0.67845	4.15
4	1.35	11.4539	205.6957	5.27	190.3743	0.679902	0.68891	3.92
5	1.8	11.4928	206.4888	5.49	191.7059	0.689877	0.69902	3.69
6	2.26	11.5294	207.2334	5.72	192.9699	0.699575	0.70884	3.46
7	2.71	11.5641	207.9368	5.94	194.1774	0.709064	0.71846	3.23
8	3.16	11.5972	208.6057	6.17	195.3394	0.718417	0.72794	3.01
9	3.61	11.6289	209.2463	6.4	196.4662	0.727709	0.73735	2.8
10	4.06	11.6596	209.8644	6.65	197.5677	0.737017	0.74678	2.59
11	4.51	11.6895	210.4652	6.9	198.6533	0.746421	0.75631	2.39
12	4.96	11.7188	211.0535	7.17	199.7316	0.756001	0.76602	2.21
13	5.41	11.7478	211.6336	7.46	200.8112	0.76584	0.77599	2.05
14	5.86	11.7766	212.2096	7.77	201.903	0.77605	0.78633	1.91
15	6.32	11.8054	212.785	8.11	203.0079	0.786651	0.79707	1.8
16	6.77	11.8345	213.3631	8.49	204.1344	0.797727	0.8083	1.72
17	7.22	11.8638	213.9467	8.9	205.2861	0.809307	0.82003	1.68
18	7.67	11.8937	214.5382	9.35	206.4629	0.821351	0.83223	1.69
19	8.12	11.9241	215.14	9.86	207.6604	0.833733	0.84478	1.74
20	8.57	11.9552	215.754	10.4	208.8681	0.8462	0.85741	1.83
21	9.02	11.987	216.3817	10.98	210.0711	0.858407	0.86978	1.96
22	9.47	12.0197	217.0246	11.58	211.2545	0.86999	0.88152	2.11
23	9.92	12.0533	217.6837	12.18	212.4077	0.880675	0.89234	2.26
24	10.38	12.0878	218.36	12.77	213.5267	0.890335	0.90213	2.4
25	10.83	12.1233	219.0542	13.34	214.6134	0.898969	0.91088	2.52
26	11.28	12.1599	219.7667	13.9	215.6731	0.906656	0.91867	2.62
27	11.73	12.1974	220.4979	14.43	216.7118	0.913509	0.92561	2.7
28	12.18	12.2361	221.2477	14.95	217.7354	0.919641	0.93183	2.77
29	12.63	12.2758	222.0163	15.44	218.749	0.925156	0.93741	2.81
30	13.08	12.3166	222.8034	15.93	219.7567	0.930143	0.94247	2.85
31	13.53	12.3584	223.6087	16.4	220.7619	0.934676	0.94706	2.86
32	13.98	12.4013	224.4319	16.86	221.767	0.938819	0.95126	2.87
33	14.44	12.4452	225.2722	17.3	222.7739	0.94262	0.95511	2.87
34	14.89	12.4901	226.1292	17.75	223.7839	0.946122	0.95866	2.86
35	15.34	12.5359	227.0021	18.18	224.798	0.949361	0.96194	2.84
36	15.79	12.5827	227.89	18.61	225.8167	0.952366	0.96498	2.82
37	16.24	12.6304	228.7923	19.03	226.8403	0.955161	0.96782	2.79
38	16.69	12.6789	229.7078	19.45	227.8689	0.957768	0.97046	2.76
39	17.14	12.7282	230.6358	19.87	228.9025	0.960204	0.97293	2.72

Table B2

Cont.

40	17.59	12.7783	231.5751	20.28	229.9406	0.962486	0.97524	2.69
41	18.04	12.8292	232.5249	20.69	230.9829	0.964626	0.97741	2.65
42	18.5	12.8806	233.484	21.1	232.0289	0.966636	0.97944	2.6
43	18.95	12.9327	234.4514	21.51	233.078	0.968527	0.98136	2.56
44	19.4	12.9854	235.4261	21.92	234.1296	0.970309	0.98317	2.52
45	19.85	13.0386	236.407	22.32	235.183	0.971988	0.98487	2.48
46	20.3	13.0922	237.3931	22.73	236.2376	0.973572	0.98647	2.43
47	20.75	13.1463	238.3835	23.14	237.2925	0.975068	0.98799	2.39
48	21.2	13.2007	239.377	23.55	238.3472	0.976483	0.98942	2.35
49	21.65	13.2554	240.3728	23.96	239.4007	0.97782	0.99078	2.31
50	22.1	13.3104	241.3699	24.37	240.4525	0.979085	0.99206	2.27
51	22.56	13.3655	242.3674	24.78	241.5018	0.980283	0.99327	2.23
52	23.01	13.4209	243.3645	25.2	242.5479	0.981416	0.99442	2.19
53	23.46	13.4764	244.3604	25.61	243.5903	0.98249	0.99551	2.16
54	23.91	13.5319	245.3542	26.03	244.6283	0.983508	0.99654	2.12
55	24.36	13.5875	246.3454	26.45	245.6612	0.984472	0.99752	2.09
56	24.81	13.6432	247.3332	26.88	246.6886	0.985385	0.99844	2.07
57	25.26	13.6987	248.317	27.31	247.7101	0.986249	0.99932	2.04
58	25.71	13.7543	249.2964	27.74	248.725	0.987068	1.00015	2.02
59	26.16	13.8097	250.2707	28.17	249.733	0.987844	1.00093	2
60	26.62	13.865	251.2396	28.6	250.7339	0.988577	1.00168	1.99
61	27.07	13.9202	252.2027	29.04	251.7273	0.989271	1.00238	1.98
62	27.52	13.9752	253.1597	29.48	252.7129	0.989927	1.00304	1.97
63	27.97	14.03	254.1102	29.93	253.6905	0.990546	1.00367	1.96
64	28.42	14.0847	255.0542	30.37	254.66	0.991129	1.00426	1.95
65	28.87	14.1391	255.9915	30.82	255.6213	0.99168	1.00482	1.95
66	29.32	14.1933	256.9219	31.27	256.5744	0.992197	1.00534	1.95
67	29.77	14.2473	257.8454	31.72	257.5193	0.992684	1.00584	1.95
68	30.22	14.3011	258.762	32.17	258.4559	0.99314	1.0063	1.95
69	30.68	14.3547	259.6717	32.62	259.3844	0.993568	1.00673	1.95
70	31.13	14.4081	260.5746	33.07	260.305	0.993968	1.00714	1.95
71	31.58	14.4612	261.4709	33.52	261.2177	0.994342	1.00752	1.94
72	32.03	14.5141	262.3606	33.97	262.1229	0.994691	1.00787	1.94
73	32.48	14.5669	263.244	34.41	263.0206	0.995017	1.0082	1.93
74	32.93	14.6194	264.1212	34.85	263.9112	0.99532	1.00851	1.92
75	33.38	14.6718	264.9924	35.28	264.7948	0.995602	1.00879	1.9
76	33.83	14.724	265.8579	35.72	265.6719	0.995864	1.00906	1.88
77	34.28	14.776	266.7178	36.14	266.5426	0.996109	1.00931	1.86
78	34.74	14.8279	267.5724	36.56	267.4073	0.996336	1.00954	1.83

Table B2

Cont.

79	35.19	14.8797	268.4218	36.98	268.2661	0.996547	1.00975	1.79
80	35.64	14.9313	269.2663	37.39	269.1193	0.996743	1.00995	1.75
81	36.09	14.9828	270.1059	37.79	269.9671	0.996927	1.01014	1.7
82	36.54	15.0342	270.9409	38.19	270.8096	0.997098	1.01031	1.65
83	36.99	15.0855	271.7712	38.59	271.647	0.997257	1.01047	1.6
84	37.44	15.1366	272.5968	38.98	272.4793	0.997406	1.01062	1.54
85	37.89	15.1877	273.4178	39.37	273.3065	0.997546	1.01076	1.48
86	38.34	15.2386	274.2339	39.75	274.1284	0.997678	1.0109	1.41
87	38.8	15.2893	275.0449	40.14	274.9449	0.997801	1.01102	1.34
88	39.25	15.3399	275.8505	40.52	275.7557	0.997917	1.01114	1.27
89	39.7	15.3903	276.6502	40.9	276.5604	0.998027	1.01125	1.2
90	40.15	15.4405	277.4436	41.28	277.3584	0.998131	1.01136	1.13
91	40.6	15.4903	278.2298	41.66	278.1491	0.99823	1.01146	1.06
92	41.05	15.5399	279.0081	42.04	278.9315	0.998324	1.01155	0.99
93	41.5	15.589	279.7774	42.43	279.7049	0.998414	1.01164	0.92
94	41.95	15.6376	280.5365	42.82	280.4679	0.998501	1.01173	0.87
95	42.4	15.6857	281.2841	43.22	281.2193	0.998585	1.01182	0.82
96	42.86	15.733	282.0185	43.64	281.9574	0.998667	1.0119	0.78
97	43.31	15.7796	282.738	44.08	282.6806	0.998748	1.01198	0.77
98	43.76	15.8252	283.4406	44.55	283.3869	0.998829	1.01206	0.79
99	44.21	15.8696	284.1239	45.08	284.074	0.998915	1.01215	0.87
100	44.66	15.9128	284.7853	45.75	284.74	0.999014	1.01225	1.09

Figure B1: Acentric factor vs carbon number fit plot

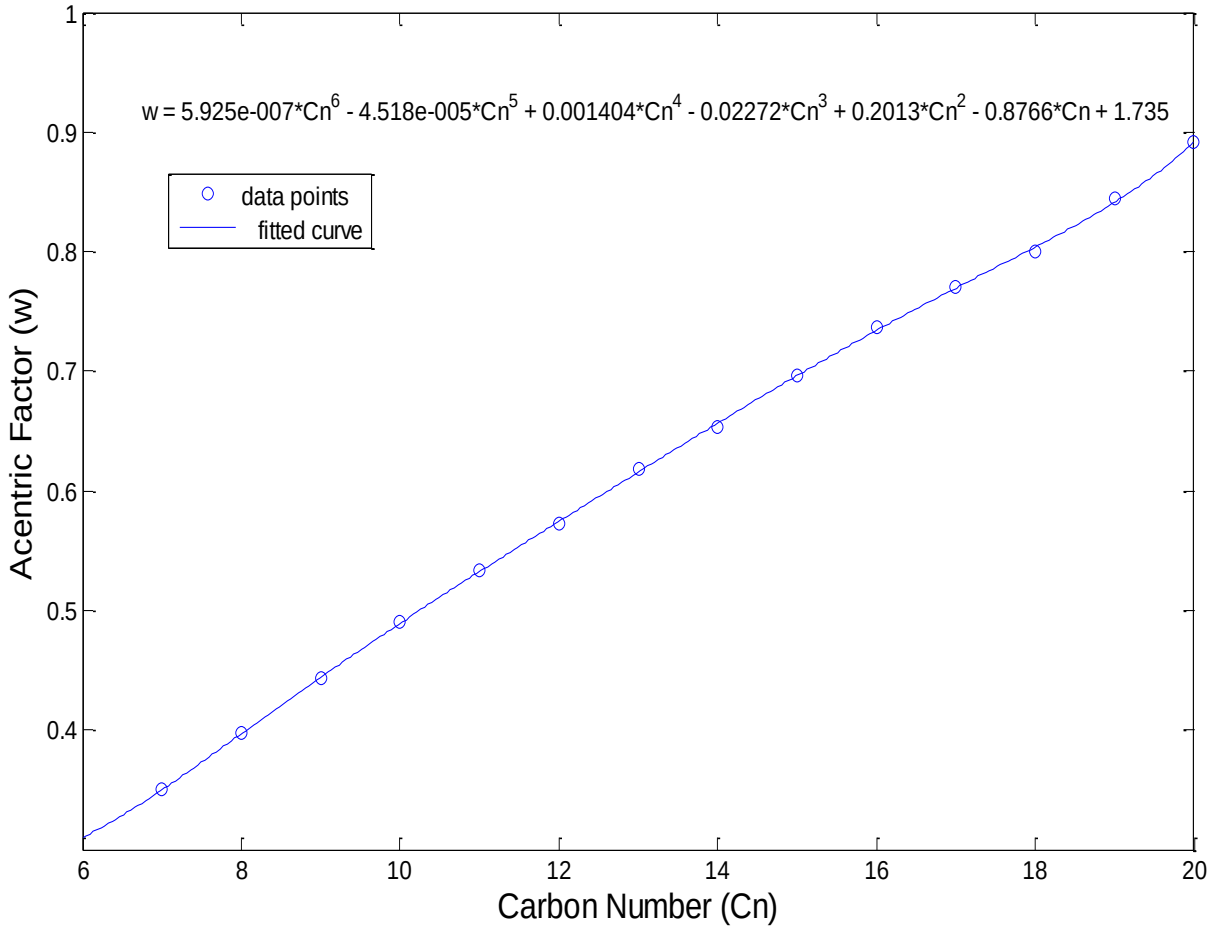

Figure B3 Acentric factor fitting curve, data reference [22]

Figure B2: Molecular weight vs carbon number fit plot

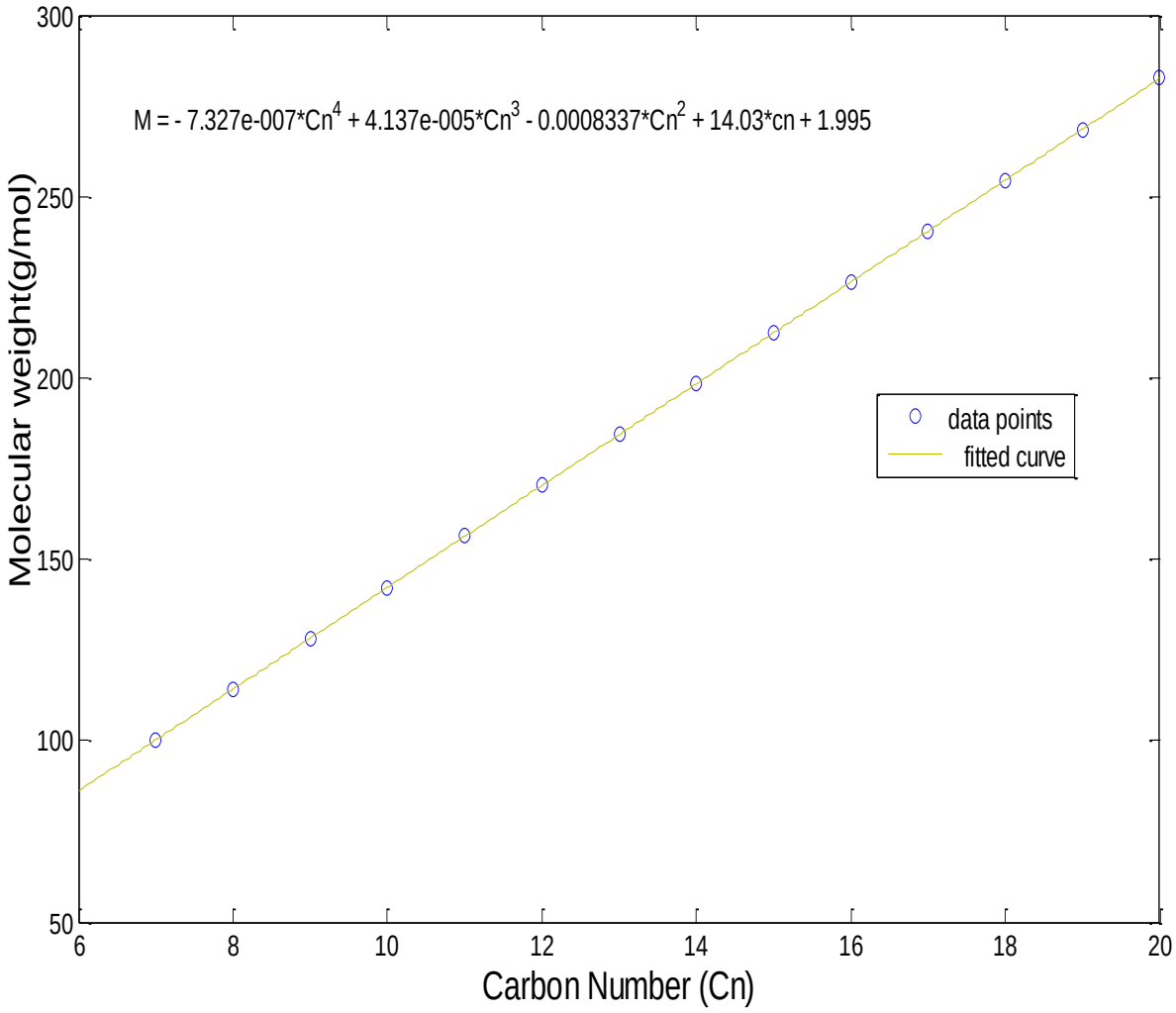

Figure B4 Molecular weight fitting, data reference [19]